

**NEW TECHNIQUES IN NUMERICAL  
INTEGRATION: THE COMPUTATION OF  
MOLECULAR INTEGRALS OVER  
EXPONENTIAL-TYPE FUNCTIONS**

by

Richard Mikaël Slevinsky

A thesis submitted in partial fulfillment of the requirements for the degree of

Doctor of Philosophy

in

Applied Mathematics

Department of Mathematical and Statistical Sciences

University of Alberta

© Richard Mikaël Slevinsky, 2014

## Abstract

The numerical evaluation of challenging integrals is a topic of interest in applied mathematics. We investigate molecular integrals in the  $B$  function basis, an exponentially decaying basis with a compact analytical Fourier transform. The Fourier property allows analytical expressions for molecular integrals to be formulated in terms of semi-infinite highly oscillatory integrals with limited exponential decay. The semi-infinite integral representations in terms of nonphysical variables stand as the bottleneck in the calculation.

To begin our numerical experiments, we conduct a comparative study of the most popular numerical steepest descent methods, extrapolation methods and sequence transformations for computing semi-infinite integrals. It concludes that having asymptotic series representations for integrals and applying sequence transformations leads to the most efficient algorithms.

For three-center nuclear attraction integrals, we find an analytical expression for the semi-infinite integrals. Numerical experiments show the resulting algorithm is approximately  $10^{2.5}$  times more efficient than the state-of-the-art. For the four-center two-electron Coulomb integrals, we take a different approach. The integrand has singularities in the complex plane that can be near the path of integration, making standard quadrature routines unreliable. The trapezoidal rule with double exponential variable transformations has been shown to have very promising properties as a general-purpose integrator. We investigate the use of conformal maps to maximize the convergence rate, resulting in a nonlinear program for the optimized variable transformation.

## Preface

The research conducted for this thesis forms part of international and institutional research collaboration, with S. Olver and H. Safouhi, with R. M. Slevinsky being the lead collaborator at the University of Alberta.

Most of chapter 3 of this thesis has been published as R. M. Slevinsky and H. Safouhi, “A comparative study of numerical steepest descent, extrapolation, and sequence transformation methods in computing semi-infinite integrals,” *Numerical Algorithms*, 60:315–337, 2012. I was responsible for the scientific computing and numerical analysis as well as the manuscript composition. H. Safouhi was the supervisory author and was involved with concept formation and manuscript composition.

Most of chapter 5 of this thesis has been submitted for publication by R. M. Slevinsky and S. Olver. I was responsible for the scientific computing and numerical analysis as well as the manuscript composition. S. Olver was the supervisory author and was involved with concept formation and manuscript composition.

## Acknowledgements

It is a pleasure to thank the people who helped me during my Ph D studies.

It is difficult to overstate my gratitude to my Ph D co-supervisors, Hassan Safouhi and Anthony To-Ming Lau. I am deeply indebted to them for their guidance and insight as supervisors. With their enthusiasm, inspiration, and passion for mathematics, they helped me succeed. Throughout my degree, they always provided the best encouragement, sound advice, and good mentoring.

The final part of my Ph D studies took place at The University of Sydney with Sheehan Olver as my host supervisor. I had a wonderful time in Sydney and this was no coincidence! I am grateful to Sheehan for the advice and inspiration, and for being the best host one could ask for. It is also a pleasure to thank Philippe Gaudreau for our regular dialogue on this work and other collaborations. Socrates would be proud.

I wish to thank my family for providing me a loving environment. My wife Katrina Slevinsky and my parents Karen Slevinsky and Richard Slevinsky have given me their unwavering support.

Last but not least, I would like to thank the Natural Sciences and Engineering Research Council for funding my Ph D studies with the Alexander Graham Bell Canada Graduate Scholarship. This funding allowed my research programme to come to fruition and was helpful in securing other sources of funding as well.

# Contents

<b>1</b>	<b>Introduction</b>	<b>1</b>
<b>2</b>	<b>The Molecular Integrals Problem</b>	<b>7</b>
2.A	The molecular Schrödinger equation . . . . .	7
2.B	General definitions and properties . . . . .	10
2.B.1	Factorials . . . . .	10
2.B.2	Spherical harmonics . . . . .	11
2.B.3	Bessel functions . . . . .	13
2.B.4	The Fourier transform . . . . .	15
2.C	Choosing a basis . . . . .	17
2.C.1	Slater-type functions . . . . .	17
2.C.2	Gaussian functions . . . . .	17
2.C.3	<i>B</i> functions . . . . .	18
2.D	The molecular integrals . . . . .	20
2.D.1	Overlap integrals . . . . .	21
2.D.2	Nuclear attraction integrals . . . . .	22
2.D.3	Four-center two-electron integrals . . . . .	24
<b>3</b>	<b>A Comparative Study</b>	<b>27</b>

3.A	Introduction . . . . .	27
3.B	Description of the methods . . . . .	30
3.B.1	Steepest descent methods . . . . .	30
3.B.2	Extrapolation methods . . . . .	33
3.B.3	Sequence transformations . . . . .	38
3.C	The integrals . . . . .	43
3.C.1	The first integral . . . . .	44
3.C.2	The second integral . . . . .	45
3.C.3	The third integral . . . . .	46
3.C.4	The fourth integral . . . . .	47
3.D	Numerical discussion . . . . .	49
3.E	Refinements of the algorithms . . . . .	52
3.E.1	Steepest descent methods . . . . .	54
3.E.2	Extrapolation methods . . . . .	57
3.E.3	Sequence transformations . . . . .	60
3.E.4	Numerical Discussion . . . . .	62
3.F	Conclusion . . . . .	63
<b>4</b>	<b>An Analytical Expression</b>	<b>67</b>
4.A	Introduction . . . . .	67
4.B	The Development . . . . .	70
4.C	Numerical Discussion . . . . .	76
4.D	Conclusion . . . . .	78
<b>5</b>	<b>Conformal Maps for the Double Exponential Transformation</b>	<b>80</b>
5.A	Introduction . . . . .	80
5.B	Quadrature and Sinc methods by variable transformation . . .	84

5.C	Maximizing the convergence rates . . . . .	90
5.D	Examples . . . . .	101
5.D.1	Example: endpoint and complex singularities . . . . .	101
5.D.2	Example: eight different complex conjugate singularities	102
5.D.3	Example: for Goursat's infinite integral . . . . .	104
5.D.4	Example: adaptive optimization via Sinc-Padé approxi- mants . . . . .	107
5.E	Applications . . . . .	109
5.E.1	Boundary value problems . . . . .	109
5.E.2	Nonlinear waves . . . . .	114
5.E.3	Multi-dimensional integrals . . . . .	118
5.E.4	Molecular integrals with exponential basis functions . .	121
5.F	Numerical Discussion . . . . .	125
5.G	Conclusion . . . . .	128
<b>6</b>	<b>Conclusion</b>	<b>129</b>
	<b>Bibliography</b>	<b>130</b>

# List of Tables

3.1	Numerical evaluation of $\mathcal{I}_1(\beta)$ . . . . .	52
3.2	Numerical evaluation of $\mathcal{I}_2(a, b)$ . . . . .	53
3.3	Numerical evaluation of $\mathcal{I}_3(\mu, \alpha, \beta)$ . . . . .	53
3.4	Numerical evaluation of $\mathcal{I}_4(\mu, \nu, \alpha, \beta, \zeta)$ . . . . .	54
3.5	Numerical evaluation of $\mathcal{I}_1(\beta)$ with the refinements. . . . .	63
3.6	Numerical evaluation of $\mathcal{I}_2(a, b)$ with the refinements. . . . .	64
3.7	Numerical evaluation of $\mathcal{I}_3(\mu, \alpha, \beta)$ with the refinements. . . . .	64
3.8	Numerical evaluation of $\mathcal{I}_4(\mu, \nu, \alpha, \beta, \zeta)$ with the refinements. . . . .	65
4.1	Numerical evaluation of the integral $\mathcal{I}(s)$ for $s = 0.25$ . . . . .	78
4.2	Numerical evaluation of the integral $\mathcal{I}(s)$ for $s = 0.75$ . . . . .	79
5.1	Variable transformations $\phi(t)$ for endpoint decay. . . . .	85
5.2	Transformations and parameters for (5.45). . . . .	101
5.3	Transformations and parameters for (5.47). . . . .	103
5.4	Transformations and parameters for (5.49). . . . .	106
5.5	Transformations and parameters for (5.51). . . . .	108
5.6	Evolution of the six nearest roots of the Sinc-Padé approximants. . . . .	108
5.7	Evolution of the coefficients of the adaptive map. . . . .	108
5.8	Transformations and parameters for (5.52). . . . .	112

5.9	Transformations and parameters for (5.64).	117
5.10	Transformations and parameters for (5.79).	119
5.11	Numerical Evaluation of (5.77) using (5.82).	121
5.12	Transformations and static parameters for (5.83).	123

# List of Figures

2.1	The configuration of four atoms located at $A, B, C,$ and $D,$ and two electrons located at $R$ and $R'.$ . . . . .	21
3.1	(a) shows the portion evaluated by quadrature and (b) shows the portion evaluated by extrapolation. . . . .	35
3.2	(a) shows the integrand in (3.72) and (b) shows the integrand in (3.73). In both cases, $a = 100$ and $b = 10.$ . . . . .	60
5.1	In (a) the plot of the strip $\mathcal{D}_{\frac{\pi}{2}}$ with singularities located on the boundary, in (b) the resulting Schwarz-Christoffel map, and in (c) a tanh map of the Schwarz-Christoffel map. In all three cases, the crosses track the singularities $\delta_1 \pm i\epsilon_1 = -1/2 \pm i$ and $\delta_2 \pm i\epsilon_2 = 1/2 \pm i/2.$ For the sake of comparison, an integral with these singularities is treated in example 5.D.1. . . . .	96
5.2	In (a) the exact solution $\mathcal{H}(0),$ in (b) the solution $\mathcal{H}(1/2),$ and in (c) the desired solution $\mathcal{H}(1).$ An integral with these singularities is treated in example 5.D.2. . . . .	98

5.3	In (a) the plot of the strip $\mathcal{D}_{\frac{\pi}{2}}$ with singularities located on the boundary, in (b) the optimized map $h(\cdot)$ , and in (c) the optimized DE map. In all three cases, the crosses track the singularities. . . . .	102
5.4	In (a) the plot of the integrand of (5.45) and in (b) the performance of the trapezoidal rule with single, double, and optimized double exponential variable transformations. . . . .	103
5.5	In (a) the plot of the strip $\mathcal{D}_{\frac{\pi}{2}}$ with singularities located on the boundary, in (b) the optimized map $h(\cdot)$ , and in (c) the optimized DE map. In all three cases, the crosses track the singularities. . . . .	104
5.6	In (a) the plot of the integrand of (5.47) and in (b) the performance of the trapezoidal rule with single, double, and optimized double exponential variable transformations. . . . .	105
5.7	In (a) the plot of the strip $\mathcal{D}_{\frac{\pi}{2}}$ with singularities located on the boundary, in (b) the optimized map $h(\cdot)$ , and in (c) the optimized DE map. In all three cases, the crosses track the singularities. . . . .	106
5.8	In (a) the plot of the integrand of (5.49) and in (b) the performance of the trapezoidal rule with single, double, and optimized double exponential variable transformations. . . . .	107
5.9	In (a) the plot of the strip $\mathcal{D}_{\frac{\pi}{2}}$ with singularities located on the boundary, in (b) the adaptive map $h(\cdot)$ , and in (c) the optimized DE map. In all three cases, the crosses track the singularities and the squares track the roots of the Sinc-Padé approximant for $n = 2^8$ . . . . .	109

5.10	In (a) the plot of the integrand of (5.51) and the Sinc-Padé approximant for $n = 2^8$ and in (b) the performance of the trapezoidal rule with single, double, optimized double, and adaptive optimized double exponential variable transformations. . . . .	110
5.11	In (a) the solution of (5.52) along with the three Sinc approximations for $n = 2^{10}$ and in (b) the performance of the Sinc approximation with single, double, and optimized double exponential variable transformations. In both cases $\epsilon = 0.2$ . . . . .	113
5.12	In (a) the solution of (5.52) along with the three Sinc approximations for $n = 2^{10}$ and in (b) the performance of the Sinc approximation with single, double, and optimized double exponential variable transformations. In both cases $\epsilon = 0.1$ . . . . .	113
5.13	In (a) the solution of (5.64) along with the three Sinc approximations for $n = 2^5$ and the scaled forcing function and in (b) the performance of the Sinc approximation with single, double, and optimized double exponential variable transformations. . . . .	117
5.14	The performance of the trapezoidal rule with single, double, and optimized double exponential variable transformations. In all figures, $\kappa = 1$ , and in (a) $m = 2$ , in (b) $m = 3$ , and in (c) $m = 4$ . . . . .	120
5.15	In (a) the plot of the strip $\mathcal{D}_{\frac{\pi}{2}}$ with singularities located on the boundary, in (b) the optimized map $h(\cdot)$ , and in (c) the composition $\zeta(h(\cdot))$ . In all three cases, the crosses track the singularities and the circle marks the saddle point. . . . .	124

5.16	In (a) the plot of the strip $\mathcal{D}_{\frac{\pi}{2}}$ with singularities located on the boundary, in (b) the optimized map $h(\cdot)$ , and in (c) the composition $\zeta(h(\cdot))$ . In all three cases, the crosses track the singularities and the circle marks the saddle point. . . . .	124
5.17	The performance of the trapezoidal rule with (a) single, (b) double, and (c) optimized double exponential variable transformations. . . . .	125

# Chapter 1

## Introduction

The numerical evaluation of challenging integrals is a topic of interest in applied mathematics. In this work, we present mathematical solutions to some outstanding issues in the numerical evaluation of molecular integrals in an exponential basis. The Fourier transform representation of the Coulomb operators allows for the expectations to be calculated with a complex linear oscillator instead. Then, using a generalized convolution property, it is equivalent to consider the expectations of the Fourier transforms of the basis elements. When using the Fourier transform representation of Coulomb operators, the  $B$  functions are the ideal exponential basis, as they have a compact analytical Fourier transform. The  $B$  functions are introduced in the Ph D thesis of Filter [Fil78] and their analytical and numerical properties are the subject of the Ph D theses of Weniger [Wen82], Grotendorst [Gro85], Homeier [Hom90].

Reducing the dimensionality of multidimensional integrals is of utmost importance for obtaining an efficient numerical program. If we naïvely consider the integration in each variable as a quadrature with  $N$  points, then an  $m$ -dimensional integral requires  $\mathcal{O}(N^m)$  function evaluations, reaching the limits

of modern computational power quite quickly. Therefore, if the reduction in dimension comes at a sub-exponential cost, such as a polynomial cost, then this will undoubtedly lead to a more promising numerical program. From a computational perspective, this was the main outcome of the  $B$  function approach.

The Fourier transform method for molecular integrals over  $B$  functions allows for compact analytical expressions for overlap integrals, and reduces the dimension of three-center nuclear integrals from three to two. The Fourier transform method for molecular integrals over  $B$  functions leads to even more savings when considering the four-center two-electron Coulomb integrals. In this setting, the Fourier decomposition of the Coulomb operator separates the integral over  $\mathbb{R}^6$  into an integral over  $\mathbb{R}^3$  over the product of two separated integrals over  $\mathbb{R}^3$ . While in the former case the integrand is a function of all six variables, in the latter case the integrands are separated, and separation ultimately reduces the dimensionality from six to three.

The major bottleneck in the  $B$  function approach occurs when evaluating highly oscillatory semi-infinite integrals with limited exponential decay in terms of non-physical variables. These semi-infinite integrals are studied scrupulously in the Ph D thesis of Safouhi [Saf99], where extrapolation methods are applied and derived to accelerate their convergence. In the three-center nuclear attraction integrals, the semi-infinite integrals contain one oscillatory Bessel function and one exponentially decaying Bessel function. In the four-center two-electron Coulomb integrals, the semi-infinite integrals contain one oscillatory Bessel function and two exponentially decaying modified Bessel functions.

To begin our numerical experiments, we conduct a comparative study of

the most popular numerical steepest descent methods, extrapolation methods and sequence transformations for computing semi-infinite integrals. It concludes that having asymptotic series representations for integrals and applying sequence transformations to accelerate their convergence or to sum their divergence leads to the most efficient algorithms for computing the integrals. While all three methods are capable of attaining a predetermined accuracy, the sequence transformations attain the same predetermined accuracy approximately  $10^3$  times faster than the other methods. The comparative study gives us a clear direction to find, whenever possible, analytical expressions for semi-infinite integrals.

Our numerical experiments continue when we find an analytical expression for the semi-infinite integral over non-physical variables for the three-center nuclear attraction integrals. The resulting algorithm is approximately  $10^{2.5}$  times more efficient than the state-of-the-art. This expression allows for the dimensionality of the three-center nuclear attraction integrals to be ultimately reduced from three to one.

When, to the best of our abilities, the same analytical techniques are fruitless for obtaining an analytical expression for the semi-infinite integrals over non-physical variables for the four-center two-electron Coulomb integrals, we focus our efforts on specifically tailoring a quadrature rule to the integrals. The integrand has singularities in the complex plane that can be very near the path of integration, thereby reducing the largest region of analyticity containing the path of integration. This reduction makes standard quadrature routines unreliable, and the number of function evaluations for a predetermined accuracy can blow up. Therefore, in the case where an analytical expression is not found, an improvement to the numerical evaluation can then be considered as

a reduction in the maximal number of function evaluations required for some predetermined accuracy.

From Liouville's theorem in complex analysis, we know that every bounded entire function is constant. Heuristically speaking, then, studying a nontrivial function is somehow equivalent to studying its singular behaviour, because unless it is constant, it will be singular *somewhere* in the extended complex plane. For most special functions, the usual singular points are 0 and  $\infty$ , and their study is often carried out at either of these points using Frobenius series, WKB methods, or otherwise. In the case of the four-center's semi-infinite integral over non-physical variables, as a function in the complex plane, the integrand has two pairs of complex conjugate poles on the imaginary axis. Therefore, we recognized that in order to construct a suitable quadrature method, it had to revolve around these singularities.

We naturally started by investigating the Gaussian quadratures. Beyond the classical rules with known three-term recurrence relations used for constructing weights and abscissas, more general weights and abscissas are either constructed by modifying the classical ones by incorporating some prescribed singular nature [Gau13], or some other integration method is used to compute the recurrence coefficients. This led us to study such other methods as they may be just as capable in singular situations in the first place. Numerical Recipes [PTVF07] contains a section on quadrature by variable transformation as their recommended solution for obtaining the coefficients of the associated recurrence relation for orthogonal polynomials. After investigating this work, we studied the works of Takahasi and Mori [TM74] on the double exponential transformation. Our initial impression was very positive because the weights and abscissas are generated in as little as  $\mathcal{O}(n)$  operations.

By studying Sugihara’s functional analysis approach on the optimality of the double exponential transformation for the trapezoidal rule [Sug97], we recognized the tremendous potential in applying it to the four-center two-electron Coulomb’s semi-infinite integrals. However, we noticed nearby singularities had a similar effect on the trapezoidal rule as it had on the Gaussian quadrature rules. The problem of maximizing the convergence rate of the double exponential transformation despite arbitrary singularities near the contour of integration was initially solved theoretically, but the numerical experiments were less than promising. With a theoretical result in hand, I packed my bags and headed south for Australia.

At The University of Sydney, Sheehan Olver introduced me to the works of Tee and Trefethen [TT06], Hale and Trefethen [HT08], Hale and Tee [HT09], and Hale’s Ph D thesis [Hal09] “On The Use of Conformal Maps to Speed Up Numerical Computations.” Inspired by this work, we are able to use conformal maps to maximize the convergence rate of the trapezoidal rule. The main idea is that from Sugihara’s functional analysis [Sug97], there is an upper bound on the maximal strip width for the analyticity of the dominating function. Therefore, by locating the pre-images of the function’s singularities on the top and bottom boundaries of the strip, it is possible to attain the upper bound exactly. For the canonical finite, infinite, and semi-infinite domains, there are double exponential variable transformations which consist of an outer transformation composed with the sinh function. So, to obtain a general framework for considering singularities, we studied the sinh conformal map. This map is actually the simplest case of the Schwarz-Christoffel map from the strip to the entire complex plane with branches emanating upward and downward at  $\pm i$ , respectively. While the Schwarz-Christoffel map is a very challenging object to

compute, we could emulate most of the properties of the Schwarz-Christoffel map with a much simpler solution strategy. Since a polynomial adjustment to the sinh map still grows at a single exponential rate, such an adjustment fits naturally in the double exponential framework, and allows for the use of the additional parameters to locate pre-images of singularities as far from the integration axis as necessary to maximize the convergence rate. It turns out that the same conformal maps maximize the convergence rate of Sinc numerical methods, and are therefore amenable to solving a variety of different problems in applied mathematics.

# Chapter 2

## The Molecular Integrals Problem

### 2.A The molecular Schrödinger equation

Consider the Schrödinger equation [Sch26] for an  $n$ -electron,  $N$ -nucleus molecule:

$$\mathcal{H}\Psi = E\Psi. \quad (2.1)$$

The Hamiltonian of the system consists of five components of kinetic and potential energies:

$$\mathcal{H} = T_e + T_N + V_{ee} + V_{eN} + V_{NN}. \quad (2.2)$$

The kinetic energies are:

$$T_e = -\frac{1}{2} \sum_{i=1}^n \frac{\Delta_i}{m_e}, \quad (2.3)$$

$$T_N = -\frac{1}{2} \sum_{K=1}^N \frac{\Delta_K}{M_K}, \quad (2.4)$$

where  $\Delta_i$  and  $\Delta_K$  are the Laplacian operators on the  $\mathbb{R}^3$  coordinate system of the  $i^{\text{th}}$  electron and  $K^{\text{th}}$  nucleus,  $m_e$  is the mass of an electron, and  $M_K$  is the mass of the  $K^{\text{th}}$  nucleus. The potential energies are:

$$V_{ee} = \sum_{i=1}^n \sum_{j>i}^n \frac{1}{r_{ij}}, \quad (2.5)$$

$$V_{eN} = - \sum_{i=1}^n \sum_{K=1}^N \frac{Z_K}{r_{iK}}, \quad (2.6)$$

$$V_{NN} = \sum_{K=1}^N \sum_{L>K}^N \frac{Z_K Z_L}{r_{KL}}, \quad (2.7)$$

where  $r_{AB}$  is the Euclidean distance between object  $A$  and object  $B$ , electrons or nuclei, and  $Z_K$  is the atomic number of the  $K^{\text{th}}$  nucleus. Then, due to the significant weight of the nuclei versus the electrons, the Hamiltonian may be separated between the electronic and the nuclear parts according to the Born-Oppenheimer approximation [BO27]:

$$\mathcal{H} = \mathcal{H}_e + \mathcal{H}_N, \quad \Psi = \Psi_e \Psi_N, \quad E = E_e + E_N. \quad (2.8)$$

Since electrons satisfy the Pauli-exclusion principle, the Slater determinant may be used to represent the electronic wavefunction in terms of the mono-electronic wave functions with no spin:

$$\Psi_e = \frac{1}{\sqrt{N!}} \begin{vmatrix} \Psi_1(\vec{r}_1) & \Psi_2(\vec{r}_1) & \cdots & \Psi_n(\vec{r}_1) \\ \Psi_1(\vec{r}_2) & \Psi_2(\vec{r}_2) & \cdots & \Psi_n(\vec{r}_2) \\ \vdots & \vdots & \ddots & \vdots \\ \Psi_1(\vec{r}_n) & \Psi_2(\vec{r}_n) & \cdots & \Psi_n(\vec{r}_n) \end{vmatrix} \equiv |\Psi_1 \ \Psi_2 \ \cdots \ \Psi_n|. \quad (2.9)$$

The electronic Hamiltonian then separates to:

$$\mathcal{H}_e \Psi_i = E_i \Psi_i, \quad i = 1, 2, \dots, n. \quad (2.10)$$

To represent each of the molecular orbitals, the Linear Combination of Atomic Orbitals (LCAO) approach may be used to further decompose:

$$\Psi_i = \sum_{k=1}^K c_{ki} \varphi_k, \quad i = 1, 2, \dots, n, \quad (2.11)$$

where  $K$  is usually a small integer. The  $i^{\text{th}}$  electron energies are found by inserting such a representation into its separated Schrödinger equation, multiplying by another atomic orbital, and integrating. We obtain an infinite system of linear equations, whose generalized eigenvalues are the eigenvalues of the  $i^{\text{th}}$  electron:

$$\begin{bmatrix} \langle \varphi_1 | \mathcal{H}_e | \varphi_1 \rangle & \langle \varphi_1 | \mathcal{H}_e | \varphi_2 \rangle & \cdots \\ \langle \varphi_2 | \mathcal{H}_e | \varphi_1 \rangle & \langle \varphi_2 | \mathcal{H}_e | \varphi_2 \rangle & \cdots \\ \vdots & \vdots & \ddots \end{bmatrix} \begin{bmatrix} c_{1i} \\ c_{2i} \\ \vdots \end{bmatrix} = E_i \begin{bmatrix} \langle \varphi_1 | \varphi_1 \rangle & \langle \varphi_1 | \varphi_2 \rangle & \cdots \\ \langle \varphi_2 | \varphi_1 \rangle & \langle \varphi_2 | \varphi_2 \rangle & \cdots \\ \vdots & \vdots & \ddots \end{bmatrix}. \quad (2.12)$$

With the condition  $\sum_{k=1}^{\infty} c_{ki} = 1$  and the normalization of the wavefunctions, then the energies can be represented as expected values of the Hamiltonian:

$$E_i = \langle \Psi_i | \mathcal{H}_e | \Psi_i \rangle. \quad (2.13)$$

This infinite system of equations is solved by truncation, and better approximations are obtained with more terms. Therefore, the total electronic energy

may be obtained by summation:

$$\begin{aligned}
E_e = & -\frac{1}{2} \sum_{i=1}^n \langle \Psi_i | \Delta_i | \Psi_i \rangle && \text{Kinetic} \\
& - \sum_{i=1}^n \sum_{K=1}^N \left\langle \Psi_i \left| \frac{Z_K}{r_{iK}} \right| \Psi_i \right\rangle && \text{Nuclear Attraction} \\
& + \sum_{i=1}^n \sum_{j>i}^n \left\langle \Psi_i \Psi_j \left| \frac{1}{r_{ij}} \right| \Psi_i \Psi_j \right\rangle && \text{Electron Repulsion} \\
& - \sum_{i=1}^n \sum_{j>i}^n \left\langle \Psi_i \Psi_j \left| \frac{1}{r_{ij}} \right| \Psi_j \Psi_i \right\rangle && \text{Exchange.}
\end{aligned} \tag{2.14}$$

A question that has been pursued in depth has been: which basis  $\varphi$  to use for the atomic orbitals? Before we introduce some of the historical choices, we require some general definitions and properties of special functions.

## 2.B General definitions and properties

### 2.B.1 Factorials

The factorial function is defined for all  $n \in \mathbb{N}_0$  as [AS65]:

$$n! = n \times (n - 1) \times \cdots \times 1, \quad 0! = 1. \tag{2.15}$$

Several generalizations of this simple concept exist. One such generalization is the double factorial function, defined for all  $n \in \mathbb{N}_0$  as [AS65]:

$$n!! = n \times (n - 2) \times \cdots \times 1, \quad 0!! = 1. \tag{2.16}$$

Another such generalization is the Gamma function which is defined for all  $z \in \mathbb{C}$  as [AS65]:

$$\Gamma(z) = \int_0^\infty x^{z-1} e^{-x} dx, \quad (2.17)$$

and satisfies the property  $\Gamma(z+1) = z\Gamma(z)$ . The Pochhammer symbol is then defined by [AS65]:

$$(x)_n = \frac{\Gamma(x+n)}{\Gamma(x)}. \quad (2.18)$$

## 2.B.2 Spherical harmonics

Consider the Laplacian  $\Delta_{\theta,\varphi}$  on the surface of the unit sphere:

$$\Delta_{\theta,\varphi} = \frac{1}{\sin \theta} \frac{\partial}{\partial \theta} \left( \sin \theta \frac{\partial}{\partial \theta} \right) + \frac{1}{\sin^2 \theta} \frac{\partial^2}{\partial \varphi^2}. \quad (2.19)$$

For  $l \in \mathbb{N}$  and  $|m| \leq l$ , the surface spherical harmonics are the eigenfunctions of the differential equation:

$$\Delta_{\theta,\varphi} Y_l^m(\theta, \varphi) + l(l+1)Y_l^m(\theta, \varphi) = 0. \quad (2.20)$$

With the Condon-Shortley phase convention [CS51], they have the form:

$$Y_l^m(\theta, \varphi) = i^{m+|m|} \sqrt{\frac{(2l+1)(l-|m|)!}{4\pi(l+|m|)!}} P_l^{|m|}(\cos \theta) e^{im\varphi}, \quad (2.21)$$

where the associated Legendre polynomials are:

$$P_l^m(x) = \frac{(-1)^m}{2^l l!} (1-x^2)^{m/2} \frac{d^{l+m}}{dx^{l+m}} (x^2-1)^l. \quad (2.22)$$

The spherical harmonics are the orthonormal basis over the unit sphere as well:

$$\int_{\varphi=0}^{2\pi} \int_{\theta=0}^{\pi} [Y_{l'}^{m'}(\theta, \varphi)]^* Y_l^m(\theta, \varphi) \sin \theta \, d\theta \, d\varphi = \delta_{l'l} \delta_{m'm}, \quad (2.23)$$

where  $\delta_{ij}$  is the Kronecker delta function and the  $*$  denotes complex conjugation. The Gaunt coefficients are defined as [Gau29, WS82, Xu96]:

$$\langle l_1 m_1 | l_2 m_2 | l_3 m_3 \rangle = \int_{\varphi=0}^{2\pi} \int_{\theta=0}^{\pi} [Y_{l_1}^{m_1}(\theta, \varphi)]^* Y_{l_2}^{m_2}(\theta, \varphi) Y_{l_3}^{m_3}(\theta, \varphi) \sin \theta \, d\theta \, d\varphi. \quad (2.24)$$

These coefficients linearize the product of two spherical harmonics:

$$[Y_{l_1}^{m_1}(\theta, \varphi)]^* Y_{l_2}^{m_2}(\theta, \varphi) = \sum_{l=l_{\min}, 2}^{l_1+l_2} \langle l_2 m_2 | l_1 m_1 | l m_2 - m_1 \rangle Y_l^{m_2 - m_1}(\theta, \varphi), \quad (2.25)$$

where the subscript  $l = l_{\min}, 2$  in the summation implies that the summation index  $l$  runs in steps of 2 from  $l_{\min}$  to  $l_1 + l_2$ , and the constant  $l_{\min}$  is given by:

$$l_{\min} = \begin{cases} \max(|l_1 - l_2|, |m_2 - m_1|), & \text{if } l_1 + l_2 + \max(|l_1 - l_2|, |m_2 - m_1|) \text{ is even} \\ \max(|l_1 - l_2|, |m_2 - m_1|) + 1, & \text{if } l_1 + l_2 + \max(|l_1 - l_2|, |m_2 - m_1|) \text{ is odd.} \end{cases} \quad (2.26)$$

The Rayleigh expansion of the plane wavefunctions is given by [Wei78]:

$$e^{\pm i \vec{p} \cdot \vec{r}} = \sum_{l=0}^{\infty} \sum_{m=-l}^l 4\pi (\pm i)^l j_l(pr) [Y_l^m(\theta_{\vec{p}}, \phi_{\vec{p}})]^* Y_l^m(\theta_{\vec{r}}, \phi_{\vec{r}}), \quad (2.27)$$

Solid harmonics are given by:

$$\mathcal{Y}_l^m(\vec{r}) = r^l Y_l^m(\theta_{\vec{r}}, \phi_{\vec{r}}). \quad (2.28)$$

The addition theorem of solid harmonics states that:

$$\mathcal{Y}_l^m(\vec{r} + \vec{r}') = 4\pi(2l + 1)!! \sum_{l'=0}^l \sum_{m'=-l'}^{l'} \frac{\langle lm|l'm'|l-l' m-m'\rangle \mathcal{Y}_{l'}^{m'}(\vec{r}) \mathcal{Y}_{l-l'}^{m-m'}(\vec{r}')}{(2l'+1)!![2(l-l')+1]!!}. \quad (2.29)$$

### 2.B.3 Bessel functions

Bessel functions of the first kind are solutions of the differential equation [Wat66]:

$$z^2 \frac{d^2}{dz^2} J_\nu(z) + z \frac{d}{dz} J_\nu(z) + (z^2 - \nu^2) J_\nu(z) = 0, \quad (2.30)$$

where  $z \in \mathbb{C}$  is the argument and  $\nu \in \mathbb{C}$  is the order. Bessel functions satisfy the following properties:

$$J_\nu(z) = \sum_{k=0}^{\infty} \frac{(-1)^k}{k! \Gamma(k + \nu + 1)} \left(\frac{z}{2}\right)^{2k+\nu}, \quad (2.31)$$

$$J_{\nu+1}(z) = \frac{2\nu}{z} J_\nu(z) - J_{\nu-1}(z), \quad (2.32)$$

$$J_{\nu-m}(z) = z^{m-\nu} \left(\frac{d}{z dz}\right)^m (z^\nu J_\nu(z)), \quad (2.33)$$

for some  $m \in \mathbb{N}_0$ . Spherical Bessel functions of the first kind of order  $n \in \mathbb{N}_0$  are defined as [Wat66]:

$$j_n(z) = \sqrt{\frac{\pi}{2z}} J_{n+1/2}(z). \quad (2.34)$$

They satisfy the following properties:

$$j_n(z) = (-z)^n \left( \frac{d}{z dz} \right)^n \left( \frac{\sin(z)}{z} \right), \quad (2.35)$$

$$j_{n+1}(z) = \frac{2n+1}{z} j_n(z) - j_{n-1}(z). \quad (2.36)$$

Bessel functions of the second kind are the second linearly independent solution to the differential equation (2.30). For  $\nu \in \mathbb{C} \setminus \mathbb{Z}$ :

$$Y_\nu(z) = \frac{J_\nu(z) \cos(\nu\pi) - J_{-\nu}(z)}{\sin(\nu\pi)}, \quad (2.37)$$

and for  $n \in \mathbb{Z}$ , they are defined by the limit:

$$Y_n(z) = \lim_{\nu \rightarrow n} Y_\nu(z). \quad (2.38)$$

Together, they allow for a second formulation of two linearly independent solutions to the differential equation (2.30), known as Hankel functions:

$$H_\nu^{(1)}(z) = J_\nu(z) + iY_\nu(z), \quad (2.39)$$

$$H_\nu^{(2)}(z) = J_\nu(z) - iY_\nu(z). \quad (2.40)$$

Modified Bessel functions of the second kind are solutions of the differential equation [Wat66]:

$$z^2 \frac{d^2}{dz^2} K_\nu(z) + z \frac{d}{dz} K_\nu(z) - (z^2 + \nu^2) K_\nu(z) = 0, \quad (2.41)$$

where  $z \in \mathbb{C}$  is the argument and  $\nu \in \mathbb{C}$  is the order. Modified Bessel functions

satisfy the following properties:

$$\frac{K_\nu(xz)}{z^\nu} = \frac{1}{2} \int_0^\infty \frac{e^{-\frac{x}{2}(t+\frac{z^2}{t})}}{t^{\nu+1}} dt, \quad (2.42)$$

$$K_{\nu+1}(z) = \frac{2\nu}{z} K_\nu(z) + K_{\nu-1}(z), \quad (2.43)$$

$$K_{\nu\mp m}(z) = (-1)^m z^{m\mp\nu} \left( \frac{d}{z dz} \right)^m (z^{\pm\nu} K_\nu(z)), \quad (2.44)$$

for some  $m \in \mathbb{N}_0$ . Reduced Bessel functions of order  $\nu \in \mathbb{C}$  are defined as [SF75, FS78]:

$$\hat{k}_\nu(z) = \sqrt{\frac{2}{\pi}} z^\nu K_\nu(z). \quad (2.45)$$

For half-integral orders, the reduced Bessel functions can be represented by an exponential multiplied by a terminating confluent hypergeometric function:

$$\hat{k}_{n+\frac{1}{2}}(z) = 2^n (1/2)_n e^{-z} {}_1F_1(-n; -2n; 2z). \quad (2.46)$$

They also satisfy the three-term recurrence relation:

$$\hat{k}_{\nu+1}(z) = 2\nu \hat{k}_\nu(z) + z^2 \hat{k}_{\nu-1}(z). \quad (2.47)$$

## 2.B.4 The Fourier transform

For Lebesgue integrable functions  $f : \mathbb{R}^3 \rightarrow \mathbb{C}$ , the symmetric Fourier transform pair is given by [AW95]:

$$\bar{f}(\vec{p}) = \frac{1}{(2\pi)^{3/2}} \int_{\vec{r}} e^{-i\vec{p}\cdot\vec{r}} f(\vec{r}) d^3\vec{r}, \quad (2.48)$$

$$f(\vec{r}) = \frac{1}{(2\pi)^{3/2}} \int_{\vec{p}} e^{i\vec{r}\cdot\vec{p}} \bar{f}(\vec{p}) d^3\vec{p}. \quad (2.49)$$

The Fourier integral representation of the Coulomb operator is given by [GS64]:

$$\frac{1}{|\vec{r} - \vec{s}|} = \frac{1}{2\pi^2} \int_{\vec{p}} \frac{e^{-i\vec{p}\cdot(\vec{r}-\vec{s})}}{p^2} d^3\vec{p}, \quad (2.50)$$

and is interpreted as the limit of the Yukawa potential  $\frac{e^{-\epsilon r}}{r}$  with vanishing screen  $\epsilon \rightarrow 0$ . Using the expression (2.50), the expectation of a Coulomb operator can then be expressed as:

$$\begin{aligned} & \left\langle f(\vec{r}) \left| \frac{1}{|\vec{r} - \vec{s}|} \right| g(\vec{r} - \vec{R}) \right\rangle_{\vec{r}} \\ &= \frac{1}{2\pi^2} \left\langle f(\vec{r}) \left| \int_{\vec{x}} \frac{e^{-i\vec{x}\cdot(\vec{r}-\vec{s})}}{x^2} d^3\vec{x} \right| g(\vec{r} - \vec{R}) \right\rangle_{\vec{r}}, \end{aligned} \quad (2.51)$$

$$= \frac{1}{2\pi^2} \int_{\vec{x}} \frac{e^{i\vec{x}\cdot\vec{s}}}{x^2} \left\langle f(\vec{r}) \left| e^{-i\vec{x}\cdot\vec{r}} \right| g(\vec{r} - \vec{R}) \right\rangle_{\vec{r}} d^3\vec{x}. \quad (2.52)$$

The Fourier transform allows for the expression:

$$\begin{aligned} & \int f^*(\vec{r}) e^{-i\vec{x}\cdot\vec{r}} g(\vec{r} - \vec{R}) d^3\vec{r}, \\ &= \frac{1}{(2\pi)^{3/2}} \int \int \bar{f}^*(\vec{p}) e^{-i\vec{p}\cdot\vec{r} - i\vec{x}\cdot\vec{r}} g(\vec{r} - \vec{R}) d^3\vec{p} d^3\vec{r}, \end{aligned} \quad (2.53)$$

$$= e^{-i\vec{x}\cdot\vec{R}} \int \bar{f}^*(\vec{p}) e^{-i\vec{p}\cdot\vec{R}} \left[ \frac{1}{(2\pi)^{3/2}} \int e^{-i(\vec{p}+\vec{x})\cdot(\vec{r}-\vec{R})} g(\vec{r} - \vec{R}) d^3\vec{r} \right] d^3\vec{p}, \quad (2.54)$$

$$= e^{-i\vec{x}\cdot\vec{R}} \int \bar{f}^*(\vec{p}) e^{-i\vec{p}\cdot\vec{R}} \bar{g}(\vec{p} + \vec{x}) d^3\vec{p}, \quad (2.55)$$

leading to the identity:

$$\left\langle f(\vec{r}) \left| e^{-i\vec{x}\cdot\vec{r}} \right| g(\vec{r} - \vec{R}) \right\rangle_{\vec{r}} = e^{-i\vec{x}\cdot\vec{R}} \left\langle \bar{f}(\vec{p}) \left| e^{-i\vec{p}\cdot\vec{R}} \right| \bar{g}(\vec{p} + \vec{x}) \right\rangle_{\vec{p}}. \quad (2.56)$$

## 2.C Choosing a basis

### 2.C.1 Slater-type functions

The first basis functions that are used are the Slater-type functions [Sla30, Sla32]:

$$\chi_{n,l}^m(\zeta, \vec{r}) = \zeta^{-n+1} [(2\zeta)^{2n+1} / (2n)!]^{1/2} r^{n-1} e^{-\zeta r} Y_l^m(\theta_{\vec{r}}, \phi_{\vec{r}}), \quad (2.57)$$

where  $n, l$ , and  $m$  are the quantum numbers such that  $n = 1, 2, \dots$ ,  $l = 0, 1, \dots, n-1$ , and  $m = -l, -l+1, \dots, l-1, l$  and  $\zeta$  is the effective charge of the nucleus after electron screening. The case of non-integral principle quantum number has also been considered. The orbitals satisfy the Kato [Kat57] conditions of 1) having a cusp at the coordinate centre and 2) exponential decay at infinity.

### 2.C.2 Gaussian functions

As a computational simplification, the second basis functions that are used are the spherical Gaussian-type functions introduced by [Boy50]:

$$G_{n,l}^m(\zeta, \vec{r}) = N_{n,l}(\zeta) R_{n,l}(\zeta, r) e^{-\zeta r^2} Y_l^m(\theta_{\vec{r}}, \varphi_{\vec{r}}), \quad (2.58)$$

where  $n, l$ , and  $m$  are the quantum numbers,  $\zeta$  is the effective charge of the nucleus after electron screening,  $N_{n,l}(\zeta)$  is a normalization constant, and  $R_{n,l}(\zeta, r)$  is a radial polynomial. While violating the Kato conditions, these functions have still provided for a very fast way to calculate the electronic energies because the integration of Gaussian orbitals is very fast. Cartesian Gaussian-type

functions have also been explored.

### 2.C.3 $B$ functions

The  $B$  functions of Filter and Steinborn [SF75, FS78] are introduced as an alternative to Gaussian-type functions that satisfy the Kato conditions. They are defined as:

$$B_{n,l}^m(\zeta, \vec{r}) = \frac{(\zeta r)^l}{2^{n+l}(n+l)!} \hat{k}_{n-\frac{1}{2}}(\zeta r) Y_l^m(\theta_{\vec{r}}, \phi_{\vec{r}}), \quad (2.59)$$

where  $n, l$ , and  $m$  are the quantum numbers and  $\zeta$  is the effective charge of the nucleus after electron screening.

Given the terminating confluent hypergeometric series representation of the reduced Bessel function, these functions are simply linear combinations of Slater-type functions, with the inverse relationship defined by [FS78]:

$$\chi_{n,l}^m(\zeta, \vec{r}) = \sum_{p=\lceil \frac{n-l}{2} \rceil}^{n-l} \frac{(-1)^{n-l-p} (n-l)! 2^{l+p} (l+p)!}{(2p-n-l)! (2n-2l-2p)!!} B_{p,l}^m(\zeta, \vec{r}). \quad (2.60)$$

The  $B$  functions have a relatively compact Fourier transform [Wen82, WS83]:

$$\bar{B}_{n,l}^m(\zeta, \vec{p}) = \sqrt{\frac{2}{\pi}} \frac{\zeta^{2n+l-1}}{(\zeta^2 + p^2)^{n+l+1}} \mathcal{Y}_l^m(-i\vec{p}). \quad (2.61)$$

Using this compact Fourier transform, the Fourier transform of a two-center density also has a compact analytical expression. From (2.56) and (2.61), we

may derive:

$$\begin{aligned} & \left\langle B_{n_1, l_1}^{m_1}(\zeta_1, \vec{r}) \left| e^{-i\vec{x}\cdot\vec{r}} \right| B_{n_2, l_2}^{m_2}(\zeta_2, \vec{r} - \vec{R}) \right\rangle_{\vec{r}} \\ &= e^{-i\vec{x}\cdot\vec{R}} \left\langle \bar{B}_{n_1, l_1}^{m_1}(\zeta_1, \vec{p}) \left| e^{-i\vec{p}\cdot\vec{R}} \right| \bar{B}_{n_2, l_2}^{m_2}(\zeta_2, \vec{p} + \vec{x}) \right\rangle_{\vec{p}} \end{aligned} \quad (2.62)$$

$$= \frac{2}{\pi} \zeta_1^{2n_1+l_1-1} \zeta_2^{2n_2+l_2-1} e^{-i\vec{x}\cdot\vec{R}} \int \frac{[\mathcal{Y}_{l_1}^{m_1}(-i\vec{p})]^* e^{-i\vec{p}\cdot\vec{R}} \mathcal{Y}_{l_2}^{m_2}(-i(\vec{p} + \vec{x}))}{(\zeta_1^2 + p^2)^{n_1+l_1+1} (\zeta_2^2 + |\vec{p} + \vec{x}|^2)^{n_2+l_2+1}} d^3\vec{p}. \quad (2.63)$$

Using the addition theorem for the solid harmonics (2.29) and the Feynman identity [Fey49]:

$$\frac{1}{ab} = \int_0^1 \frac{ds}{(a + (b-a)s)^2}, \quad (2.64)$$

the expression (2.63) can be expanded as follows, which is fundamental in the  $B$  function approach and appears in every subsequent derivation. Letting:

$$\gamma(s, x)^2 = (1-s)\zeta_1^2 + s\zeta_2^2 + s(1-s)x^2, \quad (2.65)$$

$$\Delta l = (l'_1 + l'_2 - l)/2, \quad (2.66)$$

then we obtain:

$$\begin{aligned}
& \left\langle B_{n_1, l_1}^{m_1}(\zeta_1, \vec{r}) \left| e^{-i\vec{x}\cdot\vec{r}} \right| B_{n_2, l_2}^{m_2}(\zeta_2, \vec{r} - \vec{R}) \right\rangle_{\vec{r}} \\
&= (-1)^{l_2} (4\pi)^3 (2l_1 + 1)!! (2l_2 + 1)!! \\
&\times \frac{(n_1 + l_1 + n_2 + l_2 + 1)!}{(n_1 + l_1)!(n_2 + l_2)!} \zeta_1^{2n_1 + l_1 - 1} \zeta_2^{2n_2 + l_2 - 1} \\
&\times \sum_{l'_1=0}^{l_1} \sum_{m=-l'_1}^{l'_1} \frac{\langle l_1 m_1 | l'_1 m'_1 | l_1 - l'_1 m_1 - m'_1 \rangle}{(2l'_1 + 1)!! [2(l_1 - l'_1) + 1]!!} [\mathcal{Y}_{l_1 - l'_1}^{m_1 - m'_1}(\vec{x})]^* (-1)^{l_1 - l'_1} \\
&\times \sum_{l'_2=0}^{l_2} \sum_{m=-l'_2}^{l'_2} \frac{\langle l_2 m_2 | l'_2 m'_2 | l_2 - l'_2 m_2 - m'_2 \rangle}{(2l'_2 + 1)!! [2(l_2 - l'_2) + 1]!!} \mathcal{Y}_{l_2 - l'_2}^{m_2 - m'_2}(\vec{x}) \\
&\times \sum_{l=\min, 2}^{l'_1 + l'_2} i^{l + l_1 + l_2} (-1)^{(l'_1 + l'_2 + l)/2} \langle l'_2 m'_2 | l'_1 m'_1 | l m'_2 - m'_1 \rangle \\
&\times \int_0^1 e^{-i(1-s)\vec{x}\cdot\vec{R}} \frac{s^{n_2 + l_2 + l_1 - l'_1} (1-s)^{n_1 + l_1 + l_2 - l'_2}}{[\gamma(s, x)]^{2(n_1 + l_1 + n_2 + l_2) - (l'_1 + l'_2) + 1}} \\
&\times \left[ \sum_{j=0}^{\Delta l} (-1)^j \binom{\Delta l}{j} B_{n_1 + l_1 + n_2 + l_2 - l - j + 1, l}^{m'_2 - m'_1}(\gamma(s, x), \vec{R}) \right] ds. \tag{2.67}
\end{aligned}$$

## 2.D The molecular integrals

Consider the picture in figure 2.1 describing the arrangement of two electrons and four atomic centres. In evaluating the integrals of above, they appear in three general forms: overlap integrals, nuclear attraction integrals, and repulsion integrals.

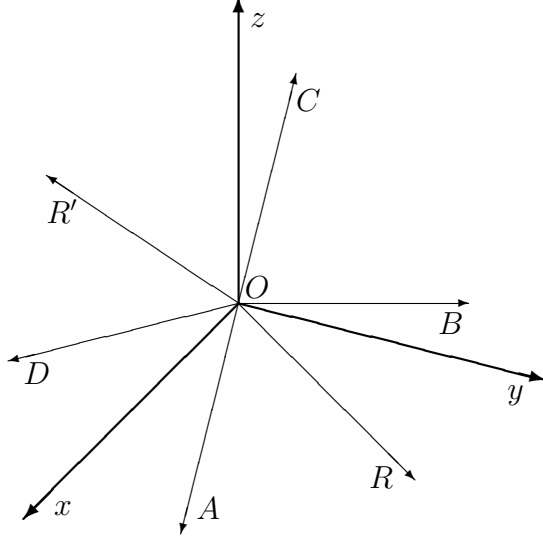


Figure 2.1: The configuration of four atoms located at  $A$ ,  $B$ ,  $C$ , and  $D$ , and two electrons located at  $R$  and  $R'$ .

### 2.D.1 Overlap integrals

Overlap integrals, which are building blocks in the expectation of the kinetic energy, take the form:

$$\mathcal{S}_{n_1 l_1 m_1}^{n_2 l_2 m_2} = \left\langle B_{n_1, l_1}^{m_1}(\zeta_1, \vec{R} - \vec{O}A) \middle| B_{n_2, l_2}^{m_2}(\zeta_2, \vec{R} - \vec{O}B) \right\rangle \quad (2.68)$$

$$= \int [B_{n_1, l_1}^{m_1}(\zeta_1, \vec{r})]^* B_{n_2, l_2}^{m_2}(\zeta_2, \vec{r} - \vec{R}_2) d^3 \vec{r}, \quad (2.69)$$

after the substitutions  $\vec{r} = \vec{R} - \vec{O}A$  and  $\vec{R}_2 = \vec{A}B$ . This integral can be obtained by formally letting  $\vec{x} \rightarrow \vec{0}$  in (2.67). An intermediate expression is then obtained and the integral over  $s$  can be expanded for an analytical

expression as follows. Letting  $\Delta l = (l_1 + l_2 - l)/2$ , we obtain:

$$\begin{aligned}
\mathcal{S}_{n_1 l_1 m_1}^{n_2 l_2 m_2} &= (-1)^{l_2} 4\pi \zeta_1^{2n_1+l_1-1} \zeta_2^{2n_2+l_2-1} \sum_{l=l_{\min}, 2}^{l_1+l_2} \langle l_2 m_2 | l_1 m_1 | l m_2 - m_1 \rangle \\
&\sum_{j=0}^{\Delta l} (-1)^j \binom{\Delta l}{j} \left\{ \frac{(-1)^{n_2+l_2+1}}{(n_2+l_2)!} \frac{\zeta_1^{l_1+l_2+1}}{(\zeta_1^2 - \zeta_2^2)^{n_1+l_1+n_2+l_2+1}} \right. \\
&\sum_{i=0}^{n_1+l_1} \frac{(n_1+l_1+n_2+l_2-i)!}{(n_1+l_1-i)!} \left( \frac{\zeta_1^2 - \zeta_2^2}{\zeta_1^2} \right)^i B_{i-j,l}^{m_2-m_1}(\zeta_1, \vec{R}_2) \\
&+ \frac{(-1)^{n_1+l_1+1}}{(n_1+l_1)!} \frac{\zeta_2^{l_1+l_2+1}}{(\zeta_2^2 - \zeta_1^2)^{n_1+l_1+n_2+l_2+1}} \\
&\left. \sum_{i=0}^{n_2+l_2} \frac{(n_1+l_1+n_2+l_2-i)!}{(n_2+l_2-i)!} \left( \frac{\zeta_2^2 - \zeta_1^2}{\zeta_2^2} \right)^i B_{i-j-l,l}^{m_2-m_1}(\zeta_2, \vec{R}_2) \right\}. \quad (2.70)
\end{aligned}$$

## 2.D.2 Nuclear attraction integrals

Three-center nuclear attraction integrals take the form:

$$\mathcal{I}_{n_1 l_1 m_1}^{n_2 l_2 m_2} = \left\langle B_{n_1, l_1}^{m_1}(\zeta_1, \vec{R} - \vec{O}A) \left| \frac{1}{|\vec{R} - \vec{O}C|} \right| B_{n_2, l_2}^{m_2}(\zeta_2, \vec{R} - \vec{O}B) \right\rangle \quad (2.71)$$

$$= \int [B_{n_1, l_1}^{m_1}(\zeta_1, \vec{r})]^* \frac{1}{|\vec{r} - \vec{R}_1|} B_{n_2, l_2}^{m_2}(\zeta_2, \vec{r} - \vec{R}_2) d^3 \vec{r}, \quad (2.72)$$

after the substitutions  $\vec{r} = \vec{R} - \vec{O}A$ ,  $\vec{R}_1 = \vec{A}C$ , and  $\vec{R}_2 = \vec{A}B$ . By using the Fourier Coulomb representation (2.50), we obtain:

$$\mathcal{I}_{n_1 l_1 m_1}^{n_2 l_2 m_2} = \frac{1}{2\pi^2} \int \frac{e^{i\vec{x} \cdot \vec{R}_1}}{x^2} \left\langle B_{n_1, l_1}^{m_1}(\zeta_1, \vec{r}) \left| e^{-i\vec{x} \cdot \vec{r}} \right| B_{n_2, l_2}^{m_2}(\zeta_2, \vec{r} - \vec{R}_2) \right\rangle_{\vec{r}} d^3 \vec{x}. \quad (2.73)$$

Then, upon inserting the result (2.67) and upon using the Rayleigh plane wavefunction expansion (2.27), we obtain:

$$\begin{aligned}
\mathcal{I}_{n_1 l_1 m_1}^{n_2 l_2 m_2} &= \frac{8(4\pi)^2 (-1)^{l_1+l_2} (2l_1+1)!! (2l_2+1)!! (n_1+l_1+n_2+l_2+1)! \zeta_1^{2n_1+l_1-1} \zeta_2^{2n_2+l_2-1}}{(n_1+l_1)!(n_2+l_2)!} \\
&\times \sum_{l'_1=0}^{l_1} \sum_{m'_1=-l'_1}^{l'_1} i^{l_1+l'_1} \frac{\langle l_1 m_1 | l'_1 m'_1 | l_1 - l'_1 m_1 - m'_1 \rangle}{(2l'_1+1)!! [2(l_1-l'_1)+1]!!} \\
&\times \sum_{l'_2=0}^{l_2} \sum_{m'_2=-l'_2}^{l'_2} i^{l_2+l'_2} (-1)^{l'_2} \frac{\langle l_2 m_2 | l'_2 m'_2 | l_2 - l'_2 m_2 - m'_2 \rangle}{(2l'_2+1)!! [2(l_2-l'_2)+1]!!} \\
&\times \sum_{l=\min(l'_1, 2)}^{l'_2+l'_1} \langle l'_2 m'_2 | l'_1 m'_1 | l m'_2 - m'_1 \rangle R_2^l Y_l^{m'_2-m'_1}(\theta_{\vec{R}_2}, \varphi_{\vec{R}_2}) \\
&\times \sum_{\lambda=l'_{\min}, 2}^{l_2-l'_2+l_1-l'_1} (-i)^\lambda \langle l_2 - l'_2 m_2 - m'_2 | l_1 - l'_1 m_1 - m'_1 | \lambda \mu \rangle \\
&\times \sum_{j=0}^{\Delta l} \binom{\Delta l}{j} \frac{(-1)^j}{2^{n_1+n_2+l_1+l_2-j+1} (n_1+n_2+l_1+l_2-j+1)!} \\
&\times \int_{s=0}^1 s^{n_2+l_2+l_1-l'_1} (1-s)^{n_1+l_1+l_2-l'_2} Y_\lambda^\mu(\theta_{\vec{v}}, \varphi_{\vec{v}}) \\
&\times \left[ \int_{x=0}^{+\infty} x^{n_x} \frac{\hat{k}_\nu [R_2 \gamma_{12}(s, x)]}{[\gamma_{12}(s, x)]^{n_\gamma}} j_\lambda(\nu x) dx \right] ds, \tag{2.74}
\end{aligned}$$

where:

$$\vec{v} = (1-s)\vec{R}_2 - \vec{R}_1$$

$$n_\gamma = 2(n_1+l_1+n_2+l_2) - (l'_1+l'_2) - l + 1$$

$$[\gamma_{12}(s, x)]^2 = (1-s)\zeta_1^2 + s\zeta_2^2 + s(1-s)x^2$$

$$\nu = n_1 + n_2 + l_1 + l_2 - l - j + \frac{1}{2}$$

$$\mu = (m_2 - m'_2) - (m_1 - m'_1)$$

$$n_x = l_1 - l'_1 + l_2 - l'_2$$

$$\Delta l = (l'_1 + l'_2 - l)/2.$$

### 2.D.3 Four-center two-electron integrals

Four-center two-electron integrals take the form:

$$\mathcal{J}_{n_1 l_1 m_1, n_3 l_3 m_3}^{n_2 l_2 m_2, n_4 l_4 m_4} = \left\langle B_{n_1, l_1}^{m_1}(\zeta_1, \vec{R} - \vec{O}A) B_{n_3, l_3}^{m_3}(\zeta_3, \vec{R}' - \vec{O}C) \left| \frac{1}{|\vec{R} - \vec{R}'|} \right| \right. \\ \left. B_{n_2, l_2}^{m_2}(\zeta_2, \vec{R} - \vec{O}B) B_{n_4, l_4}^{m_4}(\zeta_4, \vec{R}' - \vec{O}D) \right\rangle \quad (2.75)$$

$$= \iint \left[ B_{n_1, l_1}^{m_1}(\zeta_1, \vec{r} - \vec{R}_1) \right]^* \left[ B_{n_3, l_3}^{m_3}(\zeta_3, \vec{r}' - \vec{R}_3) \right]^* \frac{1}{|\vec{r} - \vec{r}'|} \\ B_{n_2, l_2}^{m_2}(\zeta_2, \vec{r} - \vec{R}_2) B_{n_4, l_4}^{m_4}(\zeta_4, \vec{r}' - \vec{R}_4) d^3 \vec{r} d^3 \vec{r}', \quad (2.76)$$

after letting  $\vec{r} = \vec{R}$ ,  $\vec{r}' = \vec{R}'$ ,  $\vec{R}_1 = \vec{O}A$ ,  $\vec{R}_2 = \vec{O}B$ ,  $\vec{R}_3 = \vec{O}C$ , and  $\vec{R}_4 = \vec{O}D$ .

By using the Fourier Coulomb representation (2.50), we obtain:

$$\mathcal{J}_{n_1 l_1 m_1, n_3 l_3 m_3}^{n_2 l_2 m_2, n_4 l_4 m_4} = \frac{1}{2\pi^2} \int \frac{e^{-i\vec{x} \cdot (\vec{R}_1 - \vec{R}_4)}}{x^2} d^3 \vec{x} \\ \times \left\langle B_{n_1, l_1}^{m_1}(\zeta_1, \vec{r} - \vec{R}_1) \left| e^{-i\vec{x} \cdot (\vec{r} - \vec{R}_1)} \right| B_{n_2, l_2}^{m_2}(\zeta_2, \vec{r} - \vec{R}_2) \right\rangle_{\vec{r}} \\ \times \left\langle B_{n_4, l_4}^{m_4}(\zeta_4, \vec{r}' - \vec{R}_4) \left| e^{-i\vec{x} \cdot (\vec{r}' - \vec{R}_4)} \right| B_{n_3, l_3}^{m_3}(\zeta_3, \vec{r}' - \vec{R}_3) \right\rangle_{\vec{r}'}^*, \quad (2.77)$$

$$= \frac{1}{2\pi^2} \int \frac{e^{-i\vec{x} \cdot \vec{R}_{14}}}{x^2} \left\langle B_{n_1, l_1}^{m_1}(\zeta_1, \vec{r}) \left| e^{-i\vec{x} \cdot \vec{r}} \right| B_{n_2, l_2}^{m_2}(\zeta_2, \vec{r} - \vec{R}_{21}) \right\rangle_{\vec{r}} \\ \times \left\langle B_{n_4, l_4}^{m_4}(\zeta_4, \vec{r}') \left| e^{-i\vec{x} \cdot \vec{r}'} \right| B_{n_3, l_3}^{m_3}(\zeta_3, \vec{r}' - \vec{R}_{34}) \right\rangle_{\vec{r}'}^* d^3 \vec{x}, \quad (2.78)$$

where  $\vec{R}_{ij} = \vec{R}_i - \vec{R}_j$ . Then, upon using the result (2.67) twice and upon using the Rayleigh plane wavefunction expansion (2.27), we obtain:

$$\begin{aligned}
\mathcal{J}_{n_1 l_1 m_1, n_3 l_3 m_3}^{n_2 l_2 m_2, n_4 l_4 m_4} &= \frac{8(4\pi)^5 (2l_1 + 1)!! (2l_2 + 1)!! (n_1 + l_1 + n_2 + l_2 + 1)! \zeta_1^{2n_1 + l_1 - 1} \zeta_2^{2n_2 + l_2 - 1}}{(n_1 + l_1)! (n_2 + l_2)!} \\
&\times \frac{(-1)^{l_1 + l_2} (2l_3 + 1)!! (2l_4 + 1)!! (n_3 + l_3 + n_4 + l_4 + 1)! \zeta_3^{2n_3 + l_3 - 1} \zeta_4^{2n_4 + l_4 - 1}}{(n_3 + l_3)! (n_4 + l_4)!} \\
&\times \sum_{l'_1=0}^{l_1} \sum_{m'_1=\mu_{11}}^{\mu_{12}} i^{l_1 + l'_1} \frac{\langle l_1 m_1 | l'_1 m'_1 | l_1 - l'_1 m_1 - m'_1 \rangle}{(2l'_1 + 1)!! [2(l_1 - l'_1) + 1]!!} \\
&\times \sum_{l'_2=0}^{l_2} \sum_{m'_2=\mu_{21}}^{\mu_{22}} i^{l_2 + l'_2} (-1)^{l'_2} \frac{\langle l_2 m_2 | l'_2 m'_2 | l_2 - l'_2 m_2 - m'_2 \rangle}{(2l'_2 + 1)!! [2(l_2 - l'_2) + 1]!!} \\
&\times \sum_{l'_3=0}^{l_3} \sum_{m'_3=\mu_{31}}^{\mu_{32}} i^{l_3 + l'_3} \frac{\langle l_3 m_3 | l'_3 m'_3 | l_3 - l'_3 m_3 - m'_3 \rangle}{(2l'_3 + 1)!! [2(l_3 - l'_3) + 1]!!} \\
&\times \sum_{l'_4=0}^{l_4} \sum_{m'_4=\mu_{41}}^{\mu_{42}} i^{l_4 + l'_4} (-1)^{l'_4} \frac{\langle l_4 m_4 | l'_4 m'_4 | l_4 - l'_4 m_4 - m'_4 \rangle}{(2l'_4 + 1)!! [2(l_4 - l'_4) + 1]!!} \\
&\times \sum_{l=l_1, \min, 2}^{l'_1 + l'_2} \langle l'_2 m'_2 | l'_1 m'_1 | l m'_2 - m'_1 \rangle R_{21}^l Y_l^{m'_2 - m'_1} (\theta_{\vec{R}_{21}}, \varphi_{\vec{R}_{21}}) \\
&\times \sum_{l_{12}=l'_{1, \min}, 2}^{l_1 - l'_1 + l_2 - l'_2} \langle l_2 - l'_2 m_2 - m'_2 | l_1 - l'_1 m_1 - m'_1 | l_{12} m_{21} \rangle \\
&\times \sum_{l'=l_{2, \min}, 2}^{l'_3 + l'_4} \langle l'_4 m'_4 | l'_3 m'_3 | l' m'_4 - m'_3 \rangle R_{34}^{l'} Y_{l'}^{m'_4 - m'_3} (\theta_{\vec{R}_{34}}, \varphi_{\vec{R}_{34}}) \\
&\times \sum_{l_{34}=l'_{2, \min}, 2}^{l_3 - l'_3 + l_4 - l'_4} \langle l_4 - l'_4 m_4 - m'_4 | l_3 - l'_3 m_3 - m'_3 | l_{34} m_{43} \rangle \\
&\times \sum_{\lambda=l''_{\min}, 2}^{l_{12} + l_{34}} (-i)^\lambda \langle l_{12} m_{21} | l_{34} m_{43} | \lambda \mu \rangle \\
&\times \sum_{j_{12}=0}^{\Delta l_{12}} \sum_{j_{34}=0}^{\Delta l_{34}} \binom{\Delta l_{12}}{j_{12}} \binom{\Delta l_{34}}{j_{34}} \frac{(-1)^{j_{12} + j_{34}}}{2^{\nu_1 + \nu_2 + l + l' + 1} (\nu_1 + \frac{1}{2} + l)! (\nu_2 + \frac{1}{2} + l')!} \\
&\times \int_{s=0}^1 \frac{s^{n_2 + l_2 + l_1} (1-s)^{n_1 + l_1 + l_2}}{s^{l'_1} (1-s)^{l'_2}} \int_{t=0}^1 \frac{t^{n_4 + l_4 + l_3} (1-t)^{n_3 + l_3 + l_4}}{t^{l'_3} (1-t)^{l'_4}} Y_\lambda^{m_2 - \mu} (\theta_{\vec{v}}, \varphi_{\vec{v}}) \\
&\times \left[ \int_{x=0}^{+\infty} x^{n_x} \frac{\hat{k}_{\nu_1} [R_{21} \gamma_{12}(s, x)]}{[\gamma_{12}(s, x)]^{n_{\gamma_{12}}}} \frac{\hat{k}_{\nu_2} [R_{34} \gamma_{34}(t, x)]}{[\gamma_{34}(t, x)]^{n_{\gamma_{34}}}} j_\lambda(vx) dx \right] dt ds,
\end{aligned}$$

where:

$$\mu_{1i} = \max(-l'_i, m_i - l_i + l'_i)$$

$$\mu_{2i} = \min(l_i, m_i + l_i - l'_i)$$

$$\mu = (m_2 - m'_2) - (m_1 - m'_1) + (m_4 - m'_4) - (m_3 - m'_3)$$

$$n_{\gamma_{12}} = 2(n_1 + l_1 + n_2 + l_2) - (l'_1 + l'_2) - l + 1$$

$$n_{\gamma_{34}} = 2(n_3 + l_3 + n_4 + l_4) - (l'_3 + l'_4) - l' + 1$$

$$[\gamma_{ij}(\alpha, x)]^2 = (1 - \alpha)\zeta_i^2 + \alpha\zeta_j^2 + \alpha(1 - \alpha)x^2$$

$$n_x = l_1 - l'_1 + l_2 - l'_2 + l_3 - l'_3 + l_4 - l'_4$$

$$\nu_1 = n_1 + n_2 + l_1 + l_2 - l - j_{12} + \frac{1}{2}$$

$$\nu_2 = n_3 + n_4 + l_3 + l_4 - l' - j_{34} + \frac{1}{2}$$

$$\vec{v} = (1 - s)\vec{R}_{21} + (1 - t)\vec{R}_{43} - \vec{R}_{41}$$

$$\Delta l_{12} = \frac{l'_1 + l'_2 - l}{2}, \quad \Delta l_{34} = \frac{l'_3 + l'_4 - l'}{2}$$

$$m_{ij} = m_i - m'_i - (m_j - m'_j).$$

Several different simplifications of this expression exist when some of the centres are equal: when  $A = B$ , they are called three-center repulsion integrals; when  $A = B = C$ , they are called two-center hybrid integrals; when  $A = C$ , they are called three-center exchange integrals; and when  $A = C$  and  $B = D$  they are called two-center exchange integrals.

## Chapter 3

# A Comparative Study of Numerical Steepest Descent, Extrapolation, and Sequence Transformation Methods in Computing Semi-Infinite Integrals

### 3.A Introduction

Semi-infinite integrals play a major role in science and engineering problems and their accurate, efficient and reliable numerical evaluation is a topic of interest in applied mathematics. Through iterative, Fourier, discretization or expansion methods, semi-infinite integrals may arise when solving the simplest to the most complicated problems. Some of the most famous examples in the extant literature are: the Twisted Tail, proposed first among ten chal-

lenging projects in numerical computation in the book *The SIAM 100-digit Challenge* [BLWW04]; Sommerfeld-type integrals [Som49, MM97], which arise in problems involving antennas or scatterers embedded in planar multilayered media; and, molecular integrals [Dal54, HM67, Huz67, GWS86, HS93, SHE<sup>+</sup>00], whose computation involves millions of semi-infinite integrals with spherical Bessel kernels and highly pathological envelope functions. From a numerical perspective, this challenging problem has also been pursued extensively [Saf01, Saf02, BS03a, BS03b].

Traditional numerical methods have failed to provide accurate approximations to highly pathological semi-infinite integrals, and consequently more powerful techniques have been developed. In the steepest descent methods [Deb09, Erd56, BH75, BO78, Zwi92], a deformation of the path of integration is used to transform oscillations or irregular exponential behaviour into linear exponential decay. In the numerical steepest descent, on the deformed contour, a Gauss-Laguerre-type quadrature is used to approximate the integral. The Levin- and Filon-type [Lev82, Fil28] methods construct quadrature rules for oscillatory integrals. Specifically for highly oscillatory integrals, the steepest descent methods have seen a revival in recent years [IN04, IN05, Olv06, HV06, CHN09, HO09]. In extrapolation methods [LS81, GA67, BRZ91, GW92, Sid03], through numerical quadrature or otherwise, one computes a sequence of approximations to the infinite-range integral and uses analytical properties of the integrand to then extrapolate on this sequence to obtain an approximation for the integral. In sequence transformations [Sha55, Wyn56, Lev73, Bre78, Wen89, Sid03], one derives the asymptotic series expansion of the integral and, whether convergent or divergent, one applies transformations to the asymptotic series hoping to approximate the limit or antilimit of the series with a

relatively small number of terms.

Numerical comparisons of sequence transformations [SF79, SF82, Mic98, PNM10] have been performed several times by just as many researchers. The context of the summation of a series by sequence transformation is different than the context of the evaluation of semi-infinite integrals by series representation. Therefore, in the comparisons, the most often used examples are convergent or divergent Taylor series, power series, perturbation series, Fourier series, or others. In the context of semi-infinite integrals, their series representations are found first, through integration by parts, Laplace's method or otherwise, and then the sequence transformations are applied to these series.

In this work: we present the three most prominent general methods for computing semi-infinite integrals; we apply these methods to four semi-infinite integrals with multiple parameters; and, we compare and contrast their performance on the bases of accuracy, reliability, and efficiency. This study is motivated by the three-way divergence we perceive in the scientific community regarding the numerical evaluation of semi-infinite integrals using the three aforementioned methods. This comparison should serve to challenge the scientific community to consider all of the aforementioned methods (and others) in the numerical evaluation of semi-infinite integrals before jumping to premature conclusions.

## 3.B Description of the methods

### 3.B.1 Steepest descent methods

We begin by describing the method of numerical steepest descent for the ideal case of an analytic integrand with no stationary points, as is used in the numerical examples in this work. To be consistent, we follow closely the developments in [IN04, IN05, Olv06, HV06, CHN09, HO09].

Let:

$$I(\omega) = \int_a^b f(x)e^{i\omega g(x)} dx, \quad (3.1)$$

where  $\omega > 0$  and  $f(x)$  and  $g(x)$  are smooth functions. We note that  $e^{i\omega g(x)}$  does not oscillate along a path in the complex plane where the real part of  $g(x)$  is fixed. Therefore, by deforming the integration contour such that paths leaving the endpoints  $a$  and  $b$  are non-oscillatory, these paths may lead to a better starting point for a numerical quadrature of the integral (3.1). In general, there may be many paths leaving the endpoints which are steepest, but for an integrand with no stationary points, there is usually only one such path. Naturally, then, the path of steepest descent is of interest. Let  $h_a(p)$  and  $h_b(p)$ , where  $p \in [0, P]$ , be parameterizations for the paths of steepest descent leaving the endpoints  $a$  and  $b$ , respectively. Then, the path  $h_a(p)$ , is found as the solution to:

$$g(h_a(p)) = g(a) + ip, \quad (3.2)$$

and the path  $h_b(p)$  is found similarly. If the inverse of  $g$  exists, then  $h_a(p) = g^{-1}(g(a) + ip)$ ,  $p \in [0, P]$ . With these paths of steepest descent, we have an

approximation for (3.1):

$$\begin{aligned}
& \int_a^b f(x)e^{i\omega g(x)} dx \\
& \approx e^{i\omega g(a)} \int_0^P f(h_a(p))h'_a(p)e^{-\omega p} dp \\
& - e^{i\omega g(b)} \int_0^P f(h_b(p))h'_b(p)e^{-\omega p} dp, \quad \text{as } \omega \rightarrow \infty. \tag{3.3}
\end{aligned}$$

It is important to note that the integrands on the right-hand side do not oscillate and actually decay exponentially as  $p$  or  $\omega$  tend to infinity. In the following theorem, the parameterization is extended to  $p \in [0, \infty)$  and, with a few additional conditions on  $f(x)$  and  $g(x)$ , is able to provide an asymptotic bound on the parameterized integrands.

**Theorem 3.1** (Huybrechs and Vandewalle [HV06]): *Assume that the functions  $f$  and  $g$  are analytic in a simply connected and sufficiently (infinitely) large complex region  $D$  containing the interval  $[a, b]$ , and that the inverse of  $g$  exists on  $D$ . If the following conditions hold in  $D$ :*

$$\exists m \in \mathbb{N} : |f(z)| = \mathcal{O}(|z|^m), \tag{3.4}$$

$$\exists \omega_0 \in \mathbb{R} : |g^{-1}(z)| = \mathcal{O}(e^{\omega_0|z|}), \quad \text{as } |z| \rightarrow \infty, \tag{3.5}$$

*then there exists a function  $F$  such that:*

$$\int_a^b f(x)e^{i\omega g(x)} dx = F(a) - F(b), \quad \forall \omega > (m+1)\omega_0, \tag{3.6}$$

where  $F$  is of the form:

$$F(a) := \int_{\Gamma_a} f(x) e^{i\omega g(x)} dx, \quad (3.7)$$

with  $\Gamma_a$  a path that starts at  $a$ . A parameterization  $h_a(p)$ ,  $p \in [0, \infty)$ , for  $\Gamma_a$  exists such that the integrand of (3.7) is  $\mathcal{O}(e^{-\omega p})$  as  $p \rightarrow \infty$ .

**Remark:** In the numerical examples of this work, the integrals are semi-infinite such that  $b = \infty$ . In these cases,  $F(b) = 0$ , and there is only one integral with path of steepest descent in the transformation.

In the cases where  $b = \infty$  and  $F(b) = 0$ , the parameterization gives:

$$I(\omega) = e^{i\omega g(a)} \int_0^\infty f(h_a(p)) h'_a(p) e^{-\omega p} dp, \quad (3.8)$$

From equation (3.8) and from Theorem 3.1 it is evident that the most noticeable characteristic is that the integrand decays exponentially in the limit as  $p \rightarrow \infty$ . Indeed, from the theory of orthogonal polynomials, Laguerre polynomials provide the ideal nodes for integration by Gaussian quadrature. The method of directly coupling Gaussian quadrature with transformed integrals along paths of steepest descent is known as the method of *numerical steepest descent* [HV06].

Let  $\lambda_\nu^n$  and  $\tau_\nu^n$  be the weights and nodes of the  $n$ -point Gauss-Laguerre quadrature rule [Gau04]. Let also  $\mathbb{P}$  be the space of real polynomials and  $\mathbb{P}_d \subset \mathbb{P}$  the space of polynomials of degree  $\leq d$ . The  $n$ -point Gauss-Laguerre quadrature rule can be written in the form:

$$\int_0^\infty f(x) e^{-x} dx = \sum_{\nu=1}^n \lambda_\nu^n f(\tau_\nu^n) + R_n[f], \quad R_n[\mathbb{P}_{2n-1}] = 0, \quad (3.9)$$

Furthermore, if  $f \in \mathcal{C}^{2n}[0, \infty)$ , then the remainder  $R_n[f]$  can be expressed as:

$$R_n[f] = \frac{(n!)^2}{(2n)!} f^{(2n)}(\tau), \quad \tau \in (0, \infty). \quad (3.10)$$

Indeed, fundamentally based on this error bound, the following theorem describes the asymptotics of a quadrature rule for the integral  $I(\omega)$ .

**Theorem 3.2** (Huybrechs and Vandewalle [HV06]): *Assume functions  $f$  and  $g$  satisfy the conditions of Theorem 3.1. Let  $I(\omega)$  in (3.8) be approximated by the  $n$ -point Gauss-Laguerre quadrature rule as in (3.9). Then, the quadrature error  $R_n[f]$  behaves asymptotically as  $\mathcal{O}(\omega^{-2n-1})$  as  $\omega \rightarrow \infty$ .*

This result demonstrates that with high oscillations, the quadrature error decays, which is in complete opposition to the straightforward application of a quadrature rule to an oscillatory integral. In some of the numerical examples in this work, where there are no oscillations and only exponential decay, the parameterization before the application of Gauss-Laguerre quadrature is not necessary.

We denote by  $GL_n$  the  $n$ -point Gauss-Laguerre quadrature rule computed by the sum on the right-hand side in (3.9).

### 3.B.2 Extrapolation methods

Consider the semi-infinite integral:

$$I[f] = \int_0^\infty f(x) dx, \quad (3.11)$$

and the monotonically increasing sequence of points  $\{x_l\}_{l=0}^\infty$  where  $x_{-1} = 0$  and  $x_{l-1} < x_l \forall l \in \mathbb{N}_0$ . Then the *integration then summation technique* of [Lon56]

gives:

$$I_n[f] = \sum_{l=0}^n \int_{x_{l-1}}^{x_l} f(x) dx, \quad \text{and} \quad \lim_{n \rightarrow \infty} I_n[f] = I[f]. \quad (3.12)$$

Any series derived from the sequence  $\{x_l\}_{l=0}^{\infty}$  described above has an equivalence with any other such series in that they all lead to a similar linear system of equations; however, this is certainly not so numerically. Now if the intervals  $[x_{l-1}, x_l]$  are sufficiently small, a Gauss-Legendre quadrature routine may be used to obtain approximations to the sub-integrals.

Supposing that a sufficiently high order quadrature is employed to achieve machine precision evaluation of the sub-integrals, then an extrapolation method ideally uses a small number of the terms  $I_n[f]$  to obtain numerical approximations to  $I[f]$ . This approximation requires knowledge of the form of the difference between  $I[f]$  and  $I_n[f]$ :

$$I[f] - I_n[f] \sim R_n[f], \quad \text{as} \quad n \rightarrow \infty. \quad (3.13)$$

The ultimate goal of any extrapolation method, then, is to have the best possible understanding of the remainder  $R_n[f]$  because with this known, the sum  $I_n[f] + R_n[f]$  serves as an extrapolated approximation to the semi-infinite integral  $I[f]$ . Below, we present the most comprehensive investigation into the remainder  $R_n[f]$ . Figure 3.1 shows a graphical depiction of this extrapolation process.

We begin by defining the class of functions we denote  $\mathbf{A}^{(\gamma)}$  by

**Definition** (Levin and Sidi [LS81]): A function  $\alpha(x)$  defined for all large  $x > 0$

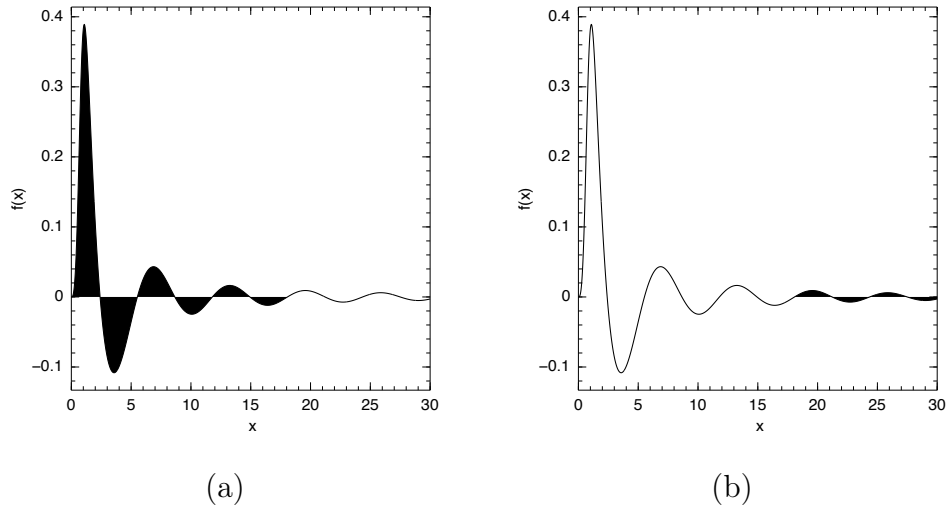


Figure 3.1: (a) shows the portion evaluated by quadrature and (b) shows the portion evaluated by extrapolation.

is in the set  $\mathbf{A}^{(\gamma)}$  if it has a Poincaré-type asymptotic expansion of the form:

$$\alpha(x) \sim \sum_{i=0}^{\infty} \alpha_i x^{\gamma-i}, \quad \text{as } x \rightarrow \infty. \quad (3.14)$$

If, in addition,  $\alpha_0 \neq 0$  in (3.14), then  $\alpha(x)$  is said to belong to  $\mathbf{A}^{(\gamma)}$  strictly. Here  $\gamma$  is complex in general.

Building on this class of functions, we also have the

**Definition** (Levin and Sidi [LS81]): A function  $f(x)$  belongs to the set  $\mathbf{B}^{(m)}$  if it satisfies a linear homogeneous differential equation of order  $m$  of the form:

$$f(x) = \sum_{k=1}^m p_k(x) f^{(k)}(x), \quad (3.15)$$

where  $p_k \in \mathbf{A}^{(k)}$ ,  $k = 1, \dots, m$ , such that  $p_k \in \mathbf{A}^{(i_k)}$  strictly for some integer  $i_k \leq k$ .

Let  $F(x) = \int_0^x f(t) dt$  and let  $I[f]$  be the semi-infinite integral. Now, for

functions in  $\mathbf{B}^{(m)}$ , we can construct the asymptotic remainder of the difference between  $I[f]$  and  $F(x)$ . We have the

**Theorem 3.3** (Levin and Sidi [LS81]): *Let  $f(x) \in \mathbf{B}^{(m)}$  and let  $f(x)$  be integrable on  $[0, \infty)$  (i.e.  $\int_0^\infty f(t) dt < \infty$ ). If for  $1 \leq i \leq m$  and  $i \leq k \leq m$ , we have  $\lim_{x \rightarrow \infty} p_k^{(i-1)}(x) f^{(k-i)}(x) = 0$  and for every integer  $l \geq -1$ , we have  $\sum_{k=1}^m l(l-1) \cdots (l-k+1) p_{k,0} \neq 1$  where  $p_{k,0} = \lim_{x \rightarrow \infty} x^{-k} p_k(x)$  for  $1 \leq k \leq m$ , then we have:*

$$I[f] - F(x) \sim \sum_{k=0}^{m-1} x^{\sigma_k} f^{(k)}(x) g_k(x), \quad \text{as } x \rightarrow \infty, \quad (3.16)$$

for some integers  $\sigma_k \leq k + 1$ , and for some functions  $g_k \in \mathbf{A}^{(0)}$ ,  $k = 0, \dots, m - 1$ .

We let the functions  $g_k(x)$  in (3.16) be given by their most general form:

$$g_k(x) = \sum_{i=0}^{\infty} \frac{\beta_{k,i}}{x^i}, \quad (3.17)$$

with the unknowns  $\beta_{k,i}$ . To solve for the unknowns  $\beta_{k,i}$ , we must set up and solve a system of linear equations. To produce this system of linear equations, few methods have been conceived. The first is called the  $D_n^{(m)}$  transformation. For this transformation, the asymptotic expansions  $g_k(x)$  are truncated after  $n$  terms and a set of interpolating points  $x_j, x_{j+1}, \dots, x_{j+mn}$  is used to solve for the unknowns. The approximation  $D_n^{(m)}$  to  $I[f]$  is given as the solution of the system of  $mn + 1$  linear equations [Sid03]:

$$D_n^{(m,j)} = F(x_l) + \sum_{k=0}^{m-1} x_l^{\sigma_k} f^{(k)}(x_l) \sum_{i=0}^{n-1} \frac{\bar{\beta}_{k,i}}{x_l^i}, \quad j \leq l \leq j + mn. \quad (3.18)$$

In the above system (3.18),  $\sigma_k = \min(s_k, k + 1)$  where  $s_k$  is the largest of the integers  $s$  such that  $\lim_{x \rightarrow \infty} x^s f^{(k)}(x) = 0$  holds,  $k = 0, 1, \dots, m - 1$ . Also,  $D_n^{(m,j)}$  and  $\bar{\beta}_{k,i}$  are the respective set of  $mn + 1$  unknowns. The monotonically increasing sequence  $\{x_l\}$  satisfies  $0 < x_0 < x_1 < \dots$  and  $\lim_{l \rightarrow \infty} x_l = \infty$ .

For the illustrated examples in this work, the integrands are either in  $\mathbf{B}^{(1)}$  or in  $\mathbf{B}^{(2)}$ . When the integrand is in  $\mathbf{B}^{(1)}$ , we apply the  $D^{(1)}$  transformation; however, when the integrand is in  $\mathbf{B}^{(2)}$ , there is often a choice of the sequence  $\{x_l\}$  such that  $f(x_l) = 0 \forall l \in \mathbb{N}_0$ . As an example, the function  $f(x) = \frac{\sin(x)}{x} \in \mathbf{B}^{(2)}$  and for the sequence  $x_l = (l+1)\pi$ ,  $f(x_l) = 0$ . This choice for the sequence  $\{x_l\}_{l=0}^{\infty}$  serves to reduce the effective asymptotic remainder by eliminating the block associated with  $x^{\sigma_0} f(x)$ . The approximation  $\bar{D}_n^{(m)}$  to  $I[f]$  is given as the solution of the system of  $(m - 1)n + 1$  linear equations [Sid80a]:

$$\bar{D}_n^{(m,j)} = F(x_l) + \sum_{k=1}^{m-1} x_l^{\sigma_k} f^{(k)}(x_l) \sum_{i=0}^{n-1} \frac{\bar{\beta}_{k,i}}{x_l^i}, \quad j \leq l \leq j + (m - 1)n. \quad (3.19)$$

To solve the system of linear equations (3.18) for  $D^{(1)}$  or (3.19) for  $\bar{D}^{(2)}$  iteratively, we employ the  $W$ -algorithm, whose rules are [Sid82]:

1. For  $j = 0, 1, \dots$ , set:

$$M_0^{(j)} = \frac{F(x_j)}{\varphi(x_j)}, \quad \text{and} \quad N_0^{(j)} = \frac{1}{\varphi(x_j)}. \quad (3.20)$$

2. For  $j = 0, 1, \dots$ , and  $n = 1, 2, \dots$ , compute  $M_n^{(j)}$  and  $N_n^{(j)}$  recursively from:

$$Q_n^{(j)} = \frac{Q_{n-1}^{(j+1)} - Q_{n-1}^{(j)}}{x_{j+n}^{-1} - x_j^{-1}}, \quad (3.21)$$

where the  $Q_n^{(j)}$  stand for either  $M_n^{(j)}$  or  $N_n^{(j)}$ .

3. For all  $j$  and  $n$ , set:

$$W_n^{(j)} = \frac{M_n^{(j)}}{N_n^{(j)}}. \quad (3.22)$$

For the  $D^{(1)}$  transformation,  $\varphi(x_j) = x_j^{\sigma_0} f(x_j)$ , whereas for the  $\bar{D}^{(2)}$  transformation,  $\varphi(x_j) = x_j^{\sigma_1} f'(x_j)$ .

It has been shown that limited power stems from fixing  $n$  while increasing  $j$  [Wen89, Wen01, Sid03], whereas substantial extrapolation can be achieved by fixing  $j$  while increasing  $n$ . In this work, we will only be considering the approximations  $D_n^{(1,0)}$  or  $\bar{D}_n^{(2,0)}$  for  $n = 0, 1, 2, \dots$ , as this sequence seems to have the best balance between accuracy and efficiency. We denote by  $W D_n^{(0)}$  the  $D_n^{(1,0)}$  transformation computed by the algorithm (3.20)–(3.22), and we denote by  $W \bar{D}_n^{(0)}$  the  $\bar{D}_n^{(2,0)}$  transformation computed by the algorithm (3.20)–(3.22).

### 3.B.3 Sequence transformations

Suppose a parameter is identified in the integrand and through integration by parts, Laplace's method, by identification with a special function, or otherwise [BH75, BO78] an asymptotic expansion in terms of functions of this parameter can be constructed:

$$I(\lambda) = \int_0^\infty f(x; \lambda) dx \quad (3.23)$$

$$\sim \sum_{k=0}^{\infty} a_k(\lambda) \quad \text{where } a_k(\lambda) = o(a_{k-1}(\lambda)) \quad \text{as } \lambda \rightarrow \infty. \quad (3.24)$$

Quite often, though asymptotic, the above series diverges. However, often the information contained in a few of the leading terms  $a_k(\lambda)$  may be extracted in such a way to provide approximations to the value of the function corre-

sponding to the general asymptotic series (3.24). Consider, more generally, the sequence  $\{a_k\}_{k=0}^{\infty}$  and the partial sums  $S_n[a] = \sum_{k=0}^n a_k$ . Then, with the limit (antilimit when the sum diverges)  $S[a]$ , there is a remainder:

$$S[a] - S_n[a] \sim R_n[a], \quad \text{as } n \rightarrow \infty. \quad (3.25)$$

As with extrapolation methods, the ultimate goal is to have the best possible understanding of the remainder  $R_n[a]$ , because with this known, the sum  $S_n[a] + R_n[a]$  serves as an approximation to the limit (antilimit)  $S[a]$ . Below, we present the most comprehensive investigation into the remainder  $R_n[a]$ .

We begin by recalling the class of functions  $\mathbf{A}^{(\gamma)}$  by definition 3.B.2. Building on this class of functions, we also have the

**Definition** (Levin and Sidi [LS81]): A sequence  $\{a_n\}$  belongs to the set  $\mathbf{b}^{(m)}$  if it satisfies a linear homogeneous difference equation of order  $m$  of the form:

$$a_n = \sum_{k=1}^m p_k(n) \Delta^k a_n, \quad (3.26)$$

where  $p_k \in \mathbf{A}^{(k)}$ ,  $k = 1, \dots, m$ , such that  $p_k \in \mathbf{A}^{(i_k)}$  strictly for some integer  $i_k \leq k$ . Here  $\Delta^0 a_n = a_n$ ,  $\Delta^1 a_n = a_{n+1} - a_n$ , and  $\Delta^k a_n = \Delta(\Delta^{k-1} a_n) = \sum_{i=0}^k (-1)^{k-i} \binom{k}{i} a_{n+i}$ .

For a convergent (divergent) series, let  $S_n[a] = \sum_{k=0}^n a_k$ , be the partial sum of the series and let  $S[a]$  be the limit (antilimit) of the series. Now, for sequences in  $\mathbf{b}^{(m)}$ , we can construct the asymptotic remainder of the difference between  $S[a]$  and  $S_n[a]$ . We have the

**Theorem 3.4** (Levin and Sidi [LS81]): *Let  $\{a_n\} \in \mathbf{b}^{(m)}$  and let  $\sum_{k=0}^{\infty} a_k$  be a*

convergent (divergent) series. If for  $1 \leq i \leq m$  and  $i \leq k \leq m$ , we have  $\lim_{n \rightarrow \infty} (\Delta^{i-1} p_k(n)) (\Delta^{k-i} a_n) = 0$  for convergent series only and for every integer  $l \geq -1$ , we have  $\sum_{k=1}^m l(l-1) \cdots (l-k+1) \bar{p}_k \neq 1$  where  $\bar{p}_k = \lim_{n \rightarrow \infty} n^{-k} p_k(n)$  for  $1 \leq k \leq m$ , then we have:

$$S[a] - S_n[a] \sim \sum_{k=0}^{m-1} n^{\rho_k} (\Delta^k a_n) g_k(n), \quad \text{as } n \rightarrow \infty, \quad (3.27)$$

for some integers  $\rho_k \leq k + 1$ , and for some functions  $g_k \in \mathbf{A}_0^{(0)}$ ,  $k = 0, \dots, m - 1$ .

We let the functions  $g_k(n)$  in (3.27) be given by their most general form:

$$g_k(n) = \sum_{i=0}^{\infty} \frac{\beta_{k,i}}{n^i}, \quad (3.28)$$

with the unknowns  $\beta_{k,i}$ . To solve for the unknowns  $\beta_{k,i}$ , we must set up and solve a system of linear equations. This system is called the  $d_n^{(m)}$  transformation. For this transformation, the asymptotic expansions  $g_k(r)$  are truncated after  $n$  terms and a set of interpolating points  $R_0, R_1, \dots, R_{mn}$  is used to solve for the unknowns. The approximation  $d_n^{(m)}$  to  $S[a]$  is given as the solution of the system of  $mn + 1$  linear equations [Sid03]:

$$d_n^{(m,j)} = S_{R_l}[a] + \sum_{k=0}^{m-1} R_l^{\rho_k} \Delta^k a_{R_l} \sum_{i=0}^{n-1} \frac{\bar{\beta}_{k,i}}{R_l^i}, \quad j \leq l \leq j + mn. \quad (3.29)$$

In the above system (3.29),  $\rho_k = \min(s_k, k + 1)$  where  $s_k$  is the largest of the integers  $s$  such that  $\lim_{n \rightarrow \infty} n^s \Delta^k a_n = 0$  holds,  $k = 0, 1, \dots, m - 1$ , when the sum is convergent. When it is divergent,  $\rho_k = k + 1$ . Also,  $d_n^{(m,j)}$  and  $\bar{\beta}_{k,i}$  are the respective set of  $mn + 1$  unknowns. The monotonically increasing sequence

$\{R_l\}$  satisfies  $0 < R_0 < R_1 < \dots$  and  $\lim_{l \rightarrow \infty} R_l = \infty$ .

In the asymptotic series representations in the illustrated examples of this work, all sequence elements  $a_k \in \mathbf{b}^{(1)}$ . In this case, we employ the  $d^{(1)}$  transformation. For linearly and logarithmically convergent series, both arithmetic progressive sampling (APS) and geometric progressive sampling (GPS) for the  $R_l$  have been used and are successful [Sid03]. However, for divergent series, the slowest possible sampling typically yields the best result. This corresponds to  $R_l = l + 1$ .

The  $d^{(1)}$  transformation with the choice of  $R_l = l + 1$  also corresponds to a different conception of a sequence transformation, one based more closely on numerical evidence for accelerated convergence of a model sequence [Lev73]. It serves our purpose to introduce this and other sequence transformations from this framework. Consider the case where the remainder in (3.25) is given more precisely by:

$$S[a] - S_n[a] \sim \omega_n \sum_{j=0}^{\infty} c_j / (n + \beta)^j, \quad \text{as } n \rightarrow \infty. \quad (3.30)$$

A Levin transformation is designed to be exact for model sequences such that:

$$L_k^{(n)}(\beta) - S_n[a] = \omega_n \sum_{j=0}^{k-1} c_j / (n + \beta)^j. \quad (3.31)$$

Isolating the sum on the right-hand side, we may annihilate the unknowns  $c_j$  one by one because:

$$(n + \beta)^{k-1} \frac{L_k^{(n)}(\beta) - S_n[a]}{\omega_n} = \sum_{j=0}^{k-1} c_j (n + \beta)^{k-j-1}, \quad (3.32)$$

and a  $k^{\text{th}}$  finite difference on  $n$  would eliminate the sum on the right-hand side. Isolating for the approximation to the series:

$$L_k^{(n)}(\beta) = \frac{\Delta^k ((n + \beta)^{k-1} S_n[a]/\omega_n)}{\Delta^k ((n + \beta)^{k-1}/\omega_n)}. \quad (3.33)$$

Expanding the finite differences, the Levin transformation is given as the ratio of two sums:

$$L_k^{(n)}(\beta) = \frac{\sum_{j=0}^k (-1)^j \binom{k}{j} \frac{(n + \beta + j)^{k-1} S_{n+j}[a]}{(n + \beta + k)^{k-1} \omega_{n+j}}}{\sum_{j=0}^k (-1)^j \binom{k}{j} \frac{(n + \beta + j)^{k-1}}{(n + \beta + k)^{k-1} \omega_{n+j}}}, \quad (3.34)$$

where the common factor  $(n + \beta + k)^{k-1}$  is added to improve stability in the computation by regulating the magnitude of each of the terms.

A recursive algorithm introduced in [FFS83] is able to compute the Levin transformation (3.34) and is summarized by:

1. For  $n = 0, 1, \dots$ , set:

$$P_0^{(n)} = \frac{S_n[a]}{\omega_n} \quad \text{and} \quad Q_0^{(n)} = \frac{1}{\omega_n}. \quad (3.35)$$

2. For  $n = 0, 1, \dots$ , and  $k = 1, 2, \dots$ , compute  $P_k^{(n)}$  and  $Q_k^{(n)}$  recursively from:

$$U_k^{(n)} = U_{k-1}^{(n+1)} - \frac{\beta + n}{\beta + n + k} \left( \frac{\beta + n + k - 1}{\beta + n + k} \right)^{k-2} U_{k-1}^{(n)}, \quad (3.36)$$

where the  $U_k^{(n)}$  stand for either  $P_k^{(n)}$  or  $Q_k^{(n)}$ .

3. For all  $n$  and  $k$ , set:

$$L_k^{(n)} = \frac{P_k^{(n)}}{Q_k^{(n)}}. \quad (3.37)$$

For the different cases of linear convergence, logarithmic convergence, series with alternating terms and divergence, specific remainder estimates have been suggested. For brevity, the remainder estimate we choose is  $\omega_n = a_n$ , which gives rise to the  $t_k^{(n)}(\beta)$  transformation<sup>1</sup>. It has been shown that limited power stems from fixing  $k$  while increasing  $n$  [Wen89, Wen01, Sid03], whereas substantial extrapolation can be achieved by fixing  $n$  while increasing  $k$ . In this work, we will only be considering the approximations  $t_n^{(0)}(\beta)$  for  $n = 0, 1, 2, \dots$ , as this sequence seems to have the best balance between accuracy and efficiency. In all cases, the numerical parameter  $\beta = 1$ . We denote by  $LT_n^{(0)}$  the  $t_n^{(0)}(1)$  transformation computed by the algorithm (3.35)–(3.37).

### 3.C The integrals

In this section, we detail the four integrals we study to compare and contrast the three general methods above. We begin by giving the integral and its representation as a special function. Then, we transform the integral to an integral with exponential decay for the method of steepest descent, if necessary. For the extrapolation method, we discuss the order of the differential equation satisfied by the integrand, and we give the sequence of extrapolation points  $\{x_l\}_{l=0}^\infty$  to be used. For the sequence transformation, we give the asymptotic

---

<sup>1</sup>Actually, it was shown in [Wen04] that the  $t_k^{(n)}(\beta, S_n[a])$  variants of the Levin-type processes are equivalent to the  $d_k^{(n-1)}(\beta+1, S_{n-1}[a])$  transformation. We refer the interested reader to [Wen89, HW95, Sid03] for more detail on the remainder estimates and their uses; however, as we are comparing significantly different methods (steepest descent, extrapolation and sequence transformations), the choice of remainder estimate does not significantly alter the results.

series of the integral with respect to one or more integral parameters in a limiting direction (i.e. we give the asymptotic series of  $\mathcal{I}_1(\beta)$  as  $\beta \rightarrow \infty$ , for example).

### 3.C.1 The first integral

The first integral is [GR07, §3.352]:

$$\mathcal{I}_1(\beta) = \int_0^\infty \frac{e^{-x}}{x + \beta} dx = -e^\beta \text{Ei}(-\beta). \quad (3.38)$$

In the form (3.38), no substitution is required to apply Gauss-Laguerre quadrature.

The integrand  $f_1(x)$  of (3.38) satisfies a first order homogeneous linear differential equation:

$$f_1(x) = -\frac{x + \beta}{x + \beta + 1} f_1'(x), \quad (3.39)$$

and therefore  $f_1(x) \in \mathbf{B}^{(1)}$ . The extrapolation points we use are  $x_l = (l + 1)(\beta + 1/2)$ .

The integral has the asymptotic expansion [GR07, §8.215]:

$$\mathcal{I}_1(\beta) \sim \frac{1}{\beta} \sum_{k=0}^{\infty} \frac{k!}{(-\beta)^k} \quad \text{as } \beta \rightarrow \infty, \quad (3.40)$$

and the sequence  $\{a_n\}$  satisfies a first order homogeneous linear difference equation:

$$a_n = -\frac{\beta}{\beta + n + 1} \Delta a_n, \quad (3.41)$$

and therefore  $\{a_n\} \in \mathbf{b}^{(1)}$ .

### 3.C.2 The second integral

The second integral is [GR07, §3.697]:

$$\mathcal{I}_2(a, b) = \int_0^\infty \sin\left(\frac{a}{x}\right) \sin(bx) dx = \frac{\pi}{2} \sqrt{\frac{a}{b}} J_1(2\sqrt{ab}). \quad (3.42)$$

By splitting the integration interval with respect to  $x_0 = \sqrt{\frac{a}{b}}$ , the point at which both oscillation frequencies are the same, we obtain the two integrals:

$$\mathcal{I}_2(a, b) = \int_0^{x_0} \sin\left(\frac{a}{x}\right) \sin(bx) dx + \int_{x_0}^\infty \sin\left(\frac{a}{x}\right) \sin(bx) dx \quad (3.43)$$

$$= \int_{x_0^{-1}}^\infty \sin\left(\frac{b}{x}\right) \frac{\sin(ax)}{x^2} dx + \int_{x_0}^\infty \sin\left(\frac{a}{x}\right) \sin(bx) dx. \quad (3.44)$$

To obtain the path of steepest descent, these integrals can be written after the substitutions  $y = ia(x_0^{-1} - x)$  and  $y = ib(x_0 - x)$  respectively, as:

$$\mathcal{I}_2(a, b) = \operatorname{Im} \left\{ \int_{x_0^{-1}}^\infty \sin\left(\frac{b}{y}\right) \frac{e^{ia y}}{y^2} dy \right\} + \operatorname{Im} \left\{ \int_{x_0}^\infty \sin\left(\frac{a}{y}\right) e^{ib y} dy \right\} \quad (3.45)$$

$$= \operatorname{Im} \left\{ \frac{i}{a} \int_0^\infty \sin\left(\frac{b}{x_0^{-1} + iy/a}\right) \frac{e^{ia x_0^{-1} e^{-y}}}{(x_0^{-1} + iy/a)^2} dy \right\} \\ + \operatorname{Im} \left\{ \frac{i}{b} \int_0^\infty \sin\left(\frac{a}{x_0 + iy/b}\right) e^{ib x_0 e^{-y}} dy \right\}. \quad (3.46)$$

The integrand  $f_2(x)$  of (3.42) satisfies a third order homogeneous linear differential equation  $f_2(x) \in \mathbf{B}^{(3)}$ . However, by considering the two integrals in (3.44) instead, one may treat one of the oscillatory sine functions as a function in  $\mathbf{A}^{(-1)}$ . For the first integral in (3.44), the extrapolation points we use are  $x_l = \frac{\pi}{a} \left( \left\lfloor \frac{x_0^{-1}}{\pi} \right\rfloor + l + 1 \right)$ . For the second integral in (3.44), the extrapolation points we use are  $x_l = \frac{\pi}{b} \left( \left\lfloor \frac{x_0}{\pi} \right\rfloor + l + 1 \right)$ . The use of the floor

function  $\lfloor \cdot \rfloor$  guarantees that the process begins at the next zero of the integrand greater than  $x_0^{-1}/a$  or  $x_0/b$ , respectively.

The integral has the asymptotic expansion [GR07, §8.451]:

$$\mathcal{I}_2(a, b) \sim \sqrt{\frac{\pi a}{2b}} \frac{1}{\sqrt{2\sqrt{ab}}} \left\{ \cos(2\sqrt{ab} - 3\pi/4) \sum_{k=0}^{\infty} \frac{(-1)^k}{(16ab)^k} \frac{\Gamma(3/2 + 2k)}{(2k)! \Gamma(3/2 - 2k)} \right. \\ \left. - \frac{\sin(2\sqrt{ab} - 3\pi/4)}{4\sqrt{ab}} \sum_{k=0}^{\infty} \frac{(-1)^k}{(16ab)^k} \frac{\Gamma(5/2 + 2k)}{(2k+1)! \Gamma(1/2 - 2k)} \right\} \quad \text{as } ab \rightarrow \infty. \quad (3.47)$$

The sequences of both series in (3.47) satisfy  $\{a_n\} \in \mathbf{b}^{(1)}$ .

### 3.C.3 The third integral

The third integral is [GR07, §6.631]:

$$\mathcal{I}_3(\mu, \alpha, \beta) = \int_0^{\infty} x^{\mu} e^{-\alpha x^2} K_0(\beta x) dx = \frac{\{\Gamma(\frac{\mu+1}{2})\}^2}{2\alpha^{\mu/2}\beta} \exp\left(\frac{\beta^2}{8\alpha}\right) W_{-\frac{\mu}{2}, 0}\left(\frac{\beta^2}{4\alpha}\right). \quad (3.48)$$

To obtain the path of steepest descent, this integral can be written after the substitution  $y = \alpha x^2 + \beta x$  as:

$$\mathcal{I}_3(\mu, \alpha, \beta) = \int_0^{\infty} \left( \frac{-\beta + \sqrt{\beta^2 + 4\alpha y}}{2\alpha} \right)^{\mu} \exp\left( \frac{-\beta^2 + \beta\sqrt{\beta^2 + 4\alpha y}}{2\alpha} \right) \\ \times K_0\left( \frac{-\beta^2 + \beta\sqrt{\beta^2 + 4\alpha y}}{2\alpha} \right) \frac{e^{-y} dy}{\sqrt{\beta^2 + 4\alpha y}}. \quad (3.49)$$

The integrand  $f_3(x)$  of (3.48) satisfies a second order homogeneous linear differential equation  $f_3(x) \in \mathbf{B}^{(2)}$  given that the Bessel function  $K_0(x) \in \mathbf{B}^{(2)}$ . However, by considering the asymptotic form of the Bessel function [AS65,

§9.7.2]:

$$K_0(x) \sim \sqrt{\frac{\pi}{2x}} e^{-x} \quad \text{as } x \rightarrow \infty, \quad (3.50)$$

the asymptotic form of the integrand  $f_3(x) \in \mathbf{B}^{(1)}$ . We use  $x_l = \frac{-\beta + \sqrt{\beta^2 + 4\alpha(l+1)}}{2\alpha}$  as the extrapolation points.

The integral has the asymptotic expansion [GR07, §9.227]:

$$\mathcal{I}_3(\mu, \alpha, \beta) \sim \frac{\{\Gamma(\frac{\mu+1}{2})\}^2}{2^{1-\mu}\beta^{\mu+1}} \sum_{k=0}^{\infty} \frac{\{(\frac{\mu+1}{2})_k\}^2}{k!} \left(-\frac{4\alpha}{\beta^2}\right)^k \quad \text{as } \frac{\beta^2}{4\alpha} \rightarrow \infty. \quad (3.51)$$

The sequence of the series in (3.51) satisfies  $\{a_n\} \in \mathbf{b}^{(1)}$ .

### 3.C.4 The fourth integral

The fourth integral is [GR07, §6.596 7.]:

$$\mathcal{I}_4(\mu, \nu, \alpha, \beta, \zeta) = \int_0^{\infty} J_{\nu}(\beta x) \frac{K_{\mu}(\alpha\sqrt{x^2 + \zeta^2})}{\sqrt{(x^2 + \zeta^2)^{\mu}}} x^{\nu+1} dx, \quad (3.52)$$

$$= \frac{\beta^{\nu}}{\alpha^{\mu}} \left(\frac{\sqrt{\alpha^2 + \beta^2}}{\zeta}\right)^{\mu-\nu-1} K_{\mu-\nu-1}(\zeta\sqrt{\alpha^2 + \beta^2}). \quad (3.53)$$

To obtain an approximate path of steepest descent, this integral can be written as:

$$\mathcal{I}_4(\mu, \nu, \alpha, \beta, \zeta) = \operatorname{Re} \left\{ \int_0^\infty H_\nu^{(1)}(\beta x) \frac{K_\mu(\alpha \sqrt{x^2 + \zeta^2})}{\sqrt{(x^2 + \zeta^2)^\mu}} x^{\nu+1} dx \right\}, \quad (3.54)$$

$$= \operatorname{Re} \left\{ \left( \frac{\alpha + i\beta}{\alpha^2 + \beta^2} \right)^{\nu+2} \int_0^\infty e^x H_\nu^{(1)} \left( \frac{\alpha\beta + i\beta^2}{\alpha^2 + \beta^2} x \right) \right. \\ \left. \times \frac{K_\mu \left( \alpha \sqrt{\left( \frac{\alpha+i\beta}{\alpha^2+\beta^2} \right)^2 x^2 + \zeta^2} \right)}{\sqrt{\left( \left( \frac{\alpha+i\beta}{\alpha^2+\beta^2} \right)^2 x^2 + \zeta^2 \right)^\mu}} x^{\nu+1} e^{-x} dx \right\}, \quad (3.55)$$

after the substitution  $y = (\alpha - i\beta)x$ . This is the case because with the correct but more complicated parameterization,  $z \sim (\alpha - i\beta)x$  and so the above parameterization is asymptotic to the path of steepest descent.

The integrand  $f_4(x)$  of (3.52) satisfies a fourth order homogeneous linear differential equation  $f_4(x) \in \mathbf{B}^{(4)}$  given that the Bessel functions  $J_\nu(x) \in \mathbf{B}^{(2)}$  and  $K_\mu(x) \in \mathbf{B}^{(2)}$  and their product  $J_\nu(x)K_\mu(x) \in \mathbf{B}^{(4)}$ . However, by considering the asymptotic form of the Bessel functions as in the case for  $\mathcal{I}_3(\mu, \alpha, \beta)$ , the asymptotic form of the integrand  $f_4(x) \in \mathbf{B}^{(2)}$ . Let  $x_{\nu,l}$  denote the  $l^{\text{th}}$  zero of the function  $J_\nu(x)$ , such that  $x_{\nu,0} = 0$ ,  $J_\nu(x_{\nu,l}) = 0$  and  $x_{\nu,l-1} < x_{\nu,l} \forall l \in \mathbb{N}$ . The extrapolation points we use are  $x_l = x_{\nu,l+1}/\beta$ .

The integral has the asymptotic expansion [GR07, 8.451 6.]:

$$\mathcal{I}_4(\mu, \nu, \alpha, \beta, \zeta) \sim \sqrt{\frac{\pi}{2\zeta\sqrt{\alpha^2 + \beta^2}}} \left( \frac{\sqrt{\alpha^2 + \beta^2}}{\zeta} \right)^{\mu-\nu-1} \frac{\beta^\nu e^{-\zeta\sqrt{\alpha^2 + \beta^2}}}{\alpha^\mu} \quad (3.56) \\ \times \sum_{k=0}^{\infty} \frac{1}{(2\zeta\sqrt{\alpha^2 + \beta^2})^k} \frac{\Gamma(\mu - \nu + k - 1/2)}{k! \Gamma(\mu - \nu - k - 1/2)}, \quad \text{as } \zeta\sqrt{\alpha^2 + \beta^2} \rightarrow \infty. \quad (3.57)$$

The sequence elements of the series satisfy  $\{a_n\} \in \mathbf{b}^{(1)}$ .

### 3.D Numerical discussion

In performing the numerical tests of three methods, the computations are performed in complex double precision arithmetic. The FORTRAN codes are compiled with Lahey/Fujitsu LF095 compiler, and the codes are run with an Intel Core 2 Duo 2.0 GHz processor.

In comparing and contrasting the three methods, we attempt to simulate such a computational environment in order to ensure a fair comparison is had. In a large program, for example, the computation of weights and nodes of a Gaussian quadrature are computed once and stored. This is replicated in our test program, as the Gauss-Legendre and the Gauss-Laguerre weights and nodes are not computed every time the steepest descent or extrapolation methods are called.

Tables 3.1, 3.2, 3.3, and 3.4 each show 10 test values of the integrals  $\mathcal{I}_1(\beta)$ ,  $\mathcal{I}_2(a, b)$ ,  $\mathcal{I}_3(\mu, \alpha, \beta)$ , and  $\mathcal{I}_4(\mu, \nu, \alpha, \beta, \zeta)$ , respectively. In these tables,  $GL_n$  denotes the approximation obtained by using the  $n$ -point Gauss-Laguerre quadrature rule on the integral along the contour of steepest descent;  $WD_n^{(1)}$  denotes the approximation obtained by using the  $W$  algorithm for the  $D_n^{(1)}$  transformation on the integral;  $W\bar{D}_n^{(2)}$  denotes the approximation obtained by using the  $W$  algorithm for the  $\bar{D}_n^{(2)}$  transformation on the integral; and,  $LT_n^{(0)}$  denotes the approximation obtained by using the algorithm (3.35)–(3.37) for the  $t_n^{(0)}(1)$  transformation on the asymptotic series representation of the integral.

For the computation of the sub-integrals in the  $D$  and  $\bar{D}$  transformations,

a 32-point Gauss-Legendre quadrature rule is used. The order 32 ensures that for the great majority of the sub-integrals, the computed approximations are accurate to 16 significant digits. A more sophisticated approach where one loops through order-for-order approximations to the sub-integrals or even a Gauss-Kronrod rule [Kro65] would certainly yield the best order  $n$  to be used to achieve 16 significant digits; however, this is seldom the approach chosen in the context of large programs, because these loops significantly increase calculation times.

In tables 3.1–3.4, all the parameters of the integrals are given in the first columns, and the order  $n$  and the relative error of the three methods are listed in the subsequent columns. In the tables:

$$\text{Error}^{\text{Method}_n} = \left| \frac{\text{Method}_n - \mathcal{I}}{\mathcal{I}} \right|, \quad (3.58)$$

represents the relative error of the value obtained from the given Method of order  $n$  with respect to a highly accurate value of the integral  $\mathcal{I}$ . These highly accurate values are computed by using the analytical expressions for the integrals and Maple’s arbitrarily high accuracy to a sufficiently high degree of precision to ensure the accuracy of the integral to 16 significant digits.

An indication of the relative computation time is given directly below each of tables 3.1–3.4. On the timing of the calculations, each integral is computed 1000 times for each method, so that the ratios below the tables are averaged over 1000 calculations. This helps ensure the accuracy of these ratios even when some of the methods are computed very rapidly compared with the CPU’s internal clock.

The three algorithms are stopped when the best approximation is obtained.

For the  $n$ -point Gauss-Laguerre quadrature rule, this stopping criterion is the simplest. If:

$$\left| \frac{GL_n - GL_{n-1}}{GL_{n-1}} \right| < \epsilon, \quad (3.59)$$

then the algorithm returns the value  $GL_n$  as a value which has approximately at least  $-\log_{10}(\epsilon)$  correct digits. The FORTRAN code we used to compute the weights and nodes was accurate to the maximal order  $n = 124$ , and so if the condition (3.59) was not met by the maximal order, then the approximation  $GL_{124}$  was taken as the best one.

For the extrapolation methods  $WD_n^{(1)}$  and  $W\bar{D}_n^{(2)}$  and the sequence transformation  $LT_n^{(0)}$ , an inherent instability in the algorithms exists, described in [Sid10], in finite-precision arithmetic which limits the maximal accuracy obtainable by the methods. To extract the best approximation, heuristic stopping criteria for related extrapolation processes have been proposed in [DS07] and extended in [GSS12]. If:

$$\left| \frac{\text{Method}_n - \text{Method}_{n-1}}{\text{Method}_{n-1}} \right| < \epsilon \quad \text{and if} \quad \left| \frac{\text{Method}_{n-1} - \text{Method}_{n-2}}{\text{Method}_{n-2}} \right| < 100\epsilon, \quad (3.60)$$

or if:

$$\rho_i = \left| \frac{\text{Method}_{n-i} - \text{Method}_{n-i-1}}{\text{Method}_{n-i-1} - \text{Method}_{n-i-2}} \right| > 1, \quad \text{for } i = 0, 1, \dots, k, \quad (3.61)$$

then the algorithm returns the value  $\text{Method}_n$  as a value which has approximately at least  $-\log_{10}(\epsilon)$  correct digits or the best approximation obtained before the algorithmic instability sets in. For the algorithms  $WD_n^{(1)}$ ,  $W\bar{D}_n^{(2)}$  and  $LT_n^{(0)}$ ,  $k = 1$  and therefore two values  $\rho_0$  and  $\rho_1$  are used in the stopping criteria. In all algorithms,  $\epsilon = 10^{-15}$ .

Tables 3.1–3.4 demonstrate that all three methods are successful in obtaining 15 significant digits for some of the test values. However, it is evident that all of the algorithms have a preferred parameter range or direction. For example, in table 3.1, it is evident that all three methods perform best as  $\beta \rightarrow \infty$ , while in table 3.2 the steepest descent and sequence transformation methods perform best as  $ab \rightarrow \infty$ , while the extrapolation method performs best as  $ab \rightarrow 0$ . There is no doubt, however, on which algorithm is the most efficient: in comparing the calculation times listed at the bottom of each table for all 40 test values, there is strong evidence to suggest that the algorithm for  $LT_n^{(0)}$  is the most efficient.

$\beta$	$n$	Error $^{GL_n}$	$n$	Error $^{WD_n^{(1)}}$	$n$	Error $^{LT_n^{(0)}}$
0.03	124	0.87D-03	17	0.22D-12	16	0.32D-01
0.10	124	0.25D-05	17	0.84D-12	17	0.11D-02
0.30	124	0.16D-09	17	0.71D-14	17	0.14D-05
1.00	124	0.13D-13	12	0.56D-15	21	0.18D-07
3.00	34	0.36D-14	8	0.13D-14	20	0.21D-12
4.00	34	0.40D-14	7	0.22D-14	19	0.40D-15
5.00	22	0.65D-15	6	0.31D-14	18	0.16D-15
10.00	15	0.61D-15	3	0.30D-14	16	0.30D-15
30.00	9	0.17D-14	3	0.47D-14	13	0.00D+00
100.00	6	0.18D-15	2	0.21D-14	9	0.18D-15

$\frac{\text{Calculation time using } WD_n^{(1)}}{\text{Calculation time using } GL_n} = 0.49$     and     $\frac{\text{Calculation time using } LT_n^{(0)}}{\text{Calculation time using } GL_n} = 0.075$ .

Table 3.1: Numerical evaluation of  $\mathcal{I}_1(\beta)$ .

### 3.E Refinements of the algorithms

In this section, we describe the best general ways to refine the methods of steepest descent, extrapolation, and sequence transformation for semi-infinite

$a$	$b$	$n$	Error $^{GL_n}$	$n$	Error $^{W\bar{D}_n^{(2)}}$	$n$	Error $^{LT_n^{(0)}}$
1.00	1.00	124	0.19D-09	16	0.86D-15	23	0.29D-08
2.00	1.00	124	0.60D-11	17	0.12D-14	24	0.34D-10
2.00	2.00	124	0.72D-12	17	0.17D-14	24	0.33D-12
3.00	1.00	124	0.12D-11	18	0.27D-15	23	0.10D-11
3.00	2.00	124	0.75D-14	17	0.55D-15	25	0.17D-14
3.00	3.00	117	0.68D-14	17	0.51D-15	18	0.13D-15
10.00	1.00	124	0.29D-14	19	0.16D-14	20	0.44D-15
100.00	1.00	124	0.76D-14	10	0.91D-01	8	0.21D-14
10.00	10.00	124	0.59D-14	7	0.79D-02	8	0.20D-14
100.00	10.00	69	0.20D-14	8	0.26D+01	5	0.16D-14

$\frac{\text{Calculation time using } W\bar{D}_n^{(2)}}{\text{Calculation time using } GL_n} = 0.096$     and     $\frac{\text{Calculation time using } LT_n^{(0)}}{\text{Calculation time using } GL_n} = 0.011$ .

Table 3.2: Numerical evaluation of  $\mathcal{I}_2(a, b)$ .

$\mu$	$\alpha$	$\beta$	$n$	Error $^{GL_n}$	$n$	Error $^{WD_n^{(1)}}$	$n$	Error $^{LT_n^{(0)}}$
0	3.00	1.00	124	0.59D-02	16	0.30D-03	18	0.57D-03
0	1.00	1.00	124	0.46D-02	15	0.33D-03	18	0.80D-06
0	3.00	3.00	124	0.39D-02	20	0.36D-03	19	0.25D-08
0	1.00	3.00	124	0.35D-02	19	0.38D-03	21	0.11D-12
1	4.00	1.00	124	0.13D-03	17	0.23D-06	17	0.11D-01
1	1.00	4.00	124	0.20D-04	17	0.24D-06	19	0.40D-15
1	1.00	8.00	124	0.17D-04	18	0.23D-06	15	0.12D-15
2	5.00	1.00	124	0.90D-05	18	0.32D-09	16	0.41D-01
2	1.00	5.00	124	0.15D-06	17	0.21D-09	19	0.73D-15
2	1.00	10.00	124	0.12D-06	19	0.19D-09	15	0.15D-15

$\frac{\text{Calculation time using } WD_n^{(1)}}{\text{Calculation time using } GL_n} = 0.089$     and     $\frac{\text{Calculation time using } LT_n^{(0)}}{\text{Calculation time using } GL_n} = 0.00022$ .

Table 3.3: Numerical evaluation of  $\mathcal{I}_3(\mu, \alpha, \beta)$ .

$\mu$	$\nu$	$\alpha$	$\beta$	$\zeta$	$n$	Error <sup>GL<sub>n</sub></sup>	$n$	Error <sup>W<math>\bar{D}_n^{(0)}</math></sup>	$n$	Error <sup>LT<sub>n</sub><sup>(0)</sup></sup>
0	0	1.00	0.50	0.50	124	0.95D-05	6	0.11D-13	19	0.45D-10
0	0	0.50	1.00	0.50	124	0.23D-05	13	0.54D-14	19	0.45D-10
0	1	0.50	0.50	1.00	124	0.28D-07	10	0.14D-13	2	0.20D+00
1	0	0.50	0.50	0.50	124	0.12D-03	8	0.29D-12	19	0.17D-08
1	1	1.00	2.00	2.00	124	0.40D-09	13	0.31D-14	15	0.40D-15
1	1	2.00	1.00	2.00	124	0.87D-10	6	0.80D-15	15	0.53D-15
2	3	2.00	2.00	1.00	124	0.19D-09	9	0.36D-15	16	0.18D-15
3	1	5.00	5.00	2.00	124	0.13D-03	11	0.19D-15	12	0.11D-14
4	3	5.00	5.00	2.00	124	0.31D-02	11	0.33D-14	12	0.15D-14
5	4	2.00	2.00	5.00	124	0.34D-01	12	0.39D-14	12	0.14D-14

Calculation time using  $W\bar{D}_n^{(0)}$  = 0.032,    and    Calculation time using  $LT_n^{(0)}$  = 0.000 032.  
 Calculation time using  $GL_n$

Table 3.4: Numerical evaluation of  $\mathcal{I}_4(\mu, \nu, \alpha, \beta, \zeta)$ .

integrals.

### 3.E.1 Steepest descent methods

In some cases, the integral transformations leading to the semi-infinite integral (3.8) may compress many of the defining characteristics of  $f(\tau)$  near the origin, such that  $f(\tau)$  may be approximated very well by a polynomial of degree  $2n - 1$  only for very large  $n$ . As  $\tau \rightarrow \infty$ , however, the function  $f(\tau)$  becomes less complicated and thus the weight  $w(\tau) = e^{-\tau}$  is legitimate. In order to remove the complications from  $f(\tau)$  at the origin, we begin by integrating via a 32-point Gauss-Legendre quadrature rule for small sub-intervals beginning from the origin until the exponential weight begins to dominate. Algorithmically:

1. For  $n = 1, 2, \dots$ , compute using Gauss-Legendre quadrature rule:

$$\int_{\tau_{n-1}}^{\tau_n} f(\tau) e^{-\tau} d\tau. \quad (3.62)$$

2. If for some  $n = 2, 3, \dots$ :

$$\left| \frac{\int_{\tau_{n-1}}^{\tau_n} f(\tau) e^{-\tau} d\tau}{\int_{\tau_{n-2}}^{\tau_{n-1}} f(\tau) e^{-\tau} d\tau} \right| < \alpha, \quad (3.63)$$

where  $\alpha \in (0, 1]$  is a numerical parameter (which is set to  $\alpha = 1/2$  for these examples) then compute via a Gauss-Laguerre quadrature rule:

$$e^{-\tau_n} \int_0^{\infty} f(\tau + \tau_n) e^{-\tau} d\tau. \quad (3.64)$$

The approximation of the semi-infinite integral is then given by:

$$\int_0^{\tau_n} f(\tau) e^{-\tau} d\tau + e^{-\tau_n} \int_0^{\infty} f(\tau + \tau_n) e^{-\tau} d\tau. \quad (3.65)$$

We denote by  $GL_n$  the approximations computed in this way where  $n$  is the larger of the number of sub-intervals computed and the order of the Gauss-Laguerre quadrature rule. On a numerical basis, we find the sequences  $x_n = n(\beta + 0.5)$  for  $\mathcal{I}_1(\beta)$ ,  $x_n = n$  for  $\mathcal{I}_2(a, b)$ ,  $x_n = n/(5\mu + 5)$  for  $\mathcal{I}_3(\mu, \alpha, \beta)$  and  $x_n = n/(\zeta\sqrt{\alpha^2 + \beta^2})$  for  $\mathcal{I}_4(\mu, \nu, \alpha, \beta, \zeta)$  work well in this algorithm. It is worth mentioning that the condition in (3.63) only works when  $f(\tau)$  does not change sign on the interval  $\tau \in [\tau_{n-1}, \tau_n]$ , because otherwise cancellation might make the integral  $\int_{\tau_{n-1}}^{\tau_n} f(\tau) e^{-\tau} d\tau$  uncharacteristically small.

This algorithm fails to improve the accuracy for the integral  $\mathcal{I}_3(\mu, \alpha, \beta)$  because the integrand  $f_3(x)$  of (3.48) contains the function  $K_0(\beta x)$ , which

has a logarithmic singularity at the origin [AS65, §9.6.54], such that:

$$f_3(x) \sim -x^\mu [\gamma + \ln(\beta x/2)] \quad \text{as } x \rightarrow 0^+, \quad (3.66)$$

where  $\gamma$  is the Euler-Mascheroni constant [AS65, §1]:  $\gamma \approx 0.57721\,56649\,01532$ .

As can be seen in table 3.3, the trouble from the logarithmic singularity is most pronounced when  $\mu = 0$ , and becomes less so as  $\mu$  increases. The logarithmic singularity at the origin present in (3.48) poses a problem that requires a more sophisticated quadrature rule for  $\mathcal{I}_3(\mu, \alpha, \beta)$ . For weak singularities on an integration contour, there exist a variety of different methods that can help increase the accuracy. For example: in [Sid80b], quadrature rules are constructed with the singularities taken into account; in [PTVF07, §4.5], the tanh-sinh substitution transforms any finite integral into an infinite one with double-exponential decay at both extremities; or, it is mentioned in [SB02, §3.4] that a sequence of sub-integrals approaching the singularity could be extrapolated to the limit. Any of these or other techniques could possibly provide a better computation. We demonstrate the improvement in accuracy by using the tanh-sinh substitution. Let:

$$\mathcal{I}_3(\mu, \alpha, \beta) = \int_0^\infty f_3(x) \, dx = \int_0^{x_s} f_3(x) \, dx + \int_{x_s}^\infty f_3(x) \, dx, \quad (3.67)$$

for some  $x_s \in (0, \infty)$ . Then, by using the substitution  $x(t) = \frac{x_s}{2} (1 + \tanh(\sinh t))$  on the first integral in (3.67), and the substitution  $y = x - x_s$  in the second

integral in (3.67), we obtain:

$$\mathcal{I}_3(\mu, \alpha, \beta) = \int_{-\infty}^{\infty} f_3\left(\frac{x_s}{2}(1 + \tanh(\sinh t))\right) x'(t) dt + \int_0^{\infty} f_3(y + x_s) dy. \quad (3.68)$$

The second integral in (3.68) can easily be approximated by Gauss-Laguerre quadrature provided  $x_s$  is large enough. And, the first integral in (3.68) can be approximated by the trapezoidal rule as:

$$\begin{aligned} & \int_{-\infty}^{\infty} f_3\left(\frac{x_s}{2}(1 + \tanh(\sinh t))\right) x'(t) dt \\ & \approx h \sum_{j=-N}^N f_3\left(\frac{x_s}{2}(1 + \tanh(\sinh(jh)))\right) x'(jh). \end{aligned} \quad (3.69)$$

It is shown in [PTVF07, §4.5] that the trapezoidal rule converges exponentially fast while decreasing step size  $h$ . Due to the term  $x'(t)$ , which decays as  $\exp(-\exp|t|)$ , as  $t \rightarrow \pm\infty$ , the infinite integral may be approximated by a finite one around the origin. For the integral  $\mathcal{I}_3(\mu, \alpha, \beta)$ , the values  $x_s = \sqrt{\beta^2/\alpha^2 + 2(\mu + 1)/\alpha}$  and  $h = 1/2^6$  work well on the finite integral from  $[-3.575, 4]$ .

### 3.E.2 Extrapolation methods

There are several ways to improve an extrapolation method when it originally fails. We believe that the best way to describe these improvements is by considering the examples individually. Comparatively speaking, the extrapolation methods work better on  $\mathcal{I}_1(\beta)$  and  $\mathcal{I}_4(\mu, \nu, \alpha, \beta, \zeta)$  than on  $\mathcal{I}_2(a, b)$  and  $\mathcal{I}_3(\mu, \alpha, \beta)$ . So, we only detail refinements to the extrapolation methods for the integrals  $\mathcal{I}_2(a, b)$  and  $\mathcal{I}_3(\mu, \alpha, \beta)$ .

When  $ab \rightarrow \infty$  in  $\mathcal{I}_2(a, b)$ , the assumption that one of the sine functions is non-oscillatory past the point  $x_0$ , resp.  $x_0^{-1}$ , is no longer valid. This causes two problems. For high-frequency interfering oscillations, the 32-point Gauss-Legendre quadrature rule is unable to provide approximations accurate to 16 significant digits. The simplest way to remedy this loss of accuracy is to further subdivide each sub-integral into  $[ab] + 1$  sub-integrals and to compute each of these with a 32-point Gauss-Legendre quadrature rule. Additionally, when the high-frequency interference is pronounced, the assumption that  $f_2(x) \in \mathbf{B}^{(2)}$  is still valid, but the remainder estimates  $\varphi(x) = \sin\left(\frac{b}{x}\right)$  for the first integral in (3.44) or  $\varphi(x) = x^2 \sin\left(\frac{a}{x}\right)$  for the second need to be simplified to reflect this assumption. They are simplified by taking on their asymptotic forms:

$$\varphi(x) = \frac{b}{x} \quad \text{for the first integral} \quad \text{or} \quad \varphi(x) = ax \quad \text{for the second.} \quad (3.70)$$

As for integral  $\mathcal{I}_3(\mu, \alpha, \beta)$ , the same tanh-sinh substitution described in (3.67)–(3.69) is used to remove the numerical difficulties stemming from the logarithmic singularity. Then, the second integral in (3.67) is extrapolated as usual.

**Remark:** In the integral  $\mathcal{I}_2(a, b)$ , the oscillations are uncoupled, in that both parameters  $a$  and  $b$  create oscillations separately. By writing the sines as complex exponentials, a quick study reveals that  $\mathcal{I}_2(a, b)$  can be written as:

$$\mathcal{I}_2(a, b) = \operatorname{Re} \int_C \frac{e^{-i(a/z+bz)}}{2} dz, \quad (3.71)$$

where  $C$  is any contour connecting the points  $z_1 = -i\sqrt{a/b}$  and  $z_2 = i\sqrt{a/b}$  not passing through the origin. As an example, consider the circular contour

$z(\theta) = \sqrt{a/b} e^{i\theta}$ ,  $-\pi/2 < \theta < \pi/2$ . Then:

$$\mathcal{I}_2(a, b) = \operatorname{Re} \left( \frac{i}{2} \sqrt{\frac{a}{b}} \int_{-\pi/2}^{\pi/2} e^{-i2\sqrt{ab} \cos(\theta)} e^{i\theta} d\theta \right). \quad (3.72)$$

This comes as no surprise as (3.72) is another integral representation for the Bessel function  $J_1(2\sqrt{ab})$  [AS65, §9.1.21]. In (3.72), the parameters  $a$  and  $b$  contribute to the oscillations equally, and this might lead one to suspect that this contour integral would be a better starting point for the extrapolation methods. After substitutions:

$$\begin{aligned} \mathcal{I}_2(a, b) = & \operatorname{Re} \left( \sqrt{\frac{a}{b}} \frac{i\pi}{4} \int_0^\infty e^{-i2\sqrt{ab} \cos\left(\frac{\pi t}{2(t+1)}\right) + i\frac{\pi t}{2(t+1)}} \frac{dt}{(t+1)^2} \right), \\ & + \operatorname{Re} \left( \sqrt{\frac{a}{b}} \frac{i\pi}{4} \int_0^\infty e^{-i2\sqrt{ab} \cos\left(\frac{\pi t}{2(t+1)}\right) - i\frac{\pi t}{2(t+1)}} \frac{dt}{(t+1)^2} \right). \end{aligned} \quad (3.73)$$

Either of these semi-infinite integrals, depicted in figure 3.2, would be unusual applications of extrapolation methods because they are oscillatory, but have a finite number of zeros. Normally, one would expect an infinite number of zeros when integrating semi-infinite oscillatory integrals. One may very well have to integrate *beyond* all the oscillations before any extrapolation is achieved. In addition, one would have to investigate the order of the differential equation satisfied by the integrand to see which order  $m$  of the  $D^{(m)}$  transformation to apply. However, the cosine in the exponential makes things difficult. And, there may not be any systematic way to reduce the system of the  $D^{(m)}$  transformation (like choosing consecutive zeros in  $\bar{D}^{(m)}$ ). So, there are real difficulties with this approach and while on a deformed contour the complete oscillatory behaviour of the integral can be treated at once, we believe that it does not render an integral that is any

less challenging.

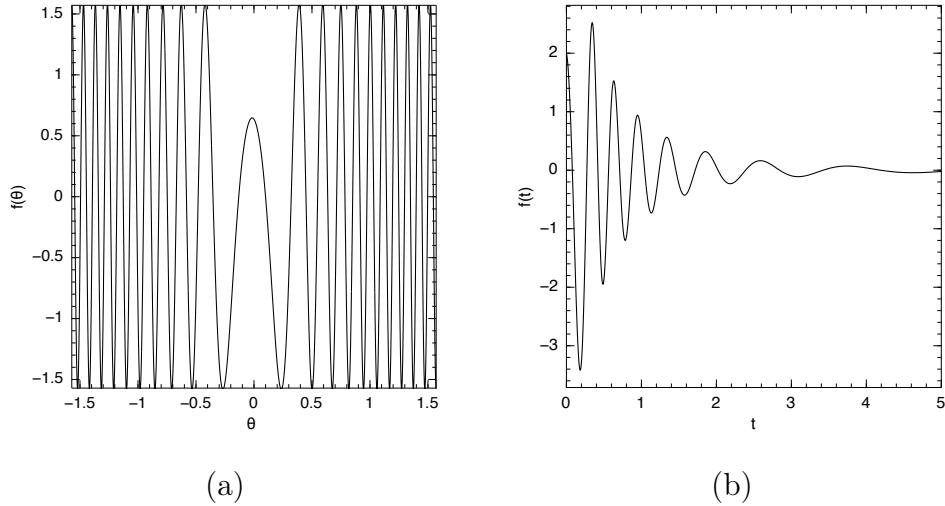


Figure 3.2: (a) shows the integrand in (3.72) and (b) shows the integrand in (3.73). In both cases,  $a = 100$  and  $b = 10$ .

### 3.E.3 Sequence transformations

In all four integrals, the sequence transformations are based on an asymptotic expansion as some governing parameter(s) tend to infinity. For  $\mathcal{I}_1(\beta)$ , the asymptotic expansion is valid as  $\beta \rightarrow \infty$ ; for  $\mathcal{I}_2(a, b)$ , the asymptotic expansion is valid as  $a b \rightarrow \infty$ ; for  $\mathcal{I}_3(\mu, \alpha, \beta)$ , the asymptotic expansion is valid as  $\frac{\beta^2}{4\alpha} \rightarrow \infty$ ; and, for  $\mathcal{I}_4(\mu, \nu, \alpha, \beta, \zeta)$ , the asymptotic expansion is valid as  $\zeta \sqrt{\alpha^2 + \beta^2} \rightarrow \infty$ . As the values of the governing parameter(s) tend to  $0^+$ , the sequence transformations do their best to approximate the antilimits of the divergent series. However, past a certain point, the stopping criteria of (3.61) return the best approximation which does not attain full precision. In this case, we resort to using a (convergent) series representation of the integrals as the governing parameter(s) in question tend to  $0^+$ .

The integral  $\mathcal{I}_1(\beta)$  also has the series representation [GR07, §8.214]:

$$\mathcal{I}_1(\beta) = -e^\beta \left( \gamma + \ln \beta + \sum_{k=1}^{\infty} \frac{(-\beta)^k}{k \cdot k!} \right) \quad \text{as } \beta \rightarrow 0^+. \quad (3.74)$$

The integral  $\mathcal{I}_2(a, b)$  also has the series representation [GR07, §8.440]:

$$\mathcal{I}_2(a, b) = \frac{\pi a}{2} \sum_{k=0}^{\infty} \frac{(-ab)^k}{k! (k+1)!} \quad \text{as } ab \rightarrow 0^+. \quad (3.75)$$

The integral  $\mathcal{I}_3(\mu, \alpha, \beta)$  also has the series representation [GR07, §9.237]:

$$\begin{aligned} \mathcal{I}_3(\mu, \alpha, \beta) &= \frac{1}{4\alpha^{\frac{\mu+1}{2}}} \sum_{k=0}^{\infty} \frac{\Gamma(k + \frac{\mu+1}{2})}{(k!)^2} \left( \frac{\beta^2}{4\alpha} \right)^k \\ &\times \left[ 2\psi(k+1) - \psi\left(k + \frac{\mu+1}{2}\right) - \ln\left(\frac{\beta^2}{4\alpha}\right) \right] \quad \text{as } \frac{\beta^2}{4\alpha} \rightarrow 0^+, \end{aligned} \quad (3.76)$$

where  $\psi$  stands for the digamma function [AS65, §6.1.3].

The integral  $\mathcal{I}_4(\mu, \nu, \alpha, \beta, \zeta)$  also has the series representation [GR07, §8.446]:

$$\begin{aligned} \mathcal{I}_4(\mu, \nu, \alpha, \beta, \zeta) &= \frac{\beta^\nu}{2\alpha^\mu} \left( \frac{\sqrt{\alpha^2 + \beta^2}}{\zeta} \right)^{\mu-\nu-1} \\ &\times \left\{ \sum_{k=0}^{\lambda-1} \frac{(-1)^k (\lambda-1-k)!}{k!} \left( \frac{\zeta \sqrt{\alpha^2 + \beta^2}}{2} \right)^{2k-\lambda} \right. \\ &+ (-1)^\lambda \sum_{k=0}^{\infty} \frac{1}{k! (\lambda+k)!} \left( \frac{\zeta \sqrt{\alpha^2 + \beta^2}}{2} \right)^{2k+\lambda} \\ &\left. \times \left[ \psi(k+1) + \psi(k+\lambda+1) - 2 \ln\left(\frac{\zeta \sqrt{\alpha^2 + \beta^2}}{2}\right) \right] \right\}, \end{aligned} \quad (3.77)$$

as  $\zeta \sqrt{\alpha^2 + \beta^2} \rightarrow 0^+$ , where  $\lambda = |\mu - \nu - 1|$ .

A simple refinement, these convergent series representations are used to approximate the integrals as the parameter(s) tend to  $0^+$ . On a numerical

basis, we find the separation points  $\beta = 4.0$  for  $\mathcal{I}_1(\beta)$ ,  $ab = 5.0$  for  $\mathcal{I}_2(a, b)$ ,  $\frac{\beta^2}{4\alpha} = 4.0$  for  $\mathcal{I}_3(\mu, \alpha, \beta)$ , and  $\zeta\sqrt{\alpha^2 + \beta^2} = 2.0$  for  $\mathcal{I}_4(\mu, \nu, \alpha, \beta, \zeta)$  work well in determining whether the convergent series or the sequence transformation on the divergent series is used.

### 3.E.4 Numerical Discussion

The performance of the three methods in tables 3.1–3.4 may not be readily impressive because each method tends to favour one direction of parameter values over another, and this would be undesirable for the computation of a semi-infinite integral with parameters not in the favourable region.

Tables 3.5, 3.6, 3.7, and 3.8 each show the same 10 test values of the integrals  $\mathcal{I}_1(\beta)$ ,  $\mathcal{I}_2(a, b)$ ,  $\mathcal{I}_3(\mu, \alpha, \beta)$ , and  $\mathcal{I}_4(\mu, \nu, \alpha, \beta, \zeta)$ , respectively, as tables 3.1, 3.2, 3.3, and 3.4 with the algorithmic refinements taken into consideration. In tables 3.5–3.8, the notation is identical to that used in tables 3.1–3.4.

Tables 3.5–3.8 demonstrate that all three methods are successful in obtaining 15 significant digits for most of the test values. The least successful region is the  $W\bar{D}_n^{(0)}$  method for high values of  $a$  and  $b$  in table 3.6. The integral  $\mathcal{I}_1(\beta)$  has a pole at  $x = -\beta$ , and this adversely affects the quadrature-dependent algorithms as  $\beta \rightarrow 0^+$ . There is no doubt that for extremely high values of  $a$  and  $b$ , the extrapolation method will require an unbearable calculation for  $\mathcal{I}_2(a, b)$ , as the accurate calculation of the sub-integrals requires an asymptotically infinite amount of subdivision, due to the infinite oscillations at 0 and  $\infty$ .

In contrast, the logarithmic singularity at the origin present in (3.48) poses a problem that requires a more sophisticated quadrature rule for  $\mathcal{I}_3(\mu, \alpha, \beta)$ . Using the tanh-sinh substitution, the numerical problems posed by the loga-

rithmic singularity are removed, and high accuracy is achieved. However, the efficiency of the quadrature-based algorithms is not change substantially.

As with tables 3.1–3.4, in comparing the calculation times listed at the bottom of each of tables 3.5–3.8 for all 40 test values, there is strong evidence to suggest that the algorithm for  $LT_n^{(0)}$  is the most efficient.

With these test examples, the authors opine that the most promising method for obtaining 15 significant digits in double precision for a semi-infinite integral consistently and efficiently, is to use a sequence transformation on the divergent series representation of the integral and to sum a (convergent) series representation where the former fails.

$\beta$	$n$	Error $^{GL_n}$	$n$	Error $^{WD_n^{(1)}}$	$n$	Error $^{LT_n^{(0)}}$
0.03	70	0.10D-12	17	0.22D-12	7	0.15D-15
0.10	53	0.18D-14	17	0.84D-12	9	0.00D+00
0.30	41	0.13D-14	17	0.71D-14	12	0.18D-15
1.00	22	0.13D-14	12	0.56D-15	17	0.00D+00
3.00	12	0.17D-14	8	0.13D-14	28	0.47D-14
4.00	12	0.17D-14	7	0.22D-14	19	0.40D-15
5.00	12	0.28D-14	6	0.31D-14	18	0.16D-15
10.00	8	0.33D-14	3	0.30D-14	16	0.30D-15
30.00	6	0.47D-14	3	0.47D-14	13	0.00D+00
100.00	5	0.19D-14	2	0.21D-14	9	0.18D-15

$$\frac{\text{Calculation time using } WD_n^{(1)}}{\text{Calculation time using } GL_n} = 2.2 \quad \text{and} \quad \frac{\text{Calculation time using } LT_n^{(0)}}{\text{Calculation time using } GL_n} = 0.27.$$

Table 3.5: Numerical evaluation of  $\mathcal{I}_1(\beta)$  with the refinements.

### 3.F Conclusion

In this work, one of the numerical steepest descent methods, one of the extrapolation methods, and one of the sequence transformations were used in the

$a$	$b$	$n$	Error $^{GL_n}$	$n$	Error $^{W\bar{D}_n^{(2)}}$	$n$	Error $^{LT_n^{(0)}}$
1.00	1.00	53	0.86D-15	16	0.16D-14	10	0.37D-15
2.00	1.00	53	0.75D-15	18	0.12D-14	12	0.12D-15
2.00	2.00	53	0.24D-14	18	0.36D-14	15	0.15D-14
3.00	1.00	53	0.13D-14	18	0.54D-15	14	0.00D+00
3.00	2.00	70	0.92D-15	17	0.15D-14	25	0.17D-14
3.00	3.00	53	0.77D-15	17	0.64D-15	18	0.13D-15
10.00	1.00	56	0.11D-14	19	0.44D-14	20	0.44D-15
100.00	1.00	34	0.38D-14	26	0.12D-12	8	0.21D-14
10.00	10.00	56	0.12D-14	29	0.98D-13	8	0.20D-14
100.00	10.00	53	0.39D-14	35	0.17D-11	5	0.16D-14

$\frac{\text{Calculation time using } W\bar{D}_n^{(2)}}{\text{Calculation time using } GL_n} = 100.0$  and  $\frac{\text{Calculation time using } LT_n^{(0)}}{\text{Calculation time using } GL_n} = 0.022$ .

Table 3.6: Numerical evaluation of  $\mathcal{I}_2(a, b)$  with the refinements.

$\mu$	$\alpha$	$\beta$	$n$	Error $^{GL_n}$	$n$	Error $^{WD_n^{(1)}}$	$n$	Error $^{LT_n^{(0)}}$
0	3.00	1.00	116	0.52D-14	14	0.78D-14	9	0.38D-15
0	1.00	1.00	44	0.12D-13	14	0.72D-14	12	0.00D+00
0	3.00	3.00	60	0.33D-14	15	0.19D-13	16	0.51D-15
0	1.00	3.00	34	0.14D-13	17	0.27D-13	24	0.12D-14
1	4.00	1.00	70	0.28D-14	12	0.22D-14	9	0.00D+00
1	1.00	4.00	20	0.89D-14	12	0.81D-14	19	0.40D-15
1	1.00	8.00	13	0.93D-14	14	0.75D-14	15	0.12D-15
2	5.00	1.00	47	0.17D-13	11	0.38D-14	9	0.00D+00
2	1.00	5.00	16	0.11D-13	14	0.10D-13	19	0.73D-15
2	1.00	10.00	14	0.89D-14	17	0.83D-14	15	0.15D-15

$\frac{\text{Calculation time using } WD_n^{(1)}}{\text{Calculation time using } GL_n} = 0.43$  and  $\frac{\text{Calculation time using } LT_n^{(0)}}{\text{Calculation time using } GL_n} = 0.00073$ .

Table 3.7: Numerical evaluation of  $\mathcal{I}_3(\mu, \alpha, \beta)$  with the refinements.

$\mu$	$\nu$	$\alpha$	$\beta$	$\zeta$	$n$	Error <sup><math>GL_n</math></sup>	$n$	Error <sup><math>W\bar{D}_n^{(0)}</math></sup>	$n$	Error <sup><math>LT_n^{(0)}</math></sup>
0	0	1.00	0.50	0.50	25	0.42D-06	6	0.11D-13	7	0.00D+00
0	0	0.50	1.00	0.50	19	0.71D-06	13	0.54D-14	7	0.00D+00
0	1	0.50	0.50	1.00	26	0.45D-14	10	0.14D-13	7	0.50D-15
1	0	0.50	0.50	0.50	16	0.70D-05	8	0.29D-12	7	0.18D-15
1	1	1.00	2.00	2.00	123	0.80D-14	13	0.31D-14	15	0.40D-15
1	1	2.00	1.00	2.00	123	0.11D-14	6	0.80D-15	15	0.53D-15
2	3	2.00	2.00	1.00	107	0.36D-15	9	0.36D-15	16	0.18D-15
3	1	5.00	5.00	2.00	124	0.10D-03	11	0.19D-15	12	0.11D-14
4	3	5.00	5.00	2.00	124	0.21D-02	11	0.33D-14	12	0.15D-14
5	4	2.00	2.00	5.00	124	0.33D-01	12	0.39D-14	12	0.14D-14

$\frac{\text{Calculation time using } W\bar{D}_n^{(0)}}{\text{Calculation time using } GL_n} = 0.048,$     and     $\frac{\text{Calculation time using } LT_n^{(0)}}{\text{Calculation time using } GL_n} = 0.000052.$

Table 3.8: Numerical evaluation of  $\mathcal{I}_4(\mu, \nu, \alpha, \beta, \zeta)$  with the refinements.

numerical evaluation of four semi-infinite integrals. We found that all three methods were capable of attaining 15 significant digits for some of the test values. By supplementing each of the methods with an algorithmic refinement, all three methods were very successful in attaining this high precision. We consider that the three methods can all be considered highly accurate in evaluating semi-infinite integrals.

However, the efficiency of the algorithms tells a different story. The algorithms based on numerical quadrature routines—the numerical steepest descent and the extrapolation methods—were markedly less efficient than the algorithm not based on numerical quadrature—the sequence transformations. For the first two test integrals, where the integrands are not so complicated, this difference in efficiency is noticeable. For the second two test integral, where the computation of the integrands necessarily involves subroutines for Bessel functions, this difference in efficiency, which is approximately between  $10^3$  and  $10^4$  times, is significant. In the construct of a large program evaluating millions of in-

tegrals, the gain in efficiency obtained by summing the series representations of semi-infinite integrals would most likely render feasible a program which would have been originally considered unfeasible.

The marked gain in efficiency and consequently the potential feasibility of the computation of challenging problems should provide the motivation to seek these series representations wherever possible. However, it is not for every integral that such convergent or divergent series representations exist. Unfortunately, for many integrals of practical interest, the integrand itself is the result of a computation and evaluating derivatives required for forming the terms of a series representation is infeasible. Similarly, evaluating the integrand in the complex plane (for steepest descent) might be difficult. Extrapolation methods seem to be the most robust, and the requirements for applicability are easily met.

There seems to be a paradox in that for the most complicated integrals these series representations are the most elusive, yet the gain in efficiency would be the greatest. In the cases where the series representations are unknown or do not lead to accurate algorithms, we suggest that both steepest descent and extrapolation methods be applied on a case-by-case approach, as neither algorithm is markedly more accurate and reliable than the other in any of the test cases above.

We hope this work opens a discussion on the comparison of these general methods and others for the numerical evaluation of semi-infinite integrals. The numerical evaluation of many challenging problems in applied mathematics is often based on one's ability to evaluate semi-infinite integrals. To seek the most accurate, reliable, and efficient method(s) for their numerical evaluation will help advance scientific research in the most complicated settings.

## Chapter 4

# An Analytical Expression for the Rapid Evaluation of Three-Center Nuclear Attraction Integrals over *B* Functions

### 4.A Introduction

The pursuit of accurate and efficient algorithms for the numerical evaluation of molecular integrals for the purpose of electronic structure calculations has led to a substantial body of work. While molecular integrals with Gaussian-type orbitals as a basis have been for a long time the most easily calculated, their theoretical deficiency both in the long range and in the short range has led to a renewed interest in an exponential-type function (ETF) basis. Examples of such a basis include the Slater-type functions, the Laguerre-type functions, and the *B* functions.

The  $B$  function basis has been at the forefront of recent developments [SW77, SW78, WS83, WGS86, GWS86, WS88], as their simple Fourier transform leads to compact analytical expressions for the integrals. Through the expansions, some of the resulting semi-infinite integrals have integrands composed of the Bessel functions. As the most complicated part of the analytical expressions, the semi-infinite integrals have become the bottleneck of the calculations in the  $B$  function approach. Since the identification of this computational problem, a large body of work is devoted to dealing with this bottleneck. The most common element to most algorithms [Saf01, BS03a, Saf04, SB06, SB07, DS07, SS09, Saf10] involves an intense integration-then-extrapolation approach, which is usually characterized by subdividing the integral between the oscillatory Bessel function's zeros, by integrating by a quadrature, and by using the resulting sequence to estimate the remainder of the integral. Many improvements to the general extrapolation procedure are documented and indeed some of the most recent of these improvements are considered state-of-the-art for multi-center integrals. While these methods and their refinements are generally highly accurate and efficient, there are some ranges of parameters where either failure is inevitable or the computation becomes extremely heavy.

In the comparative study [SS12] of the most popular extrapolation methods and sequence transformations for computing semi-infinite integrals, the authors conclude that having asymptotic series representations for integrals and applying sequence transformations to accelerate their convergence or to sum their divergence leads to the most efficient algorithms for computing the integrals. However, when such asymptotic series representations do not exist, refinements to either the numerical steepest descent method or the extrapolation methods must be made to obtain a desirable outcome. This conclu-

sion does not particularly challenge any preconceived notions. However, it does emphasize that the ultimate goal in computing semi-infinite integrals is to find analytical expressions. Several examples of this approach have been documented in the literature on molecular integrals in the  $B$  function basis [WS83,STMS10]. The expressions that are obtained have greatly simplified the calculation of one- and two-center integrals. The pursuit of such analytical expressions stopped at the three-center integrals because of the increased complexity of the integrands.

The bottleneck in the numerical evaluation of the expression (2.74) is the semi-infinite integral:

$$\mathcal{I}(s) = \int_{x=0}^{+\infty} x^{n_x} \frac{\hat{k}_\nu[R_2\gamma_{12}(s, x)]}{[\gamma_{12}(s, x)]^{n_\gamma}} j_\lambda(v x) dx, \quad (4.1)$$

where  $[\gamma_{12}(s, x)]^2 = (1 - s)\zeta_1^2 + s\zeta_2^2 + s(1 - s)x^2$ , which has varying degrees of oscillation and attenuation depending upon the values of the parameters. Originally, Gauss-Laguerre quadrature is used [TS83,GS88], ignoring the possible effects of the oscillations. Then, extrapolation methods are implemented [Saf01,BS03a,Saf04,SB06,SB07,DS07,SS09,Saf10], which use numerical integration of successive intervals, usually the Bessel function's zeros, to construct approximations the semi-infinite integral.

In this work, we report an analytical expression for the semi-infinite inte-

grals in the three-center nuclear attraction integrals. Briefly, our result is:

$$\begin{aligned}
& \int_0^\infty x^{\lambda+2r+2} \frac{\hat{k}_\nu [\alpha\sqrt{x^2+z^2}]}{(x^2+z^2)^{\nu-\mu}} j_\lambda(\beta x) dx \\
&= (-2)^r 2^\mu z^{\lambda+r+\mu-\nu+3/2} \beta^\lambda \sum_{s=0}^r \binom{r}{s} \left(\frac{\beta^2 z}{2}\right)^s (-\lambda-r-1/2)_{r-s} \\
&\times \sum_{m=0}^\mu \binom{\mu}{m} \left(\frac{\alpha^2 z}{2}\right)^m (\nu-\mu)_{\mu-m} \frac{K_{\lambda+r+\mu-\nu+3/2+s+m}(z\sqrt{\alpha^2+\beta^2})}{(\alpha^2+\beta^2)^{(\lambda+r+\mu-\nu+3/2+s+m)/2}}. \quad (4.2)
\end{aligned}$$

and it can be seen from equation (2.74) that such a formula will greatly speed up the numerical calculations. In section 4.B, we prove this result, and in section 4.C, we hold a numerical discussion on its performance and compare it to the  $S\bar{D}_n^{(2,j)}$  of [Saf01]. Our comparison leads us to believe that the analytical expression is useful in a numerical setting and performs very well. Indeed, the decrease in calculation time is on the order of  $10^{2.5}$  compared with the  $S\bar{D}_n^{(2,j)}$  of [Saf01].

## 4.B The Development

To arrive at the formula (4.2), we begin by considering Hankel transforms of the form:

$$\int_0^\infty J_\nu(\beta x) \frac{K_\mu(\alpha\sqrt{x^2+z^2})}{\sqrt{(x^2+z^2)^\mu}} x^{\nu+1} dx, \quad (4.3)$$

where  $\mu \in \mathbb{R}$ ,  $\text{Re } \nu > -1$ ,  $\alpha > 0$ ,  $\beta > 0$ , and  $|\arg z| < \frac{\pi}{2}$ . In relation to the semi-infinite integrals of (2.74), in these integrals, some of the parameters are related to one another, and cylindrical Bessel functions are used instead of spherical Bessel functions. These integrals have an analytical expression in [Wat66, §13.47] that can be proved easily. We begin by inserting the integral representation of the modified Bessel function (2.42) into the expression and

we reverse the order of integration:

$$\begin{aligned} & \int_0^\infty J_\nu(\beta x) \frac{K_\mu(\alpha\sqrt{x^2+z^2})}{\sqrt{(x^2+z^2)^\mu}} x^{\nu+1} dx \\ &= \frac{1}{2} \int_0^\infty \int_0^\infty J_\nu(\beta x) x^{\nu+1} \frac{e^{-\frac{\alpha}{2}(t+\frac{x^2+z^2}{t})}}{t^{\mu+1}} dt dx, \end{aligned} \quad (4.4)$$

$$= \frac{1}{2} \int_0^\infty \frac{e^{-\frac{\alpha}{2}(t+\frac{z^2}{t})}}{t^{\mu+1}} \int_0^\infty e^{-\frac{\alpha x^2}{2t}} J_\nu(\beta x) x^{\nu+1} dx dt, \quad (4.5)$$

By using the convergent series for the Bessel function (2.31), the inner integral is readily obtained [Wat66, §6.22]:

$$\begin{aligned} & \int_0^\infty e^{-\frac{\alpha x^2}{2t}} J_\nu(\beta x) x^{\nu+1} dx \\ &= \int_0^\infty e^{-\frac{\alpha x^2}{2t}} \sum_{k=0}^\infty \frac{(-1)^k}{k! \Gamma(k+\nu+1)} \left(\frac{\beta}{2}\right)^{2k+\nu} x^{2k+2\nu+1} dx, \end{aligned} \quad (4.6)$$

$$= \sum_{k=0}^\infty \frac{(-1)^k}{k! \Gamma(k+\nu+1)} \left(\frac{\beta}{2}\right)^{2k+\nu} \int_0^\infty e^{-\frac{\alpha x^2}{2t}} x^{2k+2\nu+1} dx, \quad (4.7)$$

$$= \sum_{k=0}^\infty \frac{(-1)^k}{k! \Gamma(k+\nu+1)} \left(\frac{\beta}{2}\right)^{2k+\nu} \frac{\Gamma(k+\nu+1)}{2} \left(\frac{2t}{\alpha}\right)^{k+\nu+1}, \quad (4.8)$$

$$= \frac{\beta^\nu t^{\nu+1}}{\alpha^{\nu+1}} \sum_{k=0}^\infty \frac{(-1)^k}{k!} \left(\frac{\beta^2 t}{2\alpha}\right)^k, \quad (4.9)$$

$$= \frac{\beta^\nu t^{\nu+1}}{\alpha^{\nu+1}} \exp\left(-\frac{\beta^2 t}{2\alpha}\right). \quad (4.10)$$

Then, the outer integral is evaluated by recognizing it as the integral representation of the modified Bessel function (2.42), and we obtain:

$$\begin{aligned} \int_0^\infty J_\nu(\beta x) \frac{K_\mu(\alpha\sqrt{x^2+z^2})}{\sqrt{(x^2+z^2)^\mu}} x^{\nu+1} dx \\ = \frac{\beta^\nu}{2\alpha^{\nu+1}} \int_0^\infty \frac{e^{-\frac{\alpha}{2}(t+\frac{z^2}{t})-\frac{\beta^2 t}{2\alpha}}}{t^{\mu-\nu}} dt, \end{aligned} \quad (4.11)$$

$$= \frac{\beta^\nu}{\alpha^\mu} \left( \frac{\sqrt{\alpha^2+\beta^2}}{z} \right)^{\mu-\nu-1} K_{\mu-\nu-1} \left( z\sqrt{\alpha^2+\beta^2} \right). \quad (4.12)$$

The semi-infinite integrals in the expression for the three-center nuclear attraction integrals are formulated using the spherical and reduced Bessel functions. In a simplified notation, they are given by:

$$\mathcal{I}_{\lambda,r}^{\nu,\mu}(\alpha, \beta, z) = \int_0^\infty x^{\lambda+2r+2} \frac{\hat{k}_\nu [\alpha\sqrt{x^2+z^2}]}{(x^2+z^2)^{\nu-\mu}} j_\lambda(\beta x) dx, \quad (4.13)$$

and the simpler case:

$$\mathcal{I}_{\lambda,0}^{\nu,0}(\alpha, \beta, z) = \int_0^\infty x^{\lambda+2} \frac{\hat{k}_\nu [\alpha\sqrt{x^2+z^2}]}{(x^2+z^2)^\nu} j_\lambda(\beta x) dx. \quad (4.14)$$

This simpler case is the essential starting point because identities can be used to increase the  $r$  and  $\mu$  parameters to obtain an expression for  $\mathcal{I}_{\lambda,r}^{\nu,\mu}(\alpha, \beta, z)$ . Applying the identities (c.f. (2.33) and (2.34)):

$$\frac{1}{\beta^{\lambda+1}} \left( \frac{\partial}{\beta\partial\beta} \right)^r (\beta^{\lambda+r+1} j_{\lambda+r}(\beta x)) = x^r j_\lambda(\beta x), \quad (4.15)$$

and (c.f. (2.44) and (2.45)):

$$(-1)^\mu \alpha^{2\nu} \left( \frac{\partial}{\alpha\partial\alpha} \right)^\mu \left( \alpha^{2\mu-2\nu} \hat{k}_{\nu-\mu} [\alpha\sqrt{x^2+z^2}] \right) = \hat{k}_\nu [\alpha\sqrt{x^2+z^2}], \quad (4.16)$$

to the integral:

$$\mathcal{I}_{\lambda+r,0}^{\nu-\mu,0}(\alpha, \beta, z) = \int_0^\infty x^{\lambda+r+2} \frac{\hat{k}_{\nu-\mu}[\alpha\sqrt{x^2+z^2}]}{(x^2+z^2)^{\nu-\mu}} j_{\lambda+r}(\beta x) dx, \quad (4.17)$$

we obtain:

$$\mathcal{I}_{\lambda,r}^{\nu,\mu}(\alpha, \beta, z) = \frac{(-1)^\mu \alpha^{2\nu}}{\beta^{\lambda+1}} \left( \frac{\partial}{\alpha \partial \alpha} \right)^\mu \left( \frac{\partial}{\beta \partial \beta} \right)^r \left( \alpha^{2\mu-2\nu} \beta^{\lambda+r+1} \mathcal{I}_{\lambda+r,0}^{\nu-\mu,0}(\alpha, \beta, z) \right). \quad (4.18)$$

Upon changing the Bessel functions to their spherical and reduced counterparts in (4.11), we obtain:

$$\mathcal{I}_{\lambda,0}^{\nu,0}(\alpha, \beta, z) = \frac{\beta^\lambda (\alpha^2 + \beta^2)^{\frac{\nu-\lambda-3/2}{2}}}{z^{\nu-\lambda-3/2}} K_{\nu-\lambda-3/2} \left( z \sqrt{\alpha^2 + \beta^2} \right), \quad (4.19)$$

and:

$$\mathcal{I}_{\lambda+r,0}^{\nu-\mu,0}(\alpha, \beta, z) = \frac{\beta^{\lambda+r} (\alpha^2 + \beta^2)^{\frac{\nu-\mu-\lambda-r-3/2}{2}}}{z^{\nu-\mu-\lambda-r-3/2}} K_{\nu-\mu-\lambda-r-3/2} \left( z \sqrt{\alpha^2 + \beta^2} \right). \quad (4.20)$$

Upon inserting the expression for  $\mathcal{I}_{\lambda+r,0}^{\nu-\mu,0}(\alpha, \beta, z)$  into (4.18), we obtain:

$$\mathcal{I}_{\lambda,r}^{\nu,\mu}(\alpha, \beta, z) = \frac{(-1)^\mu \alpha^{2\nu} z^\gamma}{\beta^{\lambda+1}} \left( \frac{\partial}{\alpha \partial \alpha} \right)^\mu \left( \frac{\partial}{\beta \partial \beta} \right)^r \left( \alpha^{2\mu-2\nu} \beta^{2\lambda+2r+1} \frac{K_\gamma(z\sqrt{\alpha^2 + \beta^2})}{(\alpha^2 + \beta^2)^{\gamma/2}} \right), \quad (4.21)$$

where  $\gamma = \lambda + r + \mu - \nu + 3/2$ . All that remains to do is to expand the derivations in (4.21), and the expression (4.2) will be obtained. We start with

the derivations with respect to  $\beta$ . Using the identities:

$$\left(\frac{\partial}{\beta\partial\beta}\right)^{r-s} (\beta^{2\lambda+2r+1}) = (-2)^{r-s}(-\lambda-r-1/2)_{r-s}\beta^{2\lambda+2s+1}, \quad (4.22)$$

$$\left(\frac{\partial}{\beta\partial\beta}\right)^s \left(\frac{K_\gamma(z\sqrt{\alpha^2+\beta^2})}{(\alpha^2+\beta^2)^{\gamma/2}}\right) = (-z)^s \frac{K_{\gamma+s}(z\sqrt{\alpha^2+\beta^2})}{(\alpha^2+\beta^2)^{(\gamma+s)/2}}, \quad (4.23)$$

for some  $s \in \mathbb{N}_0$ , the product rule yields:

$$\begin{aligned} & \left(\frac{\partial}{\beta\partial\beta}\right)^r \left(\beta^{2\lambda+2r+1} \frac{K_\gamma(z\sqrt{\alpha^2+\beta^2})}{(\alpha^2+\beta^2)^{\gamma/2}}\right) \\ &= \sum_{s=0}^r \binom{r}{s} \left(\frac{\partial}{\beta\partial\beta}\right)^{r-s} (\beta^{2\lambda+2r+1}) \left(\frac{\partial}{\beta\partial\beta}\right)^s \left(\frac{K_\gamma(z\sqrt{\alpha^2+\beta^2})}{(\alpha^2+\beta^2)^{\gamma/2}}\right), \quad (4.24) \\ &= \sum_{s=0}^r \binom{r}{s} (-2)^{r-s}(-\lambda-r-1/2)_{r-s}\beta^{2\lambda+2s+1}(-z)^s \frac{K_{\gamma+s}(z\sqrt{\alpha^2+\beta^2})}{(\alpha^2+\beta^2)^{(\gamma+s)/2}}, \\ &= (-2)^r \beta^{2\lambda+1} \sum_{s=0}^r \binom{r}{s} \left(\frac{\beta^2 z}{2}\right)^s (-\lambda-r-1/2)_{r-s} \frac{K_{\gamma+s}(z\sqrt{\alpha^2+\beta^2})}{(\alpha^2+\beta^2)^{(\gamma+s)/2}}. \quad (4.25) \end{aligned}$$

We continue with the derivations with respect to  $\alpha$ . Using the identities:

$$\left(\frac{\partial}{\alpha\partial\alpha}\right)^{\mu-m} (\alpha^{2\mu-2\nu}) = (-2)^{\mu-m}(\nu-\mu)_{\mu-m}\alpha^{2m-2\nu}, \quad (4.26)$$

$$\left(\frac{\partial}{\alpha\partial\alpha}\right)^m \left(\frac{K_{\gamma+s}(z\sqrt{\alpha^2+\beta^2})}{(\alpha^2+\beta^2)^{(\gamma+s)/2}}\right) = (-z)^m \frac{K_{\gamma+s+m}(z\sqrt{\alpha^2+\beta^2})}{(\alpha^2+\beta^2)^{(\gamma+s+m)/2}}, \quad (4.27)$$

for some  $m \in \mathbb{N}_0$ , the product rule yields:

$$\begin{aligned} & \left( \frac{\partial}{\alpha \partial \alpha} \right)^\mu \left( \alpha^{2\mu-2\nu} \frac{K_{\gamma+s}(z\sqrt{\alpha^2+\beta^2})}{(\alpha^2+\beta^2)^{(\gamma+s)/2}} \right) \\ &= \sum_{m=0}^{\mu} \binom{\mu}{m} \left( \frac{\partial}{\alpha \partial \alpha} \right)^{\mu-m} (\alpha^{2\mu-2\nu}) \left( \frac{\partial}{\alpha \partial \alpha} \right)^m \left( \frac{K_{\gamma+s}(z\sqrt{\alpha^2+\beta^2})}{(\alpha^2+\beta^2)^{(\gamma+s)/2}} \right), \end{aligned} \quad (4.28)$$

$$= \sum_{m=0}^{\mu} \binom{\mu}{m} (-2)^{\mu-m} (\nu-\mu)_{\mu-m} \alpha^{2m-2\nu} (-z)^m \frac{K_{\gamma+s+m}(z\sqrt{\alpha^2+\beta^2})}{(\alpha^2+\beta^2)^{(\gamma+s+m)/2}}, \quad (4.29)$$

$$= (-2)^\mu \alpha^{-2\nu} \sum_{m=0}^{\mu} \binom{\mu}{m} \left( \frac{\alpha^2 z}{2} \right)^m (\nu-\mu)_{\mu-m} \frac{K_{\gamma+s+m}(z\sqrt{\alpha^2+\beta^2})}{(\alpha^2+\beta^2)^{(\gamma+s+m)/2}}. \quad (4.30)$$

Then, combining these results and inserting them in (4.21), we obtain:

$$\begin{aligned} \mathcal{I}_{\lambda,r}^{\nu,\mu}(\alpha, \beta, z) &= (-2)^r 2^\mu z^\gamma \beta^\lambda \sum_{s=0}^r \binom{r}{s} \left( \frac{\beta^2 z}{2} \right)^s (-\lambda - r - 1/2)_{r-s} \\ &\quad \times \sum_{m=0}^{\mu} \binom{\mu}{m} \left( \frac{\alpha^2 z}{2} \right)^m (\nu-\mu)_{\mu-m} \frac{K_{\gamma+s+m}(z\sqrt{\alpha^2+\beta^2})}{(\alpha^2+\beta^2)^{(\gamma+s+m)/2}}. \end{aligned} \quad (4.31)$$

Finally, replacing  $\gamma$  by its original value, we obtain:

$$\begin{aligned} \mathcal{I}_{\lambda,r}^{\nu,\mu}(\alpha, \beta, z) &= (-2)^r 2^\mu z^{\lambda+r+\mu-\nu+3/2} \beta^\lambda \sum_{s=0}^r \binom{r}{s} \left( \frac{\beta^2 z}{2} \right)^s (-\lambda - r - 1/2)_{r-s} \\ &\quad \times \sum_{m=0}^{\mu} \binom{\mu}{m} \left( \frac{\alpha^2 z}{2} \right)^m (\nu-\mu)_{\mu-m} \frac{K_{\lambda+r+\mu-\nu+3/2+s+m}(z\sqrt{\alpha^2+\beta^2})}{(\alpha^2+\beta^2)^{(\lambda+r+\mu-\nu+3/2+s+m)/2}}. \end{aligned} \quad (4.32)$$

The case  $r = -1$  is also required for some values of the parameters in (2.74).

In this case, we use the identity:

$$(1/2 - \lambda)_{-s-1} = \frac{(-1)^{s+1}}{(\lambda + 1/2)_{s+1}}, \quad (4.33)$$

to obtain infinite series:

$$\begin{aligned} \mathcal{I}_{\lambda,-1}^{\nu,\mu}(\alpha, \beta, z) &= 2^{\mu-1} z^{\lambda+\mu-\nu+1/2} \beta^\lambda \sum_{s=0}^{\infty} \left( \frac{\beta^2 z}{2} \right)^s \frac{1}{(\lambda + 1/2)_{s+1}} \\ &\times \sum_{m=0}^{\mu} \binom{\mu}{m} \left( \frac{\alpha^2 z}{2} \right)^m (\nu - \mu)_{\mu-m} \frac{K_{\lambda+\mu-\nu+1/2+s+m}(z\sqrt{\alpha^2 + \beta^2})}{(\alpha^2 + \beta^2)^{(\lambda+\mu-\nu+1/2+s+m)/2}}. \end{aligned} \quad (4.34)$$

Using the asymptotics of the modified Bessel function [GR07, §8.446]:

$$K_n(z) \sim \frac{1}{2} \frac{n!}{(z/2)^n}, \quad \text{as } n \rightarrow \infty, \quad (4.35)$$

then if  $a_s$  is the  $s^{\text{th}}$  term in the infinite series (4.34), it satisfies:

$$a_s = \mathcal{O} \left\{ s^{\mu-\nu+m} \left( \frac{\beta^2}{\alpha^2 + \beta^2} \right)^s \right\}, \quad \text{as } s \rightarrow \infty. \quad (4.36)$$

If  $\beta < \sqrt{\alpha^2 + \beta^2}$ , then the series is convergent. Since  $\alpha = 0$  corresponds with  $s = 0, 1$  in (2.74), the convergence will be the fastest at the midpoint  $s = 0.5$  of the integration over  $s$ . To accelerate the convergence of the series, we employ the Levin transformation  $t_n^{(0)}(1)$  computed by the algorithm (3.35)–(3.37).

## 4.C Numerical Discussion

In contrast to most other algorithms for three-center nuclear attraction integrals, the numerical discussion for the algorithm based on the formula (4.32) is brief. Since the order of the Bessel function in (4.32) is always an integer, the accuracy and efficiency of this formula is directly related to that of the algorithm for the calculation of a sequence of Bessel functions  $\{K_\ell(\cdot)\}_{\ell \in \mathbb{N}_0}$ . Given that the recurrence relation (2.43) is stable in the upward direction, and given

the reflection formula  $K_\nu(z) = K_{-\nu}(z)$  an efficient algorithm would provide the seed values  $K_0(z)$  and  $K_1(z)$  and compute the remaining values by recurrence. In [PTVF07, §6.5], a fast algorithm for these seed values is derived based on the use of rational minimax approximants. These approximants are rational functions with unknowns that are designed to minimize the maximum error on an interval. The algorithm achieves double precision accuracy by expressing  $K_0(z)$  and  $K_1(z)$  as:

$$K_0(z) \approx \frac{p_4^{(0)}(z^2)}{q_2^{(0)}(1-z^2)} - \log(z) \frac{r_4^{(0)}(z^2)}{s_2^{(0)}(1-z^2)}, \quad (4.37)$$

$$K_1(z) \approx z \left( \frac{p_4^{(1)}(z^2)}{q_2^{(1)}(1-z^2)} + \log(z) \frac{r_4^{(1)}(z^2)}{s_2^{(1)}(1-z^2)} \right) + \frac{1}{z}, \quad (4.38)$$

for  $z \leq 1$ , and:

$$K_0(z) \approx \frac{\exp(-z) u_7^{(0)}(z^{-1})}{\sqrt{z} v_7^{(0)}(z^{-1})}, \quad (4.39)$$

$$K_1(z) \approx \frac{\exp(-z) u_7^{(1)}(z^{-1})}{\sqrt{z} v_7^{(1)}(z^{-1})}, \quad (4.40)$$

for  $z > 1$ , where  $p_n^{(m)}(z)$  stands for a polynomial of degree  $n$  in  $z$  and where  $m = 0, 1$  distinguishes between the polynomial for  $K_0(z)$  and that for  $K_1(z)$ . The coefficients of these approximants are given in the web note [Sof07].

As can be seen in tables 4.1 and 4.2, the calculation time is on the micro second scale. For the first and last two lines of both tables, the parameters require the summation of the infinite series, while for the remaining lines of both tables, the finite summation is required. While still significantly faster than the previous state-of-the-art, the infinite series is approximately 10 times slower than the finite summation. Only values of  $s$  reasonably far from the

endpoints  $s = 0, 1$  are shown. Our numerical experiments suggest that while the finite summation is a generally applicable solution, even with the Levin sequence transformation, the infinite series is not a stable representation for values of  $s$  near the endpoints. It is unclear to the authors exactly how the infinite series representation can be used in large scale computations.

$\nu - \frac{1}{2}$	$n_\gamma$	$n_x$	$\lambda$	$R_1$	$\zeta_1$	$R_2$	$\zeta_2$	$v$	Error	Time $\mu\text{s}$
2	1	0	0	1.00	1.50	1.50	0.50	0.125	0.10D-14	4.199
2	1	1	1	1.00	1.50	1.50	0.50	0.125	0.10D-14	4.240
3	5	4	0	2.00	1.50	2.50	0.50	0.125	0.53D-15	0.374
3	5	5	1	2.00	1.50	2.50	0.50	0.125	0.12D-15	0.428
5	3	2	0	3.00	0.50	2.50	0.50	1.125	0.11D-14	0.457
5	7	5	1	1.00	1.50	3.00	0.50	1.250	0.28D-15	0.511
7	3	3	1	2.00	0.50	3.50	0.50	0.625	0.87D-15	0.670
7	5	4	2	4.00	0.10	3.00	0.50	1.750	0.99D-15	0.590
8	11	3	3	3.00	1.00	3.50	0.50	0.375	0.89D-15	4.912
8	13	4	4	4.00	1.00	6.50	0.50	0.875	0.17D-14	4.215

Average time using  $S\bar{D}_n^{(2,j)}$  of [Saf01]. = 0.502 ms.      Average time using (4.32) = 2.06  $\mu\text{s}$ .  
Ratio = 0.00410.

Table 4.1: Numerical evaluation of the integral  $\mathcal{I}(s)$  for  $s = 0.25$ .

## 4.D Conclusion

In this work, we report the analytical expression (4.2) for the semi-infinite integral bottleneck occurring in the three-center nuclear attraction integrals over  $B$  functions. We describe how to compute the formula to obtain an efficient evaluation in double precision arithmetic. This requires the rational minimax approximants that minimize the maximum error on the interval of evaluation. The numerical tests show the gain in efficiency of approximately  $10^{2.5}$  over the  $S\bar{D}_n^{(2,j)}$  of [Saf01].

$\nu - \frac{1}{2}$	$n_\gamma$	$n_x$	$\lambda$	$R_1$	$\zeta_1$	$R_2$	$\zeta_2$	$v$	Error	Time $\mu\text{s}$
2	1	0	0	1.00	1.50	1.50	0.50	0.625	0.66D-14	8.553
2	1	1	1	1.00	1.50	1.50	0.50	0.625	0.90D-14	6.545
3	5	4	0	2.00	1.50	2.50	0.50	1.375	0.63D-14	0.368
3	5	5	1	2.00	1.50	2.50	0.50	1.375	0.41D-15	0.425
5	3	2	0	3.00	0.50	2.50	0.50	2.375	0.00D+00	0.457
5	7	5	1	1.00	1.50	3.00	0.50	0.250	0.17D-15	0.514
7	3	3	1	2.00	0.50	3.50	0.50	1.125	0.88D-15	0.665
7	5	4	2	4.00	0.10	3.00	0.50	3.250	0.68D-15	0.587
8	11	3	3	3.00	1.00	3.50	0.50	2.125	0.94D-11	6.832
8	13	4	4	4.00	1.00	6.50	0.50	2.375	0.57D-13	5.329

Average time using  $S\bar{D}_n^{(2,j)}$  of [Saf01]. = 0.278 ms.      Average time using (4.32) = 3.03  $\mu\text{s}$ .  
Ratio = 0.0109.

Table 4.2: Numerical evaluation of the integral  $\mathcal{I}(s)$  for  $s = 0.75$ .

# Chapter 5

## On the Use of Conformal Maps for the Acceleration of Convergence of the Trapezoidal Rule and Sinc Numerical Methods

### 5.A Introduction

The trapezoidal rule is one of the most well-known methods in numerical integration. While the composite rule has geometric convergence for periodic functions, in other cases it has been used as the starting point of effective methods, such as Richardson extrapolation [Ric11] and Romberg integration [Rom55]. The geometric convergence breaks down with endpoint singularities, and this issue inspired a different approach to improve on the composite rule. From the Euler-Maclaurin summation formula, it was noted that some form of exponential convergence can be obtained for integrands which vanish at the endpoints,

suggesting that undergoing a variable transformation may well induce this convergence [Sch69,TM71,Ste73]. After this observation, the race was on to determine exactly which variable transformation, and therefore which decay rate, is optimal. Numerical experiments showed the exceptional promise of rules such as the tanh substitution [EFH84], the erf substitution [TM73], the IMT rule [IMT87], and the tanh-sinh substitution [TM74], among others [Mor78]. But exactly which one is optimal, and in which setting?

Using a functional analysis approach, this question was beautifully answered by establishing the optimality of a double exponential endpoint decay rate for the trapezoidal rule on the real line for approximating analytic integrands [Sug97]. The domain of analyticity is described in terms of a strip of maximal width  $\pi$  centred on the real axis in the complex plane. This optimality also prescribed the optimal step size and a near-linear convergence rate  $\mathcal{O}(e^{-kN/\log N})$ , where  $N$  is the number of sample points and  $k$  is a constant proportional to the strip width.

The results allowed for displays of strong performance for integrals with integrable endpoint singularities without changing the rule in any way [Mor85, Mor05,MS01,SM04]. The double exponential transformation was also adapted to Fourier and general oscillatory integrals in [OM91,OM99]. Recognizing the trapezoidal rule as the integration of a Sinc expansion of the integrand, the double exponential advocates adapted their analysis to Sinc approximations [Sug03], and also to all the numerical methods therewith derived, such as Sinc-Galerkin and Sinc-collocation methods [HS99,Sug02,NMMS05] for initial and boundary value problems, Sinc indefinite integration [TSM04], iterated integration [MS05], and Sinc-collocation for integral equations [MNMS05,OMS10], all obtaining the near-linear convergence rate  $\mathcal{O}(e^{-kN/\log N})$ . More

recently, the researchers then focused on improving the original convergence results by developing more precise upper estimates on the error given bounds on the function [TSMM09, TSM09, OMS13, OTMS13, TOMS13].

In this work, we report an improvement of the trapezoidal rule in the context of a finite number of singularities – of any kind – near the contour of integration. This problem has been considered before, in Gaussian quadrature and in Sinc quadrature [Mon86, Bia89, Gau13]. The prevailing philosophy seems to be to characterize singularities as specifically as possible, then account for them by either adding terms from Cauchy’s residue theorem to the approximation or by modifying the weights and abscissas. While the examples and applications show exceptional performance of the algorithms, the case of general singularities is still untreated. In the optimal double exponential framework, singularities near the integration contour may reduce the width of the strip of analyticity about the real axis. As the double exponential decay rate is typically induced by a variable transformation, we seek to find variable transformations which place the threatening singularities on the upper and lower edges of the maximal strip of width  $\pi$ . In this work, such variable transformations are conformal maps which maximize the convergence rate despite the presence of the singularities.

The idea of using conformal maps to speed up numerical computations is not new. In fact, it was recently pioneered by Tee and Trefethen [TT06], Hale and Trefethen [HT08], Hale and Tee [HT09], and Hale’s so-titled Ph. D. thesis [Hal09]. Inspired by this work, we investigate the use of the Schwarz-Christoffel map from the strip of width  $\pi$  to a polygonally bounded region, with the possibility of some sides being infinite. In this way, the edges of the strip of width  $\pi$  contain the pre-images of the function’s singularities, their

possible branches, and other objects limiting analyticity. In the case dealt with in [HT09], an algorithm is constructed to solve the Schwarz-Christoffel parameter problem, and the integral definition of the Schwarz-Christoffel map is simplified by partial fraction decomposition.

For the strip map variation of the Schwarz-Christoffel map, the explicit integration of the Schwarz-Christoffel map could not be done [HT09], so in this work, an approximate map is constructed based on polynomial adjustments to the sinh map. We choose the sinh map because it appears in every double exponential map of the canonical finite, infinite, and semi-infinite domains. The polynomial adjustments add exactly enough parameters to locate a finite number of pre-images of singularities on the edges of the maximal strip of width  $\pi$ , and the parameter problem – the determination of such polynomial adjustments – is in complete analogy with the Schwarz-Christoffel parameter problem. However, the approximate map is significantly less expensive to evaluate, and therefore well-paired with the double exponential transformation for high precision numerical experiments.

The problem of poles limiting analyticity has been noted in [SM04], where Sugihara and Matsuo show the double exponential Sinc expansion of the function:

$$f(x) = \frac{x(1-x)e^{-x}}{(1/2)^2 + (x-1/2)^2}, \quad x \in [0, 1], \quad (5.1)$$

is not as efficient as methods of polynomial interpolation. To demonstrate how simple our nonlinear program can be, we note that while the original double exponential transformation for the problem is  $\phi(t) = \frac{1}{2} \tanh(\frac{\pi}{2} \sinh t) + \frac{1}{2}$ , the optimized map is  $\phi(t) = \frac{1}{2} \tanh(\frac{\pi}{4} \sinh t) + \frac{1}{2}$ , and the convergence rate is approximately tripled.

We demonstrate the merits of our algorithm on four integrals, each with its own combination of singularities. In these cases, the algorithm obtains approximately 2.5–4 times as many correct digits as a naïve double exponential transformation for the same number of function evaluations. The algorithm is applied to optimize the solution of a second order linear boundary value problem with endpoint singularities as well as two poles very near the solution interval. After this, the algorithm also shows its merit in the evaluation of an  $m$ -dimensional expectation and in the evaluation of highly oscillatory integrals.

**Remark:** The Julia code used for the numerical results is available from [Sle].

## 5.B Quadrature and Sinc methods by variable transformation

Using a variable transformation to induce exponential decay at the endpoints is first performed in [TM73] and it is extended to double exponential decay in [TM74]. They find that variable transformations that induce double exponential decay at the endpoints perform better than single exponential transformations.

For infinite and semi-infinite integrals with or without pre-existing exponential decay, various other transformations have been proposed to induce double exponential decay. Examples from [TSMM09] are included in table 5.1.

We follow closely the rigorous derivations in [Sug97,Sug03] of the optimality of the trapezoidal rule and Sinc numerical methods for functions with double exponential decay as  $x \rightarrow \pm\infty$ . Let  $d$  be a positive number and let  $\mathcal{D}_d$  denote

Interval	Single Exponential	Double Exponential
$[-1, 1]$	$\tanh(t/2)$	$\tanh(\frac{\pi}{2} \sinh t)$
$(-\infty, +\infty)$	$\sinh(t)$	$\sinh(\frac{\pi}{2} \sinh t)$
$[0, +\infty)$	$\log(\exp(t) + 1)$	$\log(\exp(\frac{\pi}{2} \sinh t) + 1)$
$[0, +\infty)$	$\exp(t)$	$\exp(\frac{\pi}{2} \sinh t)$

Table 5.1: Variable transformations  $\phi(t)$  for endpoint decay.

the strip region of width  $2d$  about the real axis:

$$\mathcal{D}_d = \{z \in \mathbb{C} : |\operatorname{Im} z| < d\}. \quad (5.2)$$

Let  $\omega(z)$  be a non-vanishing function defined on the region  $\mathcal{D}_d$ , and define the Hardy space  $H^\infty(\mathcal{D}_d, \omega)$  by [Har15]:

$$H^\infty(\mathcal{D}_d, \omega) = \{f : \mathcal{D}_d \rightarrow \mathbb{C} \mid f(z) \text{ is analytic in } \mathcal{D}_d, \text{ and } \|f\| < +\infty\}, \quad (5.3)$$

where the norm of  $f$  is given by:

$$\|f\| = \sup_{z \in \mathcal{D}_d} \left| \frac{f(z)}{\omega(z)} \right|. \quad (5.4)$$

Consequentially, for  $\omega(z)$  that decays double exponentially, the functions in  $H^\infty(\mathcal{D}_d, \omega)$  decay double exponentially as well. Let us consider the  $N(= 2n + 1)$ -point trapezoidal rule for the interval  $(-\infty, +\infty)$ :

$$\int_{-\infty}^{+\infty} f(x) dx \approx h \sum_{k=-n}^{+n} f(k h), \quad (5.5)$$

where the mesh size  $h$  is suitably chosen for a given positive integer  $n$ . For the

trapezoidal rule, let  $\mathcal{E}_{N,h}^{\text{T}}(H^\infty(\mathcal{D}_d, \omega))$  denote the error norm in  $H^\infty(\mathcal{D}_d, \omega)$ :

$$\mathcal{E}_{N,h}^{\text{T}}(H^\infty(\mathcal{D}_d, \omega)) = \sup_{\|f\| \leq 1} \left| \int_{-\infty}^{+\infty} f(x) dx - h \sum_{k=-n}^{+n} f(kh) \right|. \quad (5.6)$$

Let  $B(\mathcal{D}_d)$ , originally introduced in [Ste73], denote the family of all functions  $f$  analytic in  $\mathcal{D}_d$  such that:

$$\mathcal{N}_1(f, \mathcal{D}_d) = \int_{\partial \mathcal{D}_d} |f(z)| dz < +\infty. \quad (5.7)$$

**Theorem 5.1** (Sugihara [Sug97]): *Suppose that the function  $\omega(z)$  satisfies the following three conditions:*

1.  $\omega(z) \in B(\mathcal{D}_d)$ ;
2.  $\omega(z)$  does not vanish at any point in  $\mathcal{D}_d$  and takes real values on the real axis;
3. the decay rate of  $\omega(z)$  on the real axis is specified by:

$$\alpha_1 \exp(-(\beta|x|^\rho)) \leq |\omega(x)| \leq \alpha_2 \exp(-(\beta|x|^\rho)), \quad x \in \mathbb{R}, \quad (5.8)$$

where  $\alpha_1, \alpha_2, \beta > 0$  and  $\rho \geq 1$ .

Then:

$$\mathcal{E}_{N,h}^{\text{T}}(H^\infty(\mathcal{D}_d, \omega)) \leq C_{d,\omega} \exp\left(-(\pi d \beta N)^{\frac{\rho}{\rho+1}}\right), \quad (5.9)$$

where  $N = 2n + 1$ , the mesh size  $h$  is chosen optimally as:

$$h = (2\pi d)^{\frac{1}{\rho+1}} (\beta n)^{-\frac{\rho}{\rho+1}}, \quad (5.10)$$

and  $C_{d,\omega}$  is a constant depending on  $d$  and  $\omega$ .

**Theorem 5.2** (Sugihara [Sug97]): *Suppose that the function  $\omega(z)$  satisfies the following three conditions:*

1.  $\omega(z) \in B(\mathcal{D}_d)$ ;
2.  $\omega(z)$  does not vanish at any point in  $\mathcal{D}_d$  and takes real values on the real axis;
3. the decay rate of  $\omega(z)$  on the real axis is specified by:

$$\alpha_1 \exp(-\beta_1 e^{\gamma|x|}) \leq |\omega(x)| \leq \alpha_2 \exp(-\beta_2 e^{\gamma|x|}), \quad x \in \mathbb{R}, \quad (5.11)$$

where  $\alpha_1, \alpha_2, \beta_1, \beta_2, \gamma > 0$ .

Then:

$$\mathcal{E}_{N,h}^T(H^\infty(\mathcal{D}_d, \omega)) \leq C_{d,\omega} \exp\left(-\frac{\pi d \gamma N}{\log(\pi d \gamma N / \beta_2)}\right), \quad (5.12)$$

where  $N = 2n + 1$ , the mesh size  $h$  is chosen optimally as:

$$h = \frac{\log(2\pi d \gamma n / \beta_2)}{\gamma n}, \quad (5.13)$$

and  $C_{d,\omega}$  is a constant depending on  $d$  and  $\omega$ .

Since the trapezoidal rule is equivalent to the integration of the Sinc expansion of a function [Ste81], the entire process of analyzing the convergence rates with different endpoint decay can also be useful for the Sinc expansion of a function, with subtle differences that arise in the mesh size and convergence rates. Let us consider the  $N(= 2n + 1)$ -point Sinc approximation of a function

on the real line:

$$f(x) \approx \sum_{j=-n}^{+n} f(jh)S(j,h)(x), \quad (5.14)$$

where  $S(j,h)(x)$  is the so-called Sinc function:

$$S(j,h)(x) = \frac{\sin[\pi(x/h - j)]}{\pi(x/h - j)}, \quad (5.15)$$

and where the step size  $h$  is suitably chosen for a given positive integer  $n$ . From l'Hôpital's rule, it can easily be seen that the Sinc functions are mutually orthogonal at the so-called Sinc points  $x_k = kh$ :

$$S(j,h)(kh) = \delta_{k,j}, \quad (5.16)$$

where  $\delta_{k,j}$  is the Kronecker delta [AS65].

For the Sinc approximation, let  $\mathcal{E}_{N,h}^{\text{Sinc}}(H^\infty(\mathcal{D}_d, \omega))$  denote the error norm in  $H^\infty(\mathcal{D}_d, \omega)$ :

$$\mathcal{E}_{N,h}^{\text{Sinc}}(H^\infty(\mathcal{D}_d, \omega)) = \sup_{\|f\| \leq 1} \left\{ \sup_{x \in \mathbb{R}} \left| f(x) - \sum_{j=-n}^{+n} f(jh) S(j,h)(x) \right| \right\}. \quad (5.17)$$

**Theorem 5.3** (Sugihara [Sug03]): *Suppose that the function  $\omega(z)$  satisfies the following three conditions:*

1.  $\omega(z) \in B(\mathcal{D}_d)$ ;
2.  $\omega(z)$  does not vanish at any point in  $\mathcal{D}_d$  and takes real values on the real axis;

3. the decay rate of  $\omega(z)$  on the real axis is specified by:

$$\alpha_1 \exp(-(\beta|x|^\rho)) \leq |\omega(x)| \leq \alpha_2 \exp(-(\beta|x|^\rho)), \quad x \in \mathbb{R}, \quad (5.18)$$

where  $\alpha_1, \alpha_2, \beta > 0$  and  $\rho \geq 1$ .

Then:

$$\mathcal{E}_{N,h}^{\text{Sinc}}(H^\infty(\mathcal{D}_d, \omega)) \leq C_{d,\omega} N^{\frac{1}{\rho+1}} \exp\left(-\left(\frac{\pi d \beta N}{2}\right)^{\frac{\rho}{\rho+1}}\right), \quad (5.19)$$

where  $N = 2n + 1$ , the mesh size  $h$  is chosen optimally as:

$$h = (\pi d)^{\frac{1}{\rho+1}} (\beta n)^{-\frac{\rho}{\rho+1}}, \quad (5.20)$$

and  $C_{d,\omega}$  is a constant depending on  $d$  and  $\omega$ .

**Theorem 5.4** (Sugihara [Sug03]): *Suppose that the function  $\omega(z)$  satisfies the following three conditions:*

1.  $\omega(z) \in B(\mathcal{D}_d)$ ;
2.  $\omega(z)$  does not vanish at any point in  $\mathcal{D}_d$  and takes real values on the real axis;
3. the decay rate of  $\omega(z)$  on the real axis is specified by:

$$\alpha_1 \exp(-\beta_1 e^{\gamma|x|}) \leq |\omega(x)| \leq \alpha_2 \exp(-\beta_2 e^{\gamma|x|}), \quad x \in \mathbb{R}, \quad (5.21)$$

where  $\alpha_1, \alpha_2, \beta_1, \beta_2, \gamma > 0$ .

Then:

$$\mathcal{E}_{N,h}^{\text{Sinc}}(H^\infty(\mathcal{D}_d, \omega)) \leq C_{d,\omega} \exp\left(-\frac{\pi d \gamma N}{2 \log(\pi d \gamma N / (2\beta_2))}\right), \quad (5.22)$$

where  $N = 2n + 1$ , the mesh size  $h$  is chosen optimally as:

$$h = \frac{\log(\pi d \gamma n / \beta_2)}{\gamma n}, \quad (5.23)$$

and  $C_{d,\omega}$  is a constant depending on  $d$  and  $\omega$ .

Last but not least, there is the nonexistence theorem, which provides a fundamental bound for the proposed optimization approach.

**Theorem 5.5** (Sugihara [Sug97]): *There exists no function  $\omega(z)$  that satisfies the following three conditions:*

1.  $\omega(z) \in B(\mathcal{D}_d)$ ;
2.  $\omega(z)$  does not vanish at any point in  $\mathcal{D}_d$  and takes real values on the real axis;
3. the decay rate on the real axis of  $\omega(z)$  is specified as:

$$\omega(x) = \mathcal{O}\left(\exp(-\beta e^{\gamma|x|})\right), \quad \text{as } |x| \rightarrow \infty, \quad (5.24)$$

where  $\beta > 0$ , and  $d\gamma > \pi/2$ .

## 5.C Maximizing the convergence rates

From the previous theorems 5.2 and 5.4 on the convergence rates of the trapezoidal rule with a prescribed decay at the endpoints and the nonexistence

theorem 5.5 of analytic functions with double exponential decay in too wide a strip, we may ask the following question. How can we use a conformal map  $\phi$  to maximize the convergence rate of the trapezoidal rule:

$$\int_{-\infty}^{\infty} f(\phi(t))\phi'(t) dt \approx h \sum_{k=-n}^{+n} f(\phi(kh))\phi'(kh), \quad (5.25)$$

or the Sinc approximation:

$$f(x) \approx \sum_{j=-n}^{+n} f(\phi(jh))S(j,h)(\phi^{-1}(x)), \quad (5.26)$$

despite the singularities of  $f \in \mathbb{C}$  which limit its domain of analyticity? To formulate this problem mathematically, let  $\Phi_{\text{ad}}$  be the admissible space of all functions  $\phi$  satisfying the conditions of theorems 5.2 and 5.4:

$$\Phi_{\text{ad}} = \left\{ \begin{array}{l} \phi : f(\phi(\cdot))\phi'(\cdot) \in H^\infty(\mathcal{D}_d, \omega) \text{ for some } d > 0, \\ \text{and for some } \omega \text{ such that:} \\ 1. \omega(z) \in B(\mathcal{D}_d); \\ 2. \omega(z) \text{ does not vanish at any point in } \mathcal{D}_d \\ \text{and takes real values on the real axis;} \\ 3. \alpha_1 \exp(-\beta_1 e^{\gamma|x|}) \leq |\omega(x)| \leq \alpha_2 \exp(-\beta_2 e^{\gamma|x|}), \\ x \in \mathbb{R}, \text{ where } \alpha_1, \alpha_2, \beta_1, \beta_2, \gamma > 0. \end{array} \right\}$$

We wish to find the  $\phi \in \Phi_{\text{ad}}$  so that the convergence rates are maximized:

$$\underbrace{\operatorname{argmax}_{\phi \in \Phi_{\text{ad}}} \left( \frac{\pi d \gamma N}{\log(\pi d \gamma N / \beta_2)} \right)}_{\text{Convergence Theorem 5.2}} \quad \text{subject to} \quad \underbrace{d \gamma \leq \frac{\pi}{2}}_{\text{Nonexistence Theorem 5.5}}$$

$$\underbrace{\operatorname{argmax}_{\phi \in \Phi_{\text{ad}}} \left( \frac{\pi d \gamma N}{2 \log(\pi d \gamma N / (2\beta_2))} \right)}_{\text{Convergence Theorem 5.4}} \quad \text{subject to} \quad \underbrace{d \gamma \leq \frac{\pi}{2}}_{\text{Nonexistence Theorem 5.5}}$$

As infinite-dimensional optimization problems for  $\phi$ , these are challenging problems. However, the convergence rates of theorems 5.2 and 5.4 are asymptotic ones and therefore it is of equivalent interest to investigate the asymptotic solutions to the problem. Consider the asymptotic problems:

$$\begin{aligned} \frac{\pi d \gamma N}{\log(\pi d \gamma N / \beta_2)} &= \frac{\pi d \gamma N}{\log N + \log(\pi d \gamma / \beta_2)}, \\ &\sim \frac{\pi d \gamma N}{\log N}, \quad \text{as } N \rightarrow \infty, \end{aligned} \quad (5.27)$$

$$\begin{aligned} \frac{\pi d \gamma N}{2 \log(\pi d \gamma N / (2\beta_2))} &= \frac{\pi d \gamma N}{2 \log N + 2 \log(\pi d \gamma / (2\beta_2))}, \\ &\sim \frac{\pi d \gamma N}{2 \log N}, \quad \text{as } N \rightarrow \infty. \end{aligned} \quad (5.28)$$

Then, the linear appearance of  $d\gamma$  leads directly to the following result.

**Theorem 5.6:** *Let  $\Phi_{\text{as,ad}} = \{\Phi_{\text{ad}} : d\gamma = \pi/2\}$  be the asymptotically admissible subspace of the admissible space  $\Phi_{\text{ad}}$ . Then  $\exists \phi_{\text{as}} \in \Phi_{\text{as,ad}}$  such that:*

$$\mathcal{E}_{N,h}^{\text{T}}(H^\infty(\mathcal{D}_d, \omega)) \leq C_{d,\omega} \exp\left(-\frac{\pi^2 N}{2 \log(\pi^2 N / 2\beta_2)}\right), \quad (5.29)$$

where  $N = 2n + 1$ , the mesh size  $h$  is chosen optimally as:

$$h = \frac{\log(\pi^2 n / \beta_2)}{\gamma n}, \quad (5.30)$$

and  $C_{d,\omega}$  is a constant depending on  $d$  and  $\omega$ . This same  $\phi_{\text{as}}$  ensures that:

$$\mathcal{E}_{N,h}^{\text{Sinc}}(H^\infty(\mathcal{D}_d, \omega)) \leq C_{d,\omega} \exp\left(-\frac{\pi^2 N}{4 \log(\pi^2 N / 4\beta_2)}\right), \quad (5.31)$$

where  $N = 2n + 1$ , the mesh size  $h$  is chosen optimally as:

$$h = \frac{\log(\pi^2 n / 2\beta_2)}{\gamma n}, \quad (5.32)$$

and  $C_{d,\omega}$  is a constant depending on  $d$  and  $\omega$ .

The implication of such a theorem is that suitable mappings  $\phi$  can be found which maximize the convergence rates by neutering the terrible effects of singularities near the approximation interval. In this section, we find such mappings by starting with the observation that in all of the maps in table 5.1 for the finite, semi-infinite, and infinite canonical domains, an elementary map is composed with the sinh map. Therefore, it seems as though studying the sinh map, or some modification thereof, will be the best place to start.

Let  $f$  have a finite number of singularities located at the points  $\{\delta_k \pm i\epsilon_k\}_{k=1}^n$ .

The four maps in table 5.1 can be written as the composition of:

$$\psi(z) = \tanh(z), \quad \psi^{-1}(z) = \tanh^{-1}(z), \quad (5.33)$$

$$\psi(z) = \sinh(z), \quad \psi^{-1}(z) = \sinh^{-1}(z), \quad (5.34)$$

$$\psi(z) = \log(e^z + 1), \quad \psi^{-1}(z) = \log(e^z - 1), \quad (5.35)$$

$$\psi(z) = \exp(z), \quad \psi^{-1}(z) = \log(z). \quad (5.36)$$

with the  $\frac{\pi}{2}$  sinh function. In any of these cases, let a finite number of singularities of  $f$  be transformed as  $\{\tilde{\delta}_k \pm i\tilde{\epsilon}_k\}_{k=1}^n$  as the ordered set of  $\{\psi^{-1}(\delta_k \pm i\epsilon_k)\}_{k=1}^n$ , where  $\tilde{\delta}_1 < \tilde{\delta}_2 < \dots < \tilde{\delta}_n$ .

The sinh function is a conformal map from the strip  $\mathcal{D}_{\frac{\pi}{2}}$  to the entire complex plane with two branch cuts emanating outward from the points  $\pm i$ . It is actually the most rudimentary Schwarz-Christoffel formula mapping from the strip  $\mathcal{D}_{\frac{\pi}{2}}$  to the entire complex plane [HT90] with those two aforementioned branches. Let  $g$  map the strip  $\mathcal{D}_{\frac{\pi}{2}}$  to the polygonally bounded region  $P$  having vertices  $\{w_k\}_{k=1}^n = \{\tilde{\delta}_1 + i\tilde{\epsilon}_1, \dots, \tilde{\delta}_n + i\tilde{\epsilon}_n\}$  and interior angles  $\{\pi\alpha_k\}_{k=1}^n$ . Let also  $\frac{\pi}{2}\alpha_{\pm}$  be the divergence angles at the left and right ends of the strip  $\mathcal{D}_{\frac{\pi}{2}}$ . Then the function [HT90]:

$$g(z) = A + C \int^z e^{(\alpha_- - \alpha_+)\zeta} \prod_{k=1}^n [\sinh(\zeta - z_k)]^{\alpha_k - 1} d\zeta, \quad (5.37)$$

where  $z_k = g(w_k)$  and for some  $A$  and  $C$  maps the interior of the top half of the strip  $\mathcal{D}_{\frac{\pi}{2}}$  to the interior of the polygon  $P$ . The solution of the constants  $A$ ,  $C$ , and  $\{z_k\}_{k=1}^n$  is known as the Schwarz-Christoffel parameter problem.

Figure 5.1 shows an example of the Schwarz-Christoffel map for the polygonal restrictions on  $\mathbb{C}$  due to the possible singularities of  $f$ . The Schwarz-

Christoffel map is actually the exact solution of the problem of maximizing the convergence rates, as it maps points on the top and bottom of the strip  $\mathcal{D}_{\frac{\pi}{2}}$  to the singularities. However, the entire process is computationally intensive. Firstly, the nonlinear system of equations of the Schwarz-Christoffel parameter problem needs to be solved, and secondly, the map is defined as an integral. The parameter problem can be prohibitive to solve, requiring thousands of integrations of the map function. Also, the integral only has an analytical expression for a polygon with one finite vertex, and this gives the sinh map. The Schwarz-Christoffel Toolbox in MATLAB [Tre80,TD98,DT02] is used to solve for the maps in figure 5.1, and provides a precision of approximately  $10^{-8}$  for a computation time on the order of one minute. In figure 5.1 and subsequent figures, the plots show the mapping of lines with constant imaginary values between  $-i\pi/2$  and  $+i\pi/2$  via the conformal map from the strip, then the composition of this conformal map with one of the maps  $\psi(z)$  of (5.33)–(5.36). Were it only for the difficulties posed by the Schwarz-Christoffel parameter problem, this approach may have some promise. However, the major problem is that even after the parameter problem is solved, the map itself is defined as an integral and requires a large computational effort compared to the following proposed approach.

Fortunately, due to the framework of the double exponential transformation, we can make a polynomial adjustment to the sinh map while still retaining a variable transformation  $\phi$  which induces double exponential decay. For any real values of the  $n + 1$  parameters  $\{u_k\}_{k=0}^n$ , the function:

$$h(t) = u_0 \sinh(t) + \sum_{j=1}^n u_j t^{j-1}, \quad u_0 > 0, \quad (5.38)$$

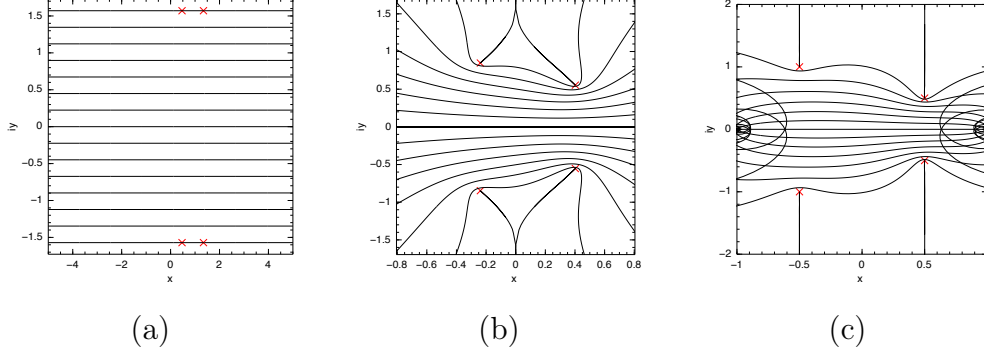


Figure 5.1: In (a) the plot of the strip  $\mathcal{D}_{\frac{\pi}{2}}$  with singularities located on the boundary, in (b) the resulting Schwarz-Christoffel map, and in (c) a tanh map of the Schwarz-Christoffel map. In all three cases, the crosses track the singularities  $\delta_1 \pm i\epsilon_1 = -1/2 \pm i$  and  $\delta_2 \pm i\epsilon_2 = 1/2 \pm i/2$ . For the sake of comparison, an integral with these singularities is treated in example 5.D.1.

still grows single exponentially. Therefore, the composition  $\psi(h(t))$  for any  $\psi$  in (5.33)–(5.36) still induces a double exponential variable transformation. The benefit of choosing such functions is that we now have sufficient parameters which we can use to ensure the pre-images of the singularities  $\{\tilde{\delta}_k \pm i\tilde{\epsilon}_k\}_{k=1}^n$  reside on the top and bottom edges of the strip  $\mathcal{D}_{\frac{\pi}{2}}$ , respectively. This is done by solving the system of equations:

$$h(x_k + i\pi/2) = \tilde{\delta}_k + i\tilde{\epsilon}_k, \quad \text{for } k = 1, \dots, n. \quad (5.39)$$

This is a system of  $n$  complex equations for the  $2n + 1$  unknowns  $\{u_k\}_{k=0}^n$  and the  $x$ -coordinates of the pre-images of the singularities  $\{x_k\}_{k=1}^n$ . Since there is one more unknown than equations, we are able to maximize the value of  $u_0$ , which is proportional to  $\beta_2$  in every case. Summing all  $n$  equations of (5.39)

leads to the nonlinear program:

$$\begin{aligned} \text{maximize } u_0 & \left( = \frac{\sum_{k=1}^n \left\{ \tilde{\epsilon}_k - \operatorname{Im} \sum_{j=1}^n u_j (x_k + i\pi/2)^{j-1} \right\}}{\sum_{k=1}^n \cosh(x_k)} \right), \\ \text{subject to } h(x_k + i\pi/2) & = \tilde{\delta}_k + i\tilde{\epsilon}_k, \quad \text{for } k = 1, \dots, n. \end{aligned} \quad (5.40)$$

Because the maximization condition is obtained by summing the constraint equations, we have one additional degree of freedom in the program (5.40). In order to save from premature convergence, we impose *ad hoc* the condition:

$$\begin{cases} x_1 = 0, & \text{for } n = 1, \\ |x_1 + x_n| \leq \bar{x}, & \text{for } n \geq 2, \end{cases} \quad (5.41)$$

where  $\bar{x}$  is a parameter which ensures the singularities stay reasonably close to the origin. In all our examples, we set  $\bar{x} = 20$  which is sufficient. This nonlinear program is in close analogy to the Schwarz-Christoffel parameter problem. However, this method has many advantages over the Schwarz-Christoffel formula. Firstly, the map  $h(t)$  is defined in terms of elementary functions and not as an integral. Secondly, the accuracy of the values of  $\{u_k\}_{k=0}^n$  does not need to equal the accuracy required of the map, allowing the map (5.38) to be evaluated in arbitrary precision. One disadvantage of this method is that the map is an approximate solution to the original problem. Therefore, while the strip width will indeed be  $2d = \pi$ , we can expect a smaller than optimal  $\beta_2$ . Nevertheless, given that  $\beta_2$  only has a secondary effect on the convergence rates, according to theorem 5.6, this is a small price to pay to obtain a solution method that emulates the Schwarz-Christoffel formula while being amenable

to arbitrary precision calculations.

A nonlinear program without any *a priori* information on the solution requires an iterative method for solving the parameter problem (5.40). An iterative method also requires a close initial guess to converge to the solution. To obtain an initial guess, we let  $\bar{\epsilon}$  be the smallest of  $\{\tilde{\epsilon}_k\}_{k=1}^n$  and  $\bar{\delta}$  be the  $\tilde{\delta}_k$  of the same index. Then the nonlinear program with singularities  $\{\bar{\delta} + i\tilde{\epsilon}_k\}_{k=1}^n$  is exactly solved by:

$$h(t) = \bar{\epsilon} \sinh t + \bar{\delta}. \quad (5.42)$$

A homotopy  $\mathcal{H}(t)$  is then constructed between the solution with singularities  $\{\bar{\delta} + i\tilde{\epsilon}_k\}_{k=1}^n$  at  $t = 0$  and the solution with singularities  $\{\tilde{\delta}_k + i\tilde{\epsilon}_k\}_{k=1}^n$  at  $t = 1$ . The interval  $t \in [0, 1]$  is discretized, and the nonlinear program is solved with singularities that vary linearly between the two problems and initial guesses from the solution of the previous iterate. Figure 5.2 shows this solution process.

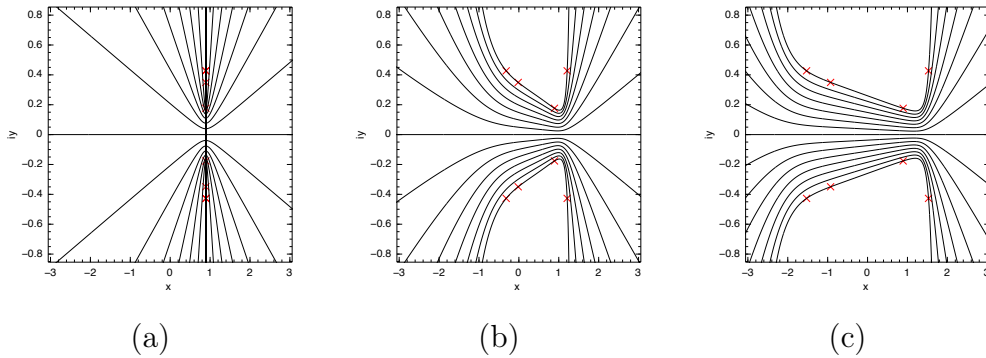


Figure 5.2: In (a) the exact solution  $\mathcal{H}(0)$ , in (b) the solution  $\mathcal{H}(1/2)$ , and in (c) the desired solution  $\mathcal{H}(1)$ . An integral with these singularities is treated in example 5.D.2.

In practice, the locations of a function’s singularities may not be known in advance. This can result from either incomplete theoretical information, or a non-local nature of singularities, such as branch cuts or “numerically singular”

terms such as the error function, which while entire, is unbounded off the real axis [HT09]. In [TT06], an adaptive approach is taken to approximating the nearby singularities, whereby the interpolatory Chebyshev-Padé approximants are constructed, and approximants' poles are taken as the loci of the singularities of the underlying function. The map is then modified to exclude these points, and the iteration of this process is the adaptive algorithm.

Because we are working with Sinc approximations, and Sinc points, we modify their algorithm to make efficient use of the information we have at hand, i.e. the Sinc sampling of the function.

**Definition:** Let  $x_k = k h$  be the Sinc points and let  $f(x_k)$  be the  $N(= 2n + 1)$  Sinc sampling of  $f$ . Then for  $r + s \leq 2n$ , the Sinc-Padé approximants  $\{r/s\}_f(x)$  are given by:

$$\{r/s\}_f(x) = \frac{\sum_{i=0}^r p_i x^i}{1 + \sum_{j=1}^s q_j x^j}, \quad (5.43)$$

where the  $r + s + 1$  coefficients solve the system:

$$\sum_{i=0}^r p_i x_k^i - f(x_k) \sum_{j=1}^s q_j x_k^j = f(x_k), \quad (5.44)$$

for  $k = -\lfloor \frac{r+s}{2} \rfloor, \dots, \lceil \frac{r+s}{2} \rceil$ .

For the Chebyshev-Padé approximants, the inverse cosine distribution of sample points leads to a stable linear system and the degrees of the numerator and denominator can add to equate the number of collocation points. For the Sinc-Padé approximants, double exponential growth of the sample points

renders the system highly ill-conditioned. Therefore, these indices must be decoupled from  $n$  and the function must only be sampled near the centre. Our adaptive algorithm is based on the following principles:

1. Sinc-Padé approximants are useful only when the Sinc approximation obtains some degree of accuracy,
2. Sinc-Padé approximants are useful for  $r, s = \mathcal{O}(\log n)$  as  $n \rightarrow \infty$ .

The first principle follows from observations of our numerical experiments, and we found that a relative error of approximately  $10^{-3}$  in the Sinc approximation allows for a useful Sinc-Padé approximant. The second principle follows from the observation that we need not identify many singularities to remove, and that even at a logarithmic increase, the sample points tend to infinity at a single exponential rate, implying that they will ultimately cover the real line. These principles form the basis of the following algorithm.

**Algorithm 5.6.1:**

```

Set  $n = 1$ ;
while |Relative Error|  $\geq 10^{-3}$  do
    Double  $n$  and naïvely compute the  $n^{\text{th}}$  double exponential approximation;
end;
while |Relative Error|  $\geq \epsilon$  do
    Compute the poles of the Sinc-Padé approximant;
    Solve the nonlinear program (5.40) for  $h(t)$ ;
    Double  $n$  and compute the  $n^{\text{th}}$  adapted optimized approximation;
end.

```

## 5.D Examples

In this section, we will use the proposed nonlinear program (5.40) to maximize the convergence rate of the double exponential transformation. We compare the results of the trapezoidal rule with single, double, and optimized double exponential variable transformations on three integrals using arbitrary precision arithmetic. On a fourth integral, we use the adaptive algorithm 5.6.1 to approximate nearby singularities.

### 5.D.1 Example: endpoint and complex singularities

We wish to evaluate the integral:

$$\int_{-1}^1 \frac{\exp((\epsilon_1^2 + (x - \delta_1)^2)^{-1}) \log(1 - x)}{(\epsilon_2^2 + (x - \delta_2)^2) \sqrt{1 + x}} dx = -2.04645 \dots, \quad (5.45)$$

for the values  $\delta_1 + i\epsilon_1 = -1/2 + i$  and  $\delta_2 + i\epsilon_2 = 1/2 + i/2$ . This integral has two different endpoint singularities and two pairs of complex conjugate singularities of different types near the integration axis. Table 5.2 summarizes the variable transformations used and the parameters in the theorems 5.1 and 5.2.

	Single	Double	Optimized Double
$\phi(t)$	$\tanh(t/2)$	$\tanh\left(\frac{\pi}{2} \sinh(t)\right)$	$\tanh(h(t))$
$\rho$ or $\gamma$	1	1	1
$\beta$ or $\beta_2$	1/2	$\pi/4$	0.06956
$d$	1.10715	0.34695	$\pi/2$

Table 5.2: Transformations and parameters for (5.45).

In addition, the optimized transformation is given by:

$$h(t) \approx 0.13912 \sinh(t) + 0.19081 + 0.21938 t. \quad (5.46)$$

Figure 5.3 shows the three stages of the optimized double exponential map.

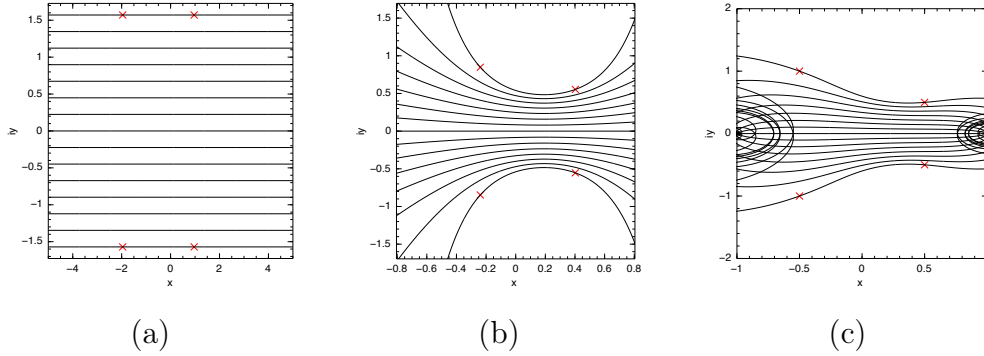


Figure 5.3: In (a) the plot of the strip  $\mathcal{D}_{\pi/2}$  with singularities located on the boundary, in (b) the optimized map  $h(\cdot)$ , and in (c) the optimized DE map. In all three cases, the crosses track the singularities.

In figure 5.4 (a), the integrand of (5.45) is shown, and in figure 5.4 (b), the logarithm of the relative errors of the trapezoidal rule of order  $n$  with single, double, and optimized double exponential variable transformations are plotted. The increase in convergence rate using the optimized variable transformation is a significant increase in efficiency over the double exponential transformation.

## 5.D.2 Example: eight different complex conjugate singularities

We wish to evaluate the integral:

$$\int_{-\infty}^{+\infty} \frac{\exp(10(\epsilon_1^2 + (x - \delta_1)^2)^{-1}) \cos(10(\epsilon_2^2 + (x - \delta_2)^2)^{-1})}{(\epsilon_3^2 + (x - \delta_3)^2) \sqrt{\epsilon_4^2 + (x - \delta_4)^2}} dx = 15.01336 \dots, \quad (5.47)$$

for the values  $\delta_1 + i\epsilon_1 = -2 + i$ ,  $\delta_2 + i\epsilon_2 = -1 + i/2$ ,  $\delta_3 + i\epsilon_3 = 1 + i/4$ , and  $\delta_4 + i\epsilon_4 = 2 + i$ . Table 5.3 summarizes the variable transformations used and the parameters in the theorems 5.1 and 5.2.

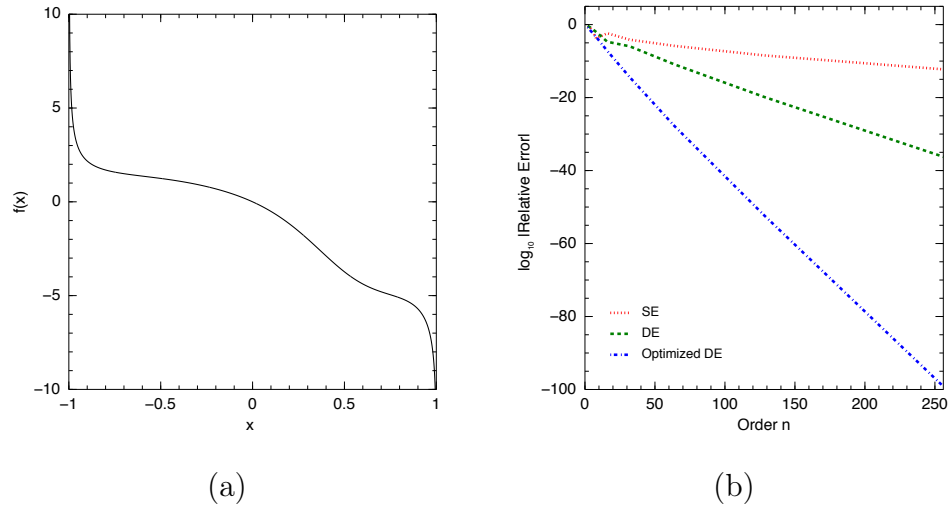


Figure 5.4: In (a) the plot of the integrand of (5.45) and in (b) the performance of the trapezoidal rule with single, double, and optimized double exponential variable transformations.

	Single	Double	Optimized Double
$\phi(t)$	$\sinh(t)$	$\sinh\left(\frac{\pi}{2} \sinh(t)\right)$	$\sinh(h(t))$
$\rho$ or $\gamma$	1	1	1
$\beta$ or $\beta_2$	2	$\pi/2$	$5.7715 \times 10^{-6}$
$d$	0.35260	0.22640	$\pi/2$

Table 5.3: Transformations and parameters for (5.47).

In addition, the optimized transformation is given by:

$$h(t) \approx 5.7715 \times 10^{-6} \sinh(t) + 0.25431 + 0.14936 t - 4.5433 \times 10^{-3} t^2 + 9.9880 \times 10^{-5} t^3. \quad (5.48)$$

Figure 5.5 shows the three stages of the optimized double exponential map.

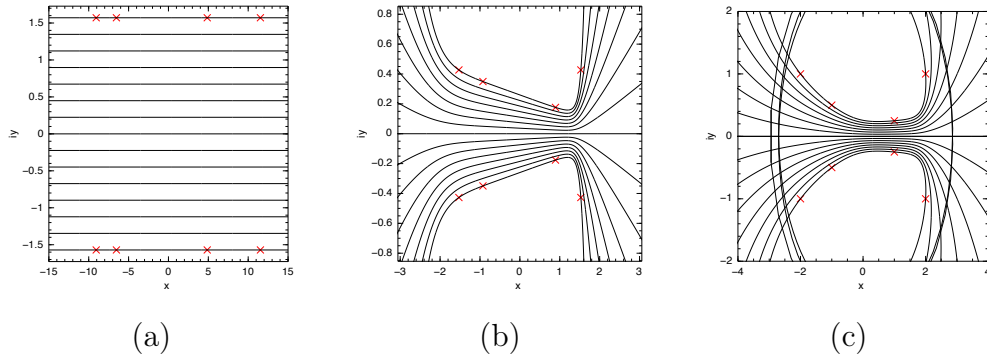


Figure 5.5: In (a) the plot of the strip  $\mathcal{D}_{\pi/2}$  with singularities located on the boundary, in (b) the optimized map  $h(\cdot)$ , and in (c) the optimized DE map. In all three cases, the crosses track the singularities.

In figure 5.6 (a), the integrand of (5.47) is shown, and in figure 5.6 (b), the logarithm of the relative errors of the trapezoidal rule of order  $n$  with single, double, and optimized double exponential variable transformations are plotted. The increase in convergence rate using the optimized variable transformation is a significant increase in efficiency over the double exponential transformation.

### 5.D.3 Example: for Goursat's infinite integral

We wish to evaluate the integral:

$$\int_0^{+\infty} \frac{x \, dx}{1 + x^6 \sinh^2 x} = 0.50368 \dots, \quad (5.49)$$

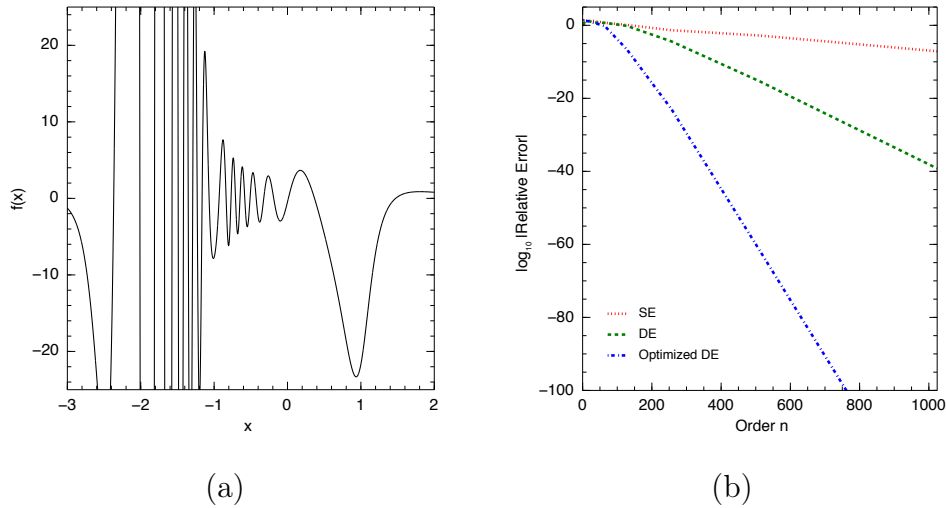


Figure 5.6: In (a) the plot of the integrand of (5.47) and in (b) the performance of the trapezoidal rule with single, double, and optimized double exponential variable transformations.

which is evaluated in [HNSH09, Oou13] as part of a high precision numerical evaluation of Goursat’s infinite integral. While there are an infinite number of poles in the complex plane due to the  $\sinh$  function, a four-parameter solution  $h(t)$  can be found using the nearest poles, while excluding the remainder. This shows the incredible versatility of the proposed optimization approach, because the same optimal asymptotic convergence rate is obtained in the complicated situation of an infinite number of singularities while not leading to a more complicated solution process. Table 5.4 summarizes the variable transformations used and the parameters in the theorems 5.1 and 5.2. For the sake of comparison, we use the same double exponential transformation used in [HNSH09].

In addition, the optimized transformation is given by:

$$h(t) \approx 0.26725 \sinh(t) + 0.30707 + 0.20337 t - 0.031966 t^2. \quad (5.50)$$

	Single	Double	Optimized Double
$\phi(t)$	$\log(e^t + 1)$	$\exp(0.22t - 0.017e^{-t})$	$\log(e^{h(t)} + 1)$
$\rho$ or $\gamma$	1	0.22	1
$\beta$ or $\beta_2$	2	2	0.26725
$d$	1.13615	1.58223	$\pi/2$

Table 5.4: Transformations and parameters for (5.49).

Figure 5.7 shows the three stages of the optimized double exponential map.

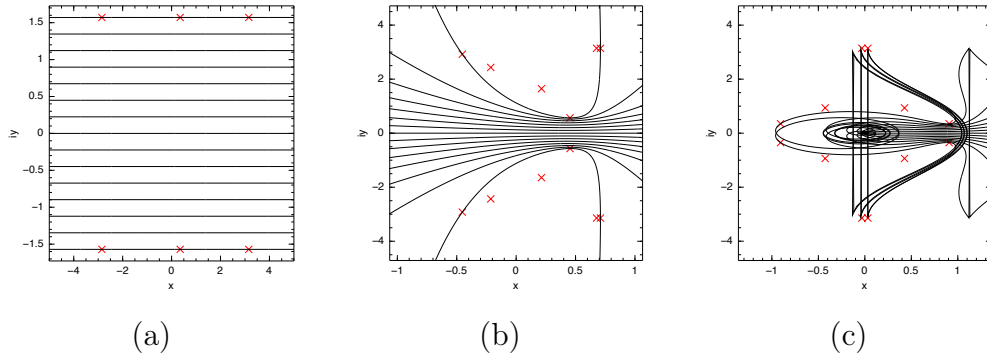


Figure 5.7: In (a) the plot of the strip  $\mathcal{D}_{\pi/2}$  with singularities located on the boundary, in (b) the optimized map  $h(\cdot)$ , and in (c) the optimized DE map. In all three cases, the crosses track the singularities.

In figure 5.8 (a), the integrand of (5.49) is shown, and in figure 5.8 (b), the logarithm of the relative errors of the trapezoidal rule of order  $n$  with single, double, and optimized double exponential variable transformations are plotted. The increase in convergence rate using the optimized variable transformation is a significant increase in efficiency over the double exponential transformation.

In [HNSH09], the authors obtained the relative error of  $10^{-72}$  with 480 function evaluations, and claim this to be a nearly minimal number. However, as can be seen in figure 5.8 (b), the optimized double exponential transformation can obtain the same relative error with only approximately 140 function evaluations. Neither of these results, however, compares to the million-digit

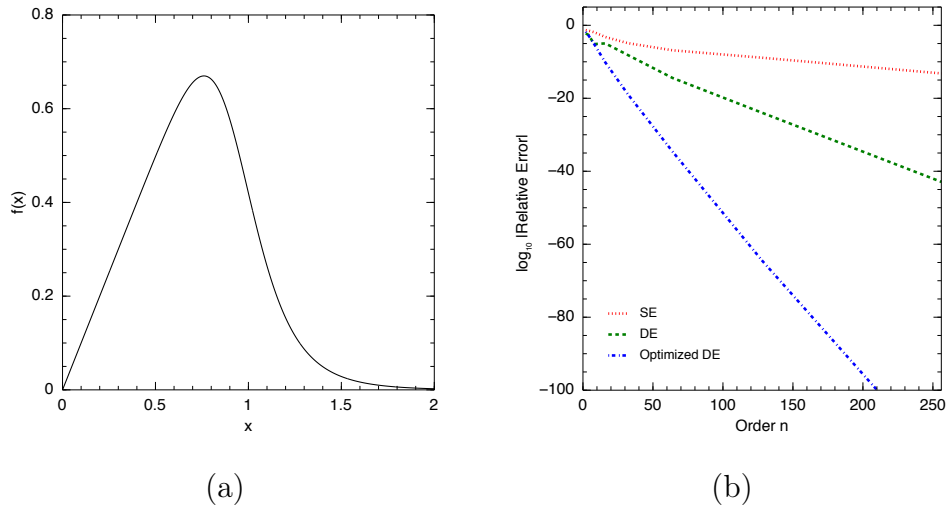


Figure 5.8: In (a) the plot of the integrand of (5.49) and in (b) the performance of the trapezoidal rule with single, double, and optimized double exponential variable transformations.

algorithm of [Oou13] using the Hilbert transform to construct a conjugate function, thereby removing all the singularities.

#### 5.D.4 Example: adaptive optimization via Sinc-Padé approximants

In this example, we will show the performance of the adaptive optimized method using the Sinc-Padé approximants to approximately locate the singularities. We wish to evaluate the integral:

$$\int_0^\infty \frac{x \, dx}{\sqrt{\epsilon_1^2 + (x - \delta_1)^2}(\epsilon_2^2 + (x - \delta_2)^2)(\epsilon_3^2 + (x - \delta_3)^2)} = 12.55613\dots, \quad (5.51)$$

for the values  $\delta_1 + i\epsilon_1 = 1 + i$ ,  $\delta_2 + i\epsilon_2 = 2 + i/2$ , and  $\delta_3 + i\epsilon_3 = 3 + i/3$ . Table 5.5 summarizes the variable transformations used and the parameters in the theorems 5.1 and 5.2.

	Single	Double	Optimized Double
$\phi(t)$	$\exp(t)$	$\exp\left(\frac{\pi}{2} \sinh(t)\right)$	$\exp(h(t))$
$\rho$ or $\gamma$	1	1	1
$\beta$ or $\beta_2$	2	$\pi/2$	$9.4353 \times 10^{-3}$
$d$	0.11066	0.05762	$\pi/2$

Table 5.5: Transformations and parameters for (5.51).

Table 5.6 shows the evolution of the six nearest roots of the Sinc-Padé approximants to the integration contour. The degrees of the Sinc-Padé approximants increase as  $r = \log_2(n) - 2$  and  $s = \log_2(n) + 2$ .

$n$	$\delta_1 \pm i\epsilon_1$	$\delta_2 \pm i\epsilon_2$	$\delta_3 \pm i\epsilon_3$
$2^5$	$-0.58097 \pm 1.2106i$	$2.0717 \pm 0.28089i$	$3.0298 \pm 0.45170i$
$2^6$	$-0.18822 \pm 1.3571i$	$2.0008 \pm 0.49777i$	$3.0004 \pm 0.33311i$
$2^7$	$0.14091 \pm 1.3982i$	$1.9963 \pm 0.48734i$	$3.0009 \pm 0.33279i$
$2^8$	$0.41762 \pm 1.3767i$	$2.0498 \pm 0.39481i$	$3.0022 \pm 0.35279i$
Exact	$1.0000 \pm 1.0000i$	$2.0000 \pm 0.50000i$	$3.0000 \pm 0.33333i$

Table 5.6: Evolution of the six nearest roots of the Sinc-Padé approximants.

Table 5.7 shows the evolution of the adaptive map. The coefficients of the optimized map are also shown for comparison.

$n$	$u_0$	$u_1$	$u_2$	$u_3$
$2^5$	$3.1344 \times 10^{-3}$	0.88233	0.072018	$-1.6222 \times 10^{-3}$
$2^6$	$9.1841 \times 10^{-3}$	0.95544	0.073207	$-7.1021 \times 10^{-3}$
$2^7$	$8.6135 \times 10^{-3}$	0.95359	0.072918	$-6.7917 \times 10^{-3}$
$2^8$	$6.1605 \times 10^{-3}$	0.93730	0.071916	$-4.7927 \times 10^{-3}$
Optimized	$9.4353 \times 10^{-3}$	0.93351	0.084087	$-9.9846 \times 10^{-3}$

Table 5.7: Evolution of the coefficients of the adaptive map.

Figure 5.9 shows the three stages of the adaptive double exponential map.

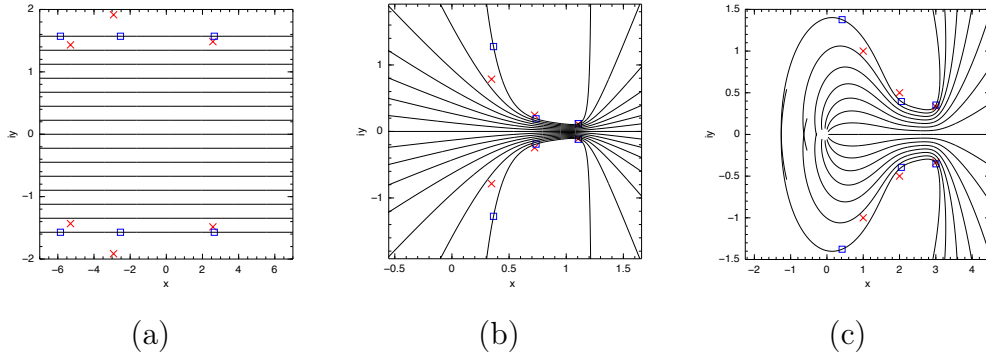


Figure 5.9: In (a) the plot of the strip  $\mathcal{D}_{\pi/2}$  with singularities located on the boundary, in (b) the adaptive map  $h(\cdot)$ , and in (c) the optimized DE map. In all three cases, the crosses track the singularities and the squares track the roots of the Sinc-Padé approximant for  $n = 2^8$ .

In figure 5.10 (a), the integrand of (5.51) is shown, and in figure 5.10 (b), the logarithm of the relative errors of the trapezoidal rule of order  $n$  with single, double, and optimized double exponential variable transformations are plotted. The increase in convergence rate using the optimized variable transformation is a significant increase in efficiency over the double exponential transformation.

## 5.E Applications

### 5.E.1 Boundary value problems

After the Sinc expansion of functions came the Sinc expansion of integral and differential equations [Sug02]. For the two-point boundary value problem (BVP):

$$\begin{aligned}
 Lf(x) &= f''(x) + \mu(x)f'(x) + \nu(x)f(x) = \sigma(x), \\
 x &\in (a, b), \quad f(a) = f(b) = 0,
 \end{aligned}
 \tag{5.52}$$

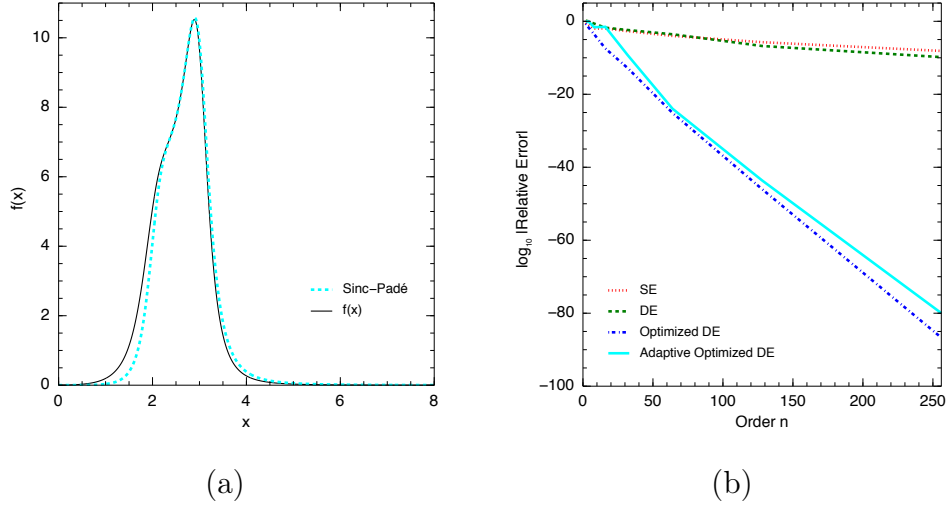


Figure 5.10: In (a) the plot of the integrand of (5.51) and the Sinc-Padé approximant for  $n = 2^8$  and in (b) the performance of the trapezoidal rule with single, double, optimized double, and adaptive optimized double exponential variable transformations.

the variable transformation  $x = \phi(t) : (-\infty, +\infty) \rightarrow (a, b)$ ,  $\lim_{t \rightarrow -\infty} \phi(t) = a$  and  $\lim_{t \rightarrow +\infty} \phi(t) = b$ , gives:

$$\begin{aligned} \tilde{L}\tilde{f} &= \tilde{f}''(t) + \tilde{\mu}(t)\tilde{f}'(t) + \tilde{\nu}(t)\tilde{f}(t) = \tilde{\sigma}(t), \\ t &\in (-\infty, +\infty), \quad \lim_{t \rightarrow \pm\infty} \tilde{f}(t) = 0, \end{aligned} \tag{5.53}$$

where:

$$\begin{aligned} \tilde{f}(t) &= f(\phi(t)), \quad \tilde{\mu}(t) = \phi'(t)\mu(\phi(t)) - \phi''(t)/\phi'(t), \\ \tilde{\nu}(t) &= (\phi'(t))^2\nu(\phi(t)), \quad \tilde{\sigma}(t) = (\phi'(t))^2\sigma(\phi(t)). \end{aligned} \tag{5.54}$$

which, for suitable variable transformations, will allow good approximations to the function  $f(x)$ . Very briefly, we let:

$$\tilde{f}_n(t; \phi) = \sum_{j=-n}^{+n} \tilde{f}_n S(j, h)(t), \quad (5.55)$$

then using the Sinc collocation points  $x_k = k h$ , we solve the linear system:

$$\tilde{L} \tilde{f}_n(k h; \phi) = \tilde{\sigma}(k h), \quad k = -n, -n + 1, \dots, n - 1, n, \quad (5.56)$$

for the  $2n + 1$  unknowns  $\tilde{f}_n$ . The approximation to the original function is then:

$$f_n(x; \phi) = \sum_{j=-n}^{+n} \tilde{f}_n S(j, h)(\phi^{-1}(x)). \quad (5.57)$$

Again, we show that using optimized double exponential maps can also be useful in the setting of two-point BVPs when singularities are near the solution interval. The problem (5.52) for  $a = -1$ ,  $b = 1$ , and:

$$\mu(x) = -\frac{4x}{(x^2 + \epsilon^2)^2} \tan\left(\frac{1}{x^2 + \epsilon^2}\right), \quad (5.58)$$

$$\begin{aligned} \nu(x) = & \frac{4x^2}{(x^2 + \epsilon^2)^4} \left(1 + 2 \tan^2\left(\frac{1}{x^2 + \epsilon^2}\right)\right) \\ & + \left(\frac{6x^2 - 2\epsilon^2}{(x^2 + \epsilon^2)^3}\right) \tan\left(\frac{1}{x^2 + \epsilon^2}\right), \end{aligned} \quad (5.59)$$

$$\sigma(x) = -(1 - x^2)^{3/2} \cos\left(\frac{1}{x^2 + \epsilon^2}\right), \quad (5.60)$$

with solution:

$$f(x) = \sqrt{1 - x^2} \cos\left(\frac{1}{x^2 + \epsilon^2}\right), \quad (5.61)$$

has branches emanating from the endpoints as well as terrible essential singu-

larities at  $\pm i\epsilon$ . In addition, at every zero of the solution, the coefficients  $\mu(x)$  and  $\nu(x)$  are singular. We use Sinc approximations with single, double, and optimized double exponential decay at the endpoints to solve the linear system. Table 5.8 summarizes the variable transformations and the parameters used.

	Single	Double	Optimized Double
$\phi(t)$	$\tanh(t/2)$	$\tanh(\pi/2 \sinh(t))$	$\tanh(\tan^{-1}(\epsilon) \sinh(t))$
$\rho$ or $\gamma$	1	1	1
$\beta$ or $\beta_2$	1/2	$\pi/4$	$\tan^{-1}(\epsilon)/2$
$d$	$2 \tan^{-1}(\epsilon)$	$\sin^{-1}(2 \tan^{-1}(\epsilon)/\pi)$	$\pi/2$

Table 5.8: Transformations and parameters for (5.52).

In figures 5.11 and 5.12 (a), the function of (5.52) is shown along with the three Sinc approximations at a high order, showing good visual agreement of the optimized Sinc approximation, and in figures 5.11 and 5.12 (b), the logarithm of the relative errors of the Sinc approximations of order  $n$  with single, double, and optimized double exponential variable transformations are plotted.

In both figures, we approximate the relative error:

$$\sup_{x \in [0,1]} \left| \frac{f(x) - f_n(x; \phi)}{f(x)} \right|, \quad (5.62)$$

by computing the maximum of the difference and quotient at 101 equally spaced points in the interval. The increase in convergence rate using the optimized variable transformation is a significant increase in efficiency over the double exponential transformation.

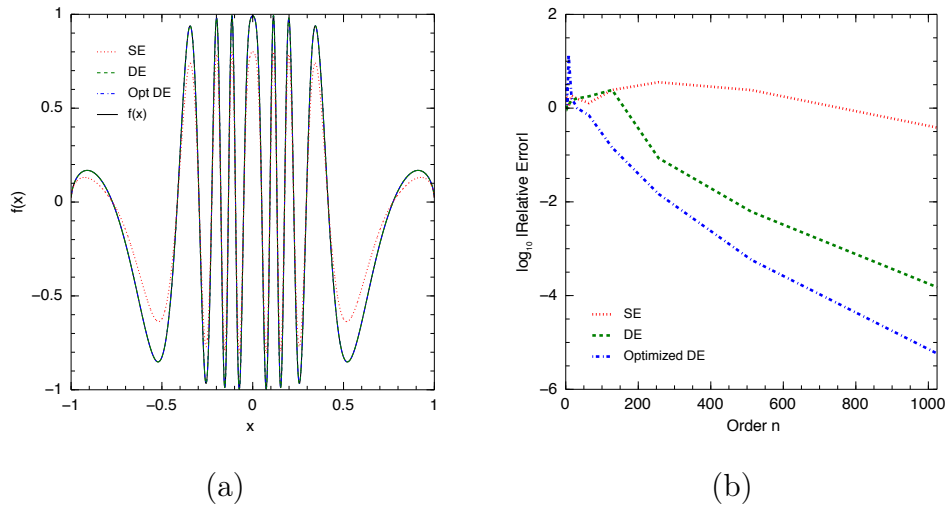


Figure 5.11: In (a) the solution of (5.52) along with the three Sinc approximations for  $n = 2^{10}$  and in (b) the performance of the Sinc approximation with single, double, and optimized double exponential variable transformations. In both cases  $\epsilon = 0.2$ .

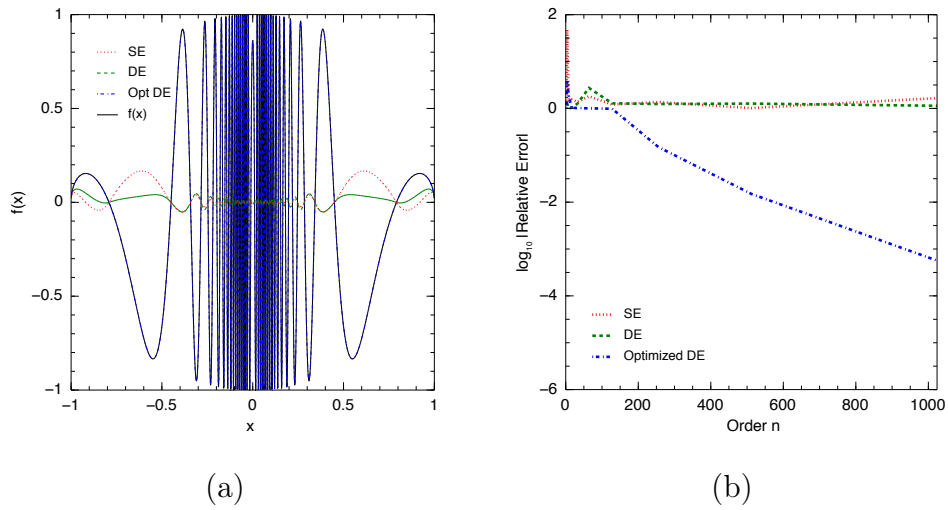


Figure 5.12: In (a) the solution of (5.52) along with the three Sinc approximations for  $n = 2^{10}$  and in (b) the performance of the Sinc approximation with single, double, and optimized double exponential variable transformations. In both cases  $\epsilon = 0.1$ .

## 5.E.2 Nonlinear waves

For internal waves in stratified fluids of great depth, the Benjamin-Ono equation [Ben67, Ono75] is a nonlinear partial integro-differential equation involving the Hilbert transform. While the KdV equation has soliton solutions that decay exponentially on the real line, the soliton solutions to the homogeneous Benjamin-Ono equation decay algebraically. The Hilbert transform on the real line is defined as [Kin09]:

$$\mathcal{H}y(x) = \frac{1}{\pi} \int_{-\infty}^{+\infty} \frac{y(s)}{s-x} ds, \quad (5.63)$$

where the dash in the integral sign denotes the Cauchy principal value. The forced Benjamin-Ono equation can then be written as:

$$y_t + yy_x + \mathcal{H}y_{xx} = g(x-ct), \quad x \in \mathbb{R}, \quad t \geq 0, \quad \lim_{x \rightarrow \pm\infty} y(x,t) = 0. \quad (5.64)$$

for some  $g$  with wave speed  $c \in \mathbb{R}$ . If we let  $y(x,t) = y(x-ct)$ , then we may consider the traveling wave solutions. Inserting such a substitution into (5.64) and integrating, we obtain:

$$-cy' + yy' + \mathcal{H}y'' = g(x-ct), \quad (5.65)$$

$$-cy + \frac{y^2}{2} + \mathcal{H}y' = f(x-ct) = \int_{-\infty}^{x-ct} g(s) ds. \quad (5.66)$$

The traveling wave is then obtained by solving this equation for  $t = 0$ .

The forced solutions to this equation have many properties that can be deduced from  $f$ . For example, if  $f$  decays algebraically on the real line, the

method of dominant balance shows that:

$$y(x) \sim -c^{-1}f(x), \quad \text{as } x \rightarrow \pm\infty, \quad (5.67)$$

and will therefore behave similarly. As well, complex singularities in  $f$  can potentially be found in  $y$ .

To continue, it is clear we require an approximation for the Hilbert transform. In [Ste93, Ste00], Stenger derives a Sinc-based approximation for the Hilbert transform. We closely follow his development which is for a general variable transformation, and show how the optimized conformal map improves the convergence rate.

By making the invertible variable transformation  $s = \phi(t) : \mathbb{R} \rightarrow \mathbb{R}$  in (5.63), we obtain:

$$\mathcal{H}y(x) = \frac{1}{\pi} \int_{-\infty}^{+\infty} \frac{y(\phi(t))\phi'(t)}{\phi(t) - x} dt. \quad (5.68)$$

The integrand multiplied by  $t - \phi^{-1}(x)$  has but a removable singularity at  $t = \phi^{-1}(x)$ . Therefore, we may approximate with a Sinc basis:

$$\frac{y(\phi(t))\phi'(t)}{\phi(t) - x} (t - \phi^{-1}(x)) \approx \sum_{j=-n}^{+n} \frac{y(\phi(jh))\phi'(jh)}{\phi(jh) - x} (jh - \phi^{-1}(x)) S(j, h)(t). \quad (5.69)$$

Using the Hilbert transform [Kin09]:

$$\mathcal{H} \frac{\sin x}{x} = \frac{1}{\pi} \int_{-\infty}^{+\infty} \frac{\sin s}{s(s-x)} ds = \frac{\cos x - 1}{x}, \quad (5.70)$$

and dividing by the linear factor  $t - \phi^{-1}(x)$  and integrating each basis function,

the approximation (5.69) leads directly to:

$$\mathcal{H}y(x) \approx \frac{h}{\pi} \sum_{j=-n}^{+n} y(\phi(jh)) \phi'(jh) \frac{\cos\left(\pi\left(\frac{\phi^{-1}(x)}{h} - j\right)\right) - 1}{x - \phi(jh)}. \quad (5.71)$$

Using the Sinc-based approximation for the Hilbert transform, the solution of the forced Benjamin-Ono equation can be obtained by approximating the solution  $y(x)$  in a Sinc basis:

$$y(x) \approx y_n(x; \phi) = \sum_{j=-n}^{+n} y_j S(j, h)(\phi^{-1}(x)), \quad (5.72)$$

and solving the system of nonlinear equations obtained by collocating at the Sinc points  $x_k = \phi(kh)$ :

$$-c y_n(kh; \phi) + y_n^2(kh, \phi) + \mathcal{H}y_n'(kh, \phi) = f(kh), \quad k = -n, \dots, n, \quad (5.73)$$

for the  $2n + 1$  unknowns  $\{y_j\}_{|j| \leq n}$  by Newton iteration.

For the purposes of illustration, we consider the functions  $f(x)$  which yield the solutions:

$$y(x) = \sum_{i=1}^m \frac{\epsilon_i^2}{((x - \delta_i)^2 + \epsilon_i^2)}, \quad (5.74)$$

for the values  $m = 3$ ,  $\delta_1 + i\epsilon_1 = -1 + 0.3i$ ,  $\delta_2 + i\epsilon_2 = 0 + 0.1i$ , and  $\delta_3 + i\epsilon_3 = 1 + 0.2i$ . This allows for an exact comparison with an analytic expression. In addition, the wave speed  $c = 1$  is used. Table 5.9 summarizes the variable transformations and the parameters used.

In addition, the optimized transformation is given by:

$$h(t) \approx 1.1451 \times 10^{-7} \sinh(t) + 0.04531 + 0.06359 t - 1.2134 \times 10^{-4} t^2. \quad (5.75)$$

	Single	Double	Optimized Double
$\phi(t)$	$\sinh(t)$	$\sinh(\pi/2 \sinh(t))$	$\sinh(h(t))$
$\rho$ or $\gamma$	1	1	1
$\beta$ or $\beta_2$	1/2	$\pi/4$	$5.7257 \times 10^{-8}$
$d$	0.10017	0.06381	$\pi/2$

Table 5.9: Transformations and parameters for (5.64).

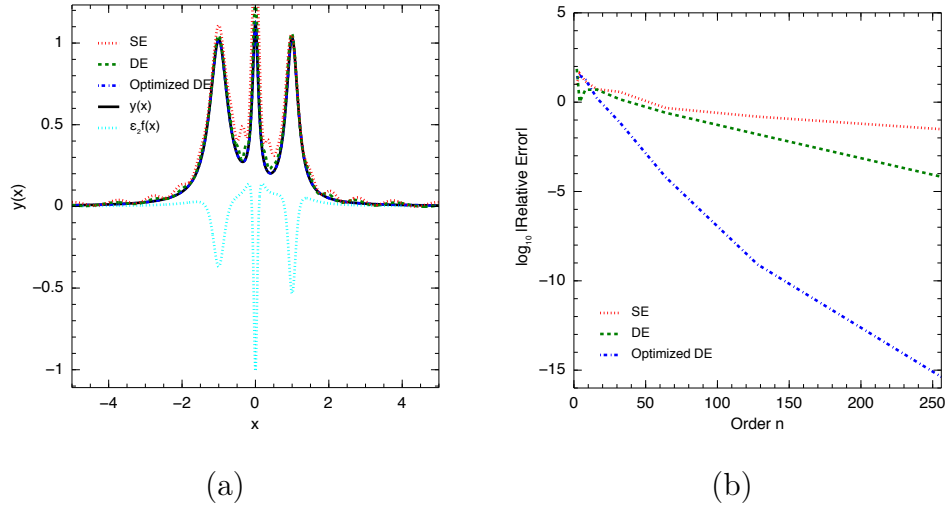


Figure 5.13: In (a) the solution of (5.64) along with the three Sinc approximations for  $n = 2^5$  and the scaled forcing function and in (b) the performance of the Sinc approximation with single, double, and optimized double exponential variable transformations.

In Figure 5.13, we approximate the relative error:

$$\sup_{x \in \mathbb{R}} \left| \frac{y(x) - y_n(x; \phi)}{y(x)} \right|, \quad (5.76)$$

by computing the maximum of the difference and quotient at 101 equally spaced points in the interval  $[-5, 5]$ . The inverse optimized map  $\phi^{-1}$  is conveniently computed via Newton iteration, as the map and its first derivative are already required in the system of collocated equations. The increase in

convergence rate using the optimized variable transformation is a significant increase in efficiency over the double exponential transformation.

### 5.E.3 Multi-dimensional integrals

There are many applications in physics that warrant the evaluation of  $m$ -dimensional integrals. Examples we are interested in include: magnetic susceptibility integrals in the Ising theory of solid-state physics [BBC06], which form terms in a series that represents the dependence of magnetic susceptibility on temperature; and, box integrals [BBC07], which are essentially  $m$ -dimensional expectations of the  $s^{\text{th}}$  power of the distance in a unit hypercube  $\langle |\vec{r}|^s \rangle_{\vec{r} \in [0,1]^m}$ . Such integrals have applications in probability theory, and in potential theory such as “jellium” potentials. After making substantial analytic advances in the theory of box integrals in [BBC10], the authors acknowledge that some of the analytical techniques they used would not apply to other  $m$ -dimensional expectations, and posit that  $\langle e^{-\kappa|\vec{r}|} \rangle_{\vec{r} \in [0,1]^m}$  should remain extremely difficult to evaluate in any general way. In this section, we construct such a general way to calculate these integrals. Explicitly:

$$\langle e^{-\kappa|\vec{r}|} \rangle_{\vec{r} \in [0,1]^m} = \int_{[0,1]^m} e^{-\kappa(r_1^2 + \dots + r_m^2)^{1/2}} dr_1 \dots dr_m. \quad (5.77)$$

Using the same dimensional-reduction technique in [BBC07], and the incomplete gamma function [GR07, §8.350 1.]:

$$\gamma(m, a) = a^m \int_0^1 x^{m-1} e^{-ax} dx = (m-1)! - e^{-a} \sum_{j=0}^{m-1} \binom{m-1}{j} \frac{j!}{a^{j-m+1}}, \quad (5.78)$$

we obtain:

$$\langle e^{-\kappa|\vec{r}|} \rangle_{\vec{r} \in [0,1]^m} = \frac{m}{2^{m-1}} \int_{[-1,1]^{m-1}} dx_1 \cdots dx_{m-1} \left( \frac{(m-1)!}{\kappa^m (x_1^2 + \cdots + x_{m-1}^2 + 1)^{m/2}} - \sum_{j=0}^{m-1} \binom{m-1}{j} \frac{j! e^{-\kappa(x_1^2 + \cdots + x_{m-1}^2 + 1)^{1/2}}}{\kappa^{j+1} (x_1^2 + \cdots + x_{m-1}^2 + 1)^{(j+1)/2}} \right). \quad (5.79)$$

Multi-dimensional integrals are a challenge for univariate numerical integration methods because of the curse of dimensionality, whereby the dimension  $m$  increases the number of sample points of the one-dimensional case  $N = 2n + 1$  geometrically as  $\mathcal{O}(N^m)$ , reaching the limits of modern computational power quite quickly. Nevertheless, positive results may be obtained for lower dimensions, especially for extremely high accuracy, for which even tens of digits qualifies in this setting. We compare and contrast the trapezoidal rule on (5.77) for the single, double, and optimized double exponential transformations. These transformations are summarized in table 5.10. Of course,  $m - 1$  transformations  $\{\phi_\ell(t_1, \dots, t_{m-1})\}_{\ell=1}^{m-1}$  will be required to induce decay at all the boundaries of the hypercube in (5.77).

	Single	Double	Optimized Double
$\phi_\ell(t_1, \dots, t_{m-1})$	$\tanh(t_\ell/2)$	$\tanh(\pi/2 \sinh(t_\ell))$	$\tanh\left(\tan^{-1}\left(\sqrt{\sum_{j=1}^{\ell-1} \phi_j^2 + 1}\right) \sinh(t_\ell)\right)$
$\rho$ or $\gamma$	1	1	1
$\beta$ or $\beta_2$	1	$\pi/2$	$\pi/4$
$d$	$\pi/2$	$\pi/6$	$\pi/2$

Table 5.10: Transformations and parameters for (5.79).

Note that while the  $\ell^{\text{th}}$  optimized double exponential transformation calls all previous ones through the term  $\sqrt{\sum_{j=1}^{\ell-1} \phi_j^2 + 1}$ , this comes at no extra cost

because it is extracted during the construction of the term  $x_1^2 + \dots + x_{m-1}^2 + 1$ , which occurs in (5.79).

In figure 5.14, the logarithm of the relative errors of the trapezoidal rule of order  $n$  with single, double, and optimized double exponential variable transformations are plotted. The increase in convergence rate using the optimized variable transformation is a significant increase in efficiency over the double exponential transformation.

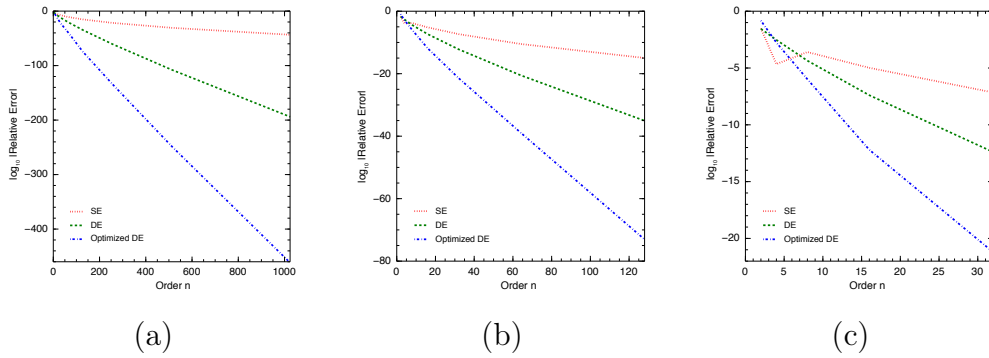


Figure 5.14: The performance of the trapezoidal rule with single, double, and optimized double exponential variable transformations. In all figures,  $\kappa = 1$ , and in (a)  $m = 2$ , in (b)  $m = 3$ , and in (c)  $m = 4$ .

The dimension of the so-called box integrals of [BBC07] was reduced completely to one in every case by using an integral representation of the integrand  $|\vec{r}|^s$ , which allowed the integrals over  $r_1, r_2$ , etc. . . to be separated and written as the  $m^{\text{th}}$  power of the error function. The authors postulated the exponential expectation to be a challenge because of an inability to reduce the dimension of the problem. Using the Bessel representation for  $K_{-1/2}(\kappa|\vec{r}|)$  from [GR07, §8.432 7.]:

$$e^{-\kappa|\vec{r}|} = \sqrt{\frac{2\kappa|\vec{r}|}{\pi}} K_{-1/2}(\kappa|\vec{r}|) = \sqrt{\frac{\kappa}{2\pi}} \int_0^\infty \frac{e^{-\frac{\kappa}{2}(t+\frac{r^2}{t})}}{t^{1/2}} dt, \quad (5.80)$$

and the error function representation [GR07, §3.321 1.]:

$$\operatorname{erf}(u) = \frac{2u}{\sqrt{\pi}} \int_0^1 e^{-u^2 x^2} dx, \quad (5.81)$$

we are able to obtain the formula:

$$\langle e^{-\kappa|\vec{r}|} \rangle_{\vec{r} \in [0,1]^m} = \frac{1}{2} \left( \frac{\pi}{2\kappa} \right)^{\frac{m-1}{2}} \int_0^\infty t^{\frac{m-1}{2}} e^{-\kappa t/2} \operatorname{erf}^m \left( \sqrt{\frac{\kappa}{2t}} \right) dt. \quad (5.82)$$

Because these are such challenging integrals, we include rounded approximate values in table 5.11 for the sake of reproducibility. The one-dimensional integral (5.82) allows for the calculation of the high precision results, and it is also used for the calculation of the relative error in figure 5.14.

$m$	$\kappa$	$\langle e^{-\kappa \vec{r} } \rangle_{\vec{r} \in [0,1]^m}$
2	1.0	0.48499 93872 72994 84128 76561 86058 31858 19718
3	1.0	0.39822 04526 88323 04659 07885 63033 98432 76981
4	1.0	0.33843 80876 94843 90404 45300 56568 55958 16022
5	1.0	0.29379 80818 76007 61424 12657 48176 65958 00955

Table 5.11: Numerical Evaluation of (5.77) using (5.82).

### 5.E.4 Molecular integrals with exponential basis functions

To compute eigenstates of the molecular Schrödinger equation [Sch26], one solution strategy is to represent molecular orbitals as a linear combination of atomic orbitals (LCAO-MO). This approach greatly simplifies the calculations by decoupling the individual particles' Hamiltonians. Evaluating the Hamiltonian elements corresponding to four-center two-electron repulsion integrals

with exponential basis functions using the Fourier transform method [WGS86, GS88], we encounter one-dimensional integrals of the form:

$$\int_{-\infty}^{+\infty} \frac{e^{i b z - a_1 \sqrt{z^2 + c_1^2} - a_2 \sqrt{z^2 + c_2^2}}}{(z^2 + c_1^2)^{\mu_1} (z^2 + c_2^2)^{\mu_2}} dz, \quad (5.83)$$

for positive real parameter values. To remove oscillations, we deform the integration contour to a path of steepest descent. While the exact path of steepest descent would require some root-finding algorithm for every evaluation point, we use an asymptotic path of steepest descent passing through the saddle point  $iy \in i(0, c_1)$ , which is the solution of:

$$g(y) = -b(c_1^2 - y^2) + a_1 y \sqrt{c_1^2 - y^2} + \frac{a_2 y (c_1^2 - y^2)}{\sqrt{c_2^2 - y^2}} + 2\mu_1 y + 2\mu_2 y \frac{c_1^2 - y^2}{c_2^2 - y^2} = 0, \quad (5.84)$$

and tending asymptotically in the direction  $\pm(a_1 + a_2) + ib$ ,  $+$  in the positive direction and  $-$  in the negative direction. To find the saddle point, we use Ridders' method [Rid79] for its quadratic convergence in the bracketed interval. An asymptotic path of steepest descent can be found with the hyperbolic substitution:

$$\zeta(x) = \lambda_1 x + i \left( \sqrt{\lambda_2^2 x^2 + \lambda_3^2 + \lambda_4} \right), \quad (5.85)$$

for some values of the parameters  $\boldsymbol{\lambda}$ . To ensure the asymptotic direction:

$$\lambda_1 = \frac{a_1 + a_2}{(a_1 + a_2)^2 + b^2}, \quad \text{and} \quad \lambda_2 = \frac{b}{(a_1 + a_2)^2 + b^2}. \quad (5.86)$$

Then, this leaves  $\lambda_3$  and  $\lambda_4$  to determine the locations of pre-images of the singularities  $\pm ic_1$  and  $\pm ic_2$  in relation to the saddle point  $iy$ . Due to symmetry,

we will want the saddle point to have a pre-image of 0:

$$\zeta(0) = iy = i(|\lambda_3| + \lambda_4), \quad (5.87)$$

which readily gives us an equation relating  $\lambda_3$  and  $\lambda_4$ . Due to horizontal and vertical symmetries in the singularities  $\pm ic_1$  and  $\pm ic_2$ , we can consider the two-parameter map:

$$h(t) = u_0 \sinh(t) + u_2 t. \quad (5.88)$$

Then, to ensure the solution of  $u_0$  and  $u_2$  is well-posed, we use:

$$\lambda_3 = \frac{b(c_1 - y)}{(\sqrt{(a_1 + a_2)^2 + b^2} - b)}, \quad \text{and} \quad \lambda_4 = y - |\lambda_3|. \quad (5.89)$$

Table 5.12 summarizes the variable transformations after the substitution  $\zeta(x)$  is used and the static parameters in the theorems 5.1 and 5.2. The dash indicates that parameters change from one integral to the next.

	Single	Double	Optimized Double
$\phi(t)$	$t$	$\frac{\pi}{2} \sinh(t)$	$h(t)$
$\rho$ or $\gamma$	1	1	1
$\beta$ or $\beta_2$	1	$\pi/2$	—
$d$	—	—	$\pi/2$

Table 5.12: Transformations and static parameters for (5.83).

Figure 5.15 shows plots of the three stages of the optimized double exponential map when the optimal value of  $\beta_2$  is reached. Figure 5.16 shows plots of the three stages of the optimized double exponential map when the optimal value of  $\beta_2$  is not reached and is additionally constrained by the singularity  $-ic_1$ .

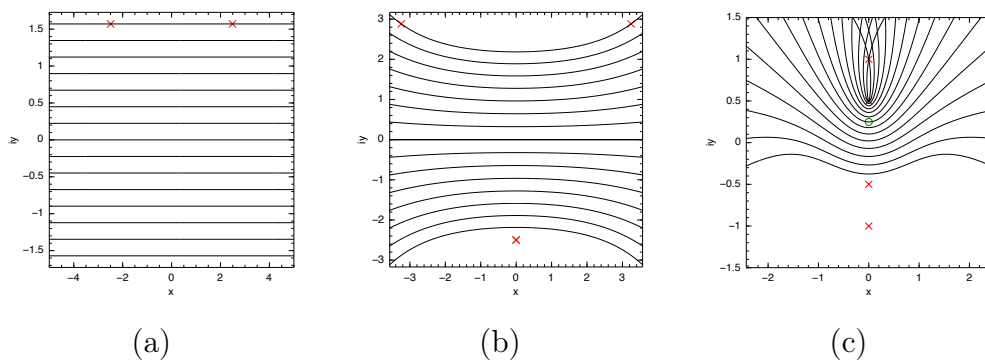


Figure 5.15: In (a) the plot of the strip  $\mathcal{D}_{\frac{\pi}{2}}$  with singularities located on the boundary, in (b) the optimized map  $h(\cdot)$ , and in (c) the composition  $\zeta(h(\cdot))$ . In all three cases, the crosses track the singularities and the circle marks the saddle point.

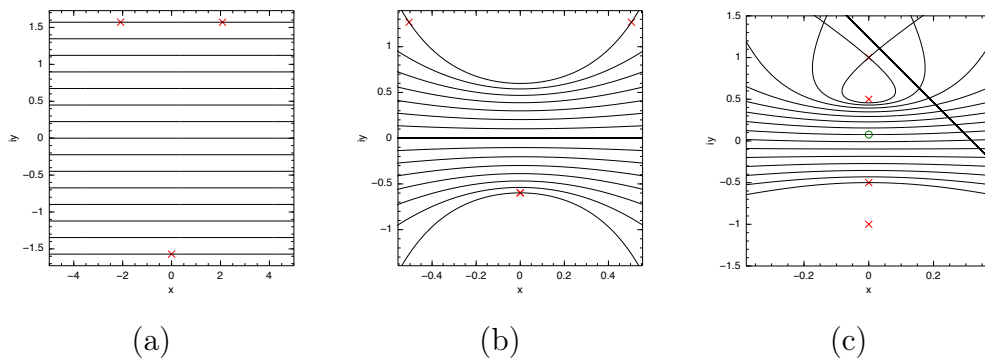


Figure 5.16: In (a) the plot of the strip  $\mathcal{D}_{\frac{\pi}{2}}$  with singularities located on the boundary, in (b) the optimized map  $h(\cdot)$ , and in (c) the composition  $\zeta(h(\cdot))$ . In all three cases, the crosses track the singularities and the circle marks the saddle point.

In order to show the performance of the three algorithms, 20 runs are performed with randomized values for the parameters in (5.83). They are distributed uniformly according to:

$$\begin{aligned} a_1 &\sim U(0, 1), & a_2 &\sim U(0, 1), & b &\sim U(0, 20), \\ c_1 &\sim U(0, 1), & c_2 &\sim U(0, 2), & \mu_1 &\sim U(0, 1), & \mu_2 &\sim U(0, 1). \end{aligned} \tag{5.90}$$

The results of the 20 runs are depicted in figure 5.17. In addition, we keep track of the relative performance of the three transformations because this may not be clear from the image. In every run, the optimized transformation outperforms the single and double exponential transformations, while in 16 runs, the double exponential transformation outperforms the single exponential transformation.

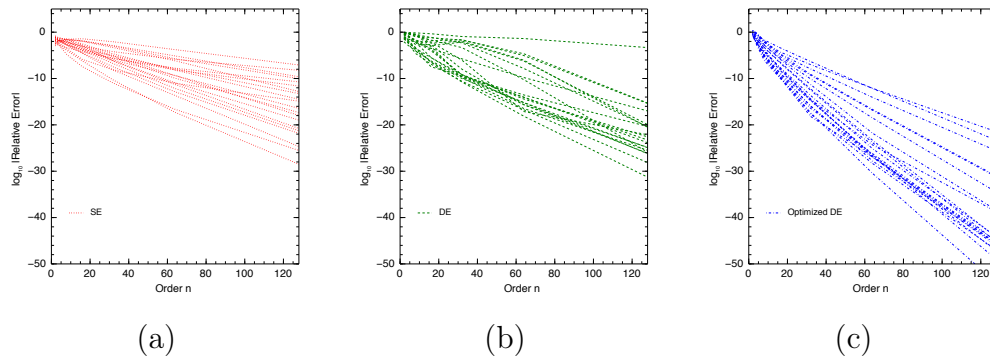


Figure 5.17: The performance of the trapezoidal rule with (a) single, (b) double, and (c) optimized double exponential variable transformations.

## 5.F Numerical Discussion

The numerical experiments are all programmed in Julia [BKSE12], calling at times GNU's MPFR library for arbitrary precision arithmetic, OpenBLAS for

solving the linear systems and Ipopt [WB06] for solving the nonlinear program (5.40). As can be seen in the figures showing the relative errors, the maximization of the convergence rates provides a significant improvement for the double exponential variable transformations. With an equal number of function evaluations, the optimized double exponential formulas provide approximately 2.5–4 times as many correct digits. The conformal maps achieve this by locating singularity pre-images on the boundary of the strip  $\partial\mathcal{D}_{\frac{\pi}{2}}$ . A degree of caution should be used when calculating the nodes and weights of the double exponential quadrature, as they reach the solution intervals' endpoints extremely rapidly. We worked around this issue by using high precision arithmetic.

In examples 5.D.1–5.D.4, one integral is treated on each of the canonical domains: in example 5.D.1, two different endpoint and two pairs of different near-contour singularities are treated; in example 5.D.2, four pairs of different near-contour singularities are treated; in example 5.D.3, an infinite array of singularities is treated; and, in example 5.D.4, the adaptive optimized method is shown to successfully approximate the loci of the three pairs of near-contour singularities.

In every case, the nonlinear program (5.40) still does not ensure analyticity in the strip  $\mathcal{D}_{\frac{\pi}{2}}$ . In examples 5.D.1, 5.D.2 and 5.D.4, the compositions  $\psi(h(t))$  actually cross the branches of the square root functions, and in example 5.D.3, there are even more poles than are shown in figure 5.7. Yet still, a significant increase in convergence is observed. It is quite clear that some singular effects are numerically more damaging than others.

Example 5.D.4 shows the use of the Sinc-Padé approximants for the adaptive optimized algorithm 5.6.1. While in figure 5.10, the Sinc-Padé approxi-

ants serve as relatively poor approximations of the integrand, their ability to approximate singular points is acceptable. In table 5.6, the Sinc-Padé approximants obtain 2-3 correct digits for the first order poles  $\delta_2 \pm i\epsilon_2$  and  $\delta_3 \pm i\epsilon_3$ , but struggle to obtaining an accurate location of the branch points  $\delta_1 \pm i\epsilon_1$ . This is entirely related to the rational limitations of the Sinc-Padé approximants, and suggests that approximating essential singularities, for example, surpasses the capabilities of the Padé methods.

While the nonlinear program (5.40) is successful in the current endeavours, further research in other conformal maps would be fruitful. For example, it is still unclear how to maximize the convergence rate in cases of countably infinite singularities, such as:

$$\int_{-\infty}^{+\infty} \frac{\tanh x}{x(1+x^2)} dx. \quad (5.91)$$

A single exponential transformation such as  $\frac{\pi}{2} \sinh$  creates an array of singularities along  $\pm \frac{i\pi}{2}$ . Therefore, any further composition will inevitably cause the limits of this array to approach the real axis without bound. The problem has been discussed in [OTMS13, TOMS13], and the result is almost the same convergence property as a single exponential transformation.

Nevertheless, the applications show how the conformal maps can be used to obtain substantial increases in accuracy. In the boundary value problem, only the optimized double exponential transformation is able to provide any accuracy that resembles the solution. For the multi-dimensional integrals, the gain in accuracy is also significant. And for the highly oscillatory integrals, the deformation to the contour of steepest descent, coupled with the conformal map provides an algorithm that is insensitive to the many parameters in the

integral.

## 5.G Conclusion

In this work, we investigate the use of conformal maps for the acceleration of convergence of the trapezoidal rule and Sinc numerical methods. The conformal map is a polynomial adjustment to the sinh map, and allows the treatment of a finite number of singularities in the complex plane. In the case where locations are unknown, the so-called Sinc-Padé approximants are used to provide approximate results. This adaptive method is shown to have almost the same convergence properties. We use the conformal maps to generate high accuracy solutions to challenging boundary value problems, multi-dimensional integrals, and highly oscillatory integrals.

# Chapter 6

## Conclusion

To the best of my abilities, I am pleased to have provided what can be considered as optimal solutions to the numerical evaluation of semi-infinite integrals arising in molecular integrals over  $B$  functions, and in the process, solutions to other problems as well. I am grateful to Hassan Safouhi for suggesting this problem as my Ph D thesis. I am confident this thesis can be used as the starting point for future work. Firstly, the large scale calculations of the molecular integrals over  $B$  functions could greatly benefit from using the analytical expression (4.32) and the algorithm for (5.83). Secondly, the trapezoidal rule and Sinc numerical methods have received a significant improvement. The main advantage of the trapezoidal rule and Sinc numerical methods over polynomial interpolation methods is the ability to succeed despite endpoint singularities. With the use of specific conformal maps, it can succeed with other types of singularities as well. There is no doubt that very challenging problems in applied mathematics can be solved with accelerated convergence from the use of conformal maps for the trapezoidal rule and Sinc numerical methods.

# Bibliography

- [AS65] M. Abramowitz and I. A. Stegun. *Handbook of Mathematical Functions*. Dover, New York, 1965.
- [AW95] G. B. Arfken and H. J. Weber. *Mathematical Methods for Physicists*. Academic Press, Fifth edition, 1995.
- [BBC06] D. H. Bailey, J. M. Borwein, and R. E. Crandall. Integrals of the Ising class. *J. Phys. A: Math. Gen.*, 39:12271–12302, 2006.
- [BBC07] D. H. Bailey, J. M. Borwein, and R. E. Crandall. Box integrals. *J. Comp. Appl. Math.*, 206:196–208, 2007.
- [BBC10] D. H. Bailey, J. M. Borwein, and R. E. Crandall. Advances in the theory of box integrals. *Math. Comp.*, 79:1839–1866, 2010.
- [Ben67] T. B. Benjamin. Internal waves of permanent form in fluids of great depth. *J. Fluid Mech.*, 29:559–592, 1967.
- [BH75] N. Bleistein and R. Handelsman. *Asymptotic Expansions of Integrals*. Holt, Rinehart and Winston, New York, 1975.
- [Bia89] B. Bialecki. A modified Sinc quadrature rule for functions with poles near the arc of integration. *BIT*, 29:464–476, 1989.
- [BKSE12] J. Bezanson, S. Karpinski, V. B. Shah, and A. Edelman. Julia: a fast dynamic language for technical computing. arXiv:1209.5145, 2012.
- [BLWW04] F. Bornemann, D. Laurie, S. Wagon, and J. Waldvogel. *The SIAM 100-Digit Challenge. A Study in High-Accuracy Numerical Computing*. SIAM, Philadelphia, 2004.
- [BO27] M. Born and J.R. Oppenheimer. Zur Quantentheorie der Molekeln. *Annalen der Physik*, 389:457–484, 1927.
- [BO78] C. M. Bender and S. A. Orszag. *Advanced Mathematical Methods for Scientists and Engineers*. McGraw-Hill, New York, 1978.

- [Boy50] S. F. Boys. Electronic wave functions. I. A general method of calculation for the stationary states of any molecular system. *Proc. R. Soc. Lond. Series A, Math. & Phys. Sciences.*, 200:542–554, 1950.
- [Bre78] C. Brezinski. *Algorithmes d’Accélération de la Convergence*. Edition Technip, Paris, 1978.
- [BRZ91] C. Brezinski and M. Redivo-Zaglia. *Extrapolation Methods: Theory and Practice*. Edition North-Holland, Amsterdam, 1991.
- [BS03a] L. Berlu and H. Safouhi. An extremely efficient and rapid algorithm for a numerical evaluation of three-center nuclear attraction integrals over Slater type functions. *J. Phys. A: Math. Gen.*, 36:11791–11805, 2003.
- [BS03b] L. Berlu and H. Safouhi. A new algorithm for accurate and fast numerical evaluation of hybrid and three-center two-electron Coulomb integrals over Slater type functions. *J. Phys. A: Math. Gen.*, 36:11267–11283, 2003.
- [CHN09] R. Cools, D. Huybrechs, and D. Nuyens. Recent topics in numerical integration. *Int. J. Quant. Chem.*, 109:1748–1755, 2009.
- [CS51] E. U. Condon and G. H. Shortley. *The Theory of Atomic Spectra*. Cambridge University Press, Cambridge, England, 1951.
- [Dal54] A. Dalgarno. Integrals occurring in problems of molecular structure. *Math. Tables Aids Comput.*, 8:203–212, 1954.
- [Deb09] P. Debye. Näherungsformeln für die Zylinderfunktionen für grosse Werte des Arguments und unbeschränkt veränderliche Werte des Index. *Math. Anal.*, 67:535–558, 1909.
- [DS07] S. Duret and H. Safouhi. The  $W$  algorithm and the  $\bar{D}$  transformation for the numerical evaluation of three-center nuclear attraction integrals. *Int. J. Quantum Chem.*, 107:1060–1066, 2007.
- [DT02] T. A. Driscoll and L. N. Trefethen. *Schwarz-Christoffel Mapping*. Cambridge University Press, 2002.
- [EFH84] G. A. Evans, R. C. Forbes, and J. Hyslop. The tanh transformation for singular integrals. *Int. J. Computer Mathematics*, 15:339–358, 1984.
- [Erd56] A. Erdelyi. *Asymptotic Expansions*. Dover Publications, 1956.

- [Fey49] R. Feynman. Space-time approach to quantum electrodynamics. *Phys. Rev.*, 76:769–789, 1949.
- [FFS83] T. Fessler, W. F. Ford, and D. A. Smith. HURRY: An acceleration algorithm for scalar sequences and series. *ACM Trans. Math. Software*, 9:346–354, 1983.
- [Fil28] L. N. G. Filon. On a quadrature formula for trigonometric integrals. *Proc. Roy. Soc. Edinburgh*, 49:38–47, 1928.
- [Fil78] E. Filter. *Analytische Methoden zur Auswertung von Mehrzentren-Matrixelementen in der Theorie der Molekülorbitale bei Verwendung exponentialartiger Basissätze*. PhD thesis, Universität Regensburg, 1978.
- [FS78] E. Filter and E. O. Steinborn. Extremely compact formulas for molecular one-electron integrals and Coulomb integrals over Slater-type orbitals. *Phys. Rev. A.*, 18:1–11, 1978.
- [GA67] H. L. Gray and T. A. Atchison. Nonlinear transformation related to the evaluation of improper integrals. I. *SIAM J. Numer. Anal.*, 4:363–371, 1967.
- [Gau29] J. A. Gaunt. The triplets of helium. *Phil. Trans. Roy. Soc., A.* 228:151–196, 1929.
- [Gau04] W. Gautschi. *Orthogonal Polynomials: Computation and Approximation*. Clarendon Press, Oxford, UK, 2004.
- [Gau13] W. Gautschi. Neutralizing nearby singularities in numerical quadrature. *Numer. Algor.*, 64:417–425, 2013.
- [GR07] I. S. Gradshteyn and I. M. Ryzhik. *Table of Integrals, Series, and Products, Seventh Edition*. Elsevier Academic Press, Burlington, MA, 2007.
- [Gro85] J. Grotendorst. *Berechnung der Mehrzentren-Molekülintegrale mit exponentialartigen Basisfunktionen durch systematische Anwendung der Fourier-Transformationsmethode*. PhD thesis, Universität Regensburg, 1985.
- [GS64] I. M. Gel'fand and G. E. Shilov. *Generalized functions I, properties and operations*. Academic, New York, 1964.

- [GS88] J. Grotendorst and E. O. Steinborn. Numerical evaluation of molecular one- and two-electron multicenter integrals with exponential-type orbitals via the Fourier-transform method. *Phys. Rev. A.*, 38:3857–3876, 1988.
- [GSS12] P. Gaudreau, R. M. Slevinsky, and H. Safouhi. Computation of tail probability distributions via extrapolation methods and connection with rational and Padé approximants. *SIAM J. Sci. Comput.*, 34:B65–B85, 2012.
- [GW92] H. L. Gray and S. Wang. A new method for approximating improper integrals. *SIAM J. Numer. Anal.*, 29:271–283, 1992.
- [GWS86] J. Grotendorst, E. J. Weniger, and E. O. Steinborn. Efficient evaluation of infinite-series representations for overlap, two-center nuclear attraction, and Coulomb integrals using nonlinear convergence accelerators. *Phys. Rev. A.*, 33:3706–3726, 1986.
- [Hal09] N. Hale. *On The Use Of Conformal Maps To Speed Up Numerical Computations*. PhD thesis, University of Oxford, 2009.
- [Har15] G. H. Hardy. The mean value of the modulus of an analytic function. *Proc. Lond. Math. Soc.*, 1:269–277, 1915.
- [HM67] F. E. Harris and H. H. Michels. The evaluation of molecular integrals for Slater-type orbitals. *Adv. Chem. Phys.*, 13:205–266, 1967.
- [HNSH09] Y. Hatano, I. Ninomiya, H. Sugiura, and T. Hasegawa. Numerical evaluation of Goursat’s infinite integral. *Numer. Algor.*, 52:213–224, 2009.
- [HO09] D. Huybrechs and S. Olver. *Highly Oscillatory Quadrature, in Highly Oscillatory Problems: Computation, Theory and Applications*. Cambridge University Press, Cambridge, 2009.
- [Hom90] H. H. H. Homeier. *Integraltransformationmethoden und Quadraturverfahren für Molekülintegrale mit B-Funktionen*. PhD thesis, Universität Regensburg, 1990.
- [HS93] H. H. H. Homeier and E. O. Steinborn. Programs for the evaluation of nuclear attraction integrals with  $B$  functions. *Comput. Phys. Commun.*, 77:135–151, 1993.
- [HS99] K. Horiuchi and M. Sugihara. Sinc-Galerkin method with the double exponential transformation for the two point boundary problems. *Tech. Rep.*, 99-05, University of Tokyo, 5, 1999.

- [HT90] L. H. Howell and L. N. Trefethen. A modified Schwarz-Christoffel transformation for elongated regions. *SIAM J. Sci. Sta. Comput.*, 11:928–949, 1990.
- [HT08] N. Hale and L. N. Trefethen. New quadrature formulas from conformal maps. *SIAM J. Numer. Anal.*, 46:930–948, 2008.
- [HT09] N. Hale and T. W. Tee. Conformal maps to multiply slit domains and applications. *SIAM J. Sci. Comput.*, 31:3195–3215, 2009.
- [Huz67] S. Huzinaga. Molecular integrals. *Prog. Theor. Phys. Suppl.*, 40:52–77, 1967.
- [HV06] D. Huybrechs and S. Vandewalle. On the evaluation of highly oscillatory integrals by analytic continuation. *SIAM J. Numer. Anal.*, 44:1026–1048, 2006.
- [HW95] H. H. H. Homeier and E. J. Weniger. On remainder estimates for Levin-type sequence transformations. *Comput. Phys. Commun.*, 92:1–10, 1995.
- [IMT87] M. Iri, S. Moriguti, and Y. Takasawa. On a certain quadrature formula (Japanese version originally published in 1970). *J. Comp. Appl. Math.*, 17:3–20, 1987.
- [IN04] A. Iserles and S. P. Nørsett. On quadrature methods for highly oscillatory integrals and their implementation. *BIT*, 44:755–772, 2004.
- [IN05] A. Iserles and S. P. Nørsett. Efficient quadrature of highly oscillatory integrals using derivatives. *Proc. R. Soc. Lond. A*, 461:1383–1399, 2005.
- [Kat57] T. Kato. On the eigenfunctions of many-particle systems in quantum mechanics. *Commun. Pure Appl. Math.*, 10:151–177, 1957.
- [Kin09] F. W. King. *Hilbert Transforms*, volume 1. Cambridge University Press, 2009.
- [Kro65] A. Kronrod. *Nodes and Weights of Quadrature Formulas. Sixteen-Place Tables*. New York: Consultants Bureau (Authorized translation from the Russian), New York, NY, 1965.
- [Lev73] D. Levin. Development of non-linear transformations for improving convergence of sequences. *Int. J. Comput. Math.*, B3:371–388, 1973.

- [Lev82] D. Levin. Procedure for computing one- and two-dimensional integrals of functions with rapid irregular oscillations. *Math. Comp.*, 38:531–538, 1982.
- [Lon56] I. M. Longman. Note on a method for computing infinite integrals of oscillatory functions. *Proc. Cambridge Philos. Soc.*, 52:764–768, 1956.
- [LS81] D. Levin and A. Sidi. Two new classes of non-linear transformations for accelerating the convergence of infinite integrals and series. *Appl. Math. Comput.*, 9:175–215, 1981.
- [Mic98] K. A. Michalski. Extrapolation methods for Sommerfeld integral tails. *IEEE Transactions on Antennas and Propagation*, 46:1405–1418, 1998.
- [MM97] K. A. Michalski and J. R. Mosig. Multilayered media Green’s functions in integral equation formulations. *IEEE Transactions on Antennas and Propagation*, 45:508–519, 1997.
- [MNMS05] M. Muhammad, A. Nurmuhammad, M. Mori, and M. Sugihara. Numerical solution of integral equations by means of the Sinc collocation method based on the double exponential transformation. *J. Comput. Appl. Math.*, 177:269–286, 2005.
- [Mon86] G. Monegato. Quadrature formulas for functions with poles near the interval of integration. *Math. Comp.*, 47:301–312, 1986.
- [Mor78] M. Mori. An IMT-type double exponential formula for numerical integration. *Publ. RIMS, Kyoto Univ.*, 14:713–729, 1978.
- [Mor85] M. Mori. Quadrature formulas obtained by variable transformation and DE rule. *J. Comp. Appl. Math.*, 12 & 13:119–130, 1985.
- [Mor05] M. Mori. Discovery of the double exponential transformation and its developments. *Publ. RIMS, Kyoto Univ.*, 41:897–935, 2005.
- [MS01] M. Mori and M. Sugihara. The double-exponential transformation in numerical analysis. *J. Comp. Appl. Math.*, 127:287–296, 2001.
- [MS05] M. Muhammad and M. Sugihara. Numerical iterated integration based on the double exponential transformation. *Japan J. Indust. Appl. Math.*, 22:77–86, 2005.

- [NMMS05] A. Nurmuhammad, M. Muhammad, M. Mori, and M. Sugihara. Double exponential transformation in the Sinc-collocation method for a boundary value problem of fourth-order ordinary differential equation. *J. Comput. Appl. Math.*, 182:32–50, 2005.
- [Olv06] S. Olver. Moment-free numerical integration of highly oscillatory functions. *IMA J. Num. Anal.*, 26:213–227, 2006.
- [OM91] T. Ooura and M. Mori. The double exponential formula for oscillatory functions over the half infinite interval. *J. Comp. Appl. Math.*, 38:353–360, 1991.
- [OM99] T. Ooura and M. Mori. A robust double exponential formula for Fourier type integrals. *J. Comp. Appl. Math.*, 112:229–241, 1999.
- [OMS10] T. Okayama, T. Matsuo, and M. Sugihara. Sinc-collocation methods for weakly singular Fredholm integral equations of the second kind. *J. Comp. Appl. Math.*, 234:1211–1227, 2010.
- [OMS13] T. Okayama, T. Matsuo, and M. Sugihara. Error estimates with explicit constants for Sinc approximation, Sinc quadrature and Sinc indefinite integration. *Numer. Math.*, 124:361–394, 2013.
- [Ono75] H. Ono. Algebraic solitary waves in stratified fluids. *J. Phys. Soc. Japan*, 39:1082–1091, 1975.
- [Oou13] T. Ooura. Fast computation of Goursat’s infinite integral with very high accuracy. *J. Comp. Appl. Math.*, 249:1–8, 2013.
- [OTMS13] T. Okayama, K. Tanaka, T. Matsuo, and M. Sugihara. DE-Sinc methods have almost the same convergence property as SE-Sinc methods even for a family of functions fitting the SE-Sinc methods: Part I: definite integration and function approximation. *Numer. Math.*, 125:511–543, 2013.
- [PNM10] A. G. Polimeridis, R. M. Golubovic Niciforovic, and J. R. Mosig. Acceleration of slowly convergent series via the generalized weighted-averages method. *Progress In Electromagnetics Research M*, 14:233–245, 2010.
- [PTVF07] W. H. Press, S. A. Teukolsky, W. T. Vetterling, and B. P. Flannery. *Numerical Recipes: The Art of Scientific Computing, Third Edition*. Cambridge University Press, New York, 2007.

- [Ric11] L. F. Richardson. The approximate arithmetical solution by finite differences of physical problems including differential equations, with an application to the stresses in a masonry dam. *Phil. Trans. of the Royal Society A*, 210:459–470, 1911.
- [Rid79] C. Ridders. A new algorithm for computing a single root of a real continuous function. *IEEE Trans. Circ. Sys.*, 26:979–980, 1979.
- [Rom55] W. Romberg. Vereinfachte numerische Integration. *Det Kongelige Norske Videnskabers Selskab Forhandlinger*, 28:30–36, 1955.
- [Saf99] H. Safouhi. *Nonlinear transformations for accelerating the convergence of molecular multicenter bielectronic integrals*. PhD thesis, Université de Blaise Pascal, 1999.
- [Saf01] H. Safouhi. The properties of sine, spherical Bessel and reduced Bessel functions for improving convergence of semi-infinite very oscillatory integrals: The evaluation of three-center nuclear attraction integrals over  $B$  functions. *J. Phys. A: Math. Gen.*, 34:2801–2818, 2001.
- [Saf02] H. Safouhi. Convergence properties of the  $s\bar{D}$  transformation and a fast and accurate numerical evaluation of molecular integrals. *J. Phys. A: Math. Gen.*, 35:9685–9698, 2002.
- [Saf04] H. Safouhi. Highly accurate numerical results for three-center nuclear attraction and two-electron Coulomb and exchange integrals over Slater type functions. *Int. J. Quantum Chem.*, 100:172–183, 2004.
- [Saf10] H. Safouhi. Bessel, sine and cosine functions and extrapolation methods for computing molecular multi-center integrals. *Numer. Algor.*, 54:141–167, 2010.
- [SB02] J. Stoer and R. Bulirsch. *Introduction to Numerical Analysis, Third Edition. Texts in Applied Mathematics 12*. Springer-Verlag, New York, 2002.
- [SB06] H. Safouhi and A. Bouferguene. Extrapolation methods for improving convergence of spherical Bessel integrals for the two-center Coulomb integrals. *Int. J. Quantum Chem.*, 106:2318–2323, 2006.
- [SB07] H. Safouhi and A. Bouferguene. Nonlinear transformation methods for accelerating the convergence of Coulomb integrals over exponential type functions. *Theo. Chem. Acc.*, 117:213–222, 2007.

- [Sch26] E. Schrödinger. An undulatory theory of the mechanics of atoms and molecules. *Phys. Rev.*, 28:1049–1070, 1926.
- [Sch69] C. Schwartz. Numerical integration of analytic functions. *J. Comp. Phys.*, 4:19–29, 1969.
- [SF75] E. O. Steinborn and E. Filter. Translations of fields represented by spherical-harmonics expansions for molecular calculations. III. Translations of reduced Bessel functions, Slater-type s-orbitals, and other functions. *Theor. Chim. Acta.*, 38:273–281, 1975.
- [SF79] D. A. Smith and W. F. Ford. Acceleration of linear and logarithmic convergence. *SIAM J. Numer. Anal.*, 16:223–240, 1979.
- [SF82] D. A. Smith and W. F. Ford. Numerical comparisons of nonlinear convergence accelerators. *Math. Comput.*, 38:481–499, 1982.
- [Sha55] D. Shanks. Non-linear transformations of divergent and slowly convergent sequences. *J. Math. and Phys.*, 34:1–42, 1955.
- [SHE<sup>+</sup>00] E. O. Steinborn, H. H. H. Homeier, I. Ema, R. López, and G. Ramírez. Molecular calculations with  $B$  functions. *Int. J. Quantum Chem.*, 76:244–251, 2000.
- [Sid80a] A. Sidi. Extrapolation methods for oscillating infinite integrals. *J. Inst. Math. Appl.*, 26:1–20, 1980.
- [Sid80b] A. Sidi. Numerical quadrature and non-linear sequence transformations; unified rules for the efficient computation of integrals with algebraic and logarithmic end-point singularities. *Math. Comp.*, 35:851–874, 1980.
- [Sid82] A. Sidi. An algorithm for a special case of a generalization of the Richardson extrapolation process. *Numer. Math.*, 38:299–307, 1982.
- [Sid03] A. Sidi. *Practical Extrapolation Methods: Theory and Applications*. Cambridge U. P., Cambridge, 2003.
- [Sid10] A. Sidi. Survey of numerical stability issues in convergence acceleration. *Appl. Num. Math.*, 60:1395–1410, 2010.
- [Sla30] J. C. Slater. Atomic shielding constants. *Phys. Rev.*, 36:57–64, 1930.
- [Sla32] J. C. Slater. Analytic atomic wave functions. *Phys. Rev.*, 42:33–43, 1932.

- [Sle] R. M. Slevinsky. <https://github.com/MikaelSlevinsky/DEQuadrature.jl>.
- [SM04] M. Sugihara and T. Matsuo. Recent developments of the Sinc numerical methods. *J. Comput. Appl. Math.*, 164 & 165:673–689, 2004.
- [Sof07] Numerical Recipes Software. Coefficients used in the bessjy and bessik objects. <http://www.nr.com/webnotes?7>, 2007.
- [Som49] A. Sommerfeld. *Partial Differential Equations in Physics (Pure and Applied Mathematics: A Series of Monographs and Textbooks, Vol. 1)*. Academic Press, New York, NY, 1949.
- [SS09] R. M. Slevinsky and H. Safouhi. The  $S$  and  $G$  transformations for computing three-center nuclear attraction integrals. *Int. J. Quant. Chem.*, 109:1741–1747, 2009.
- [SS12] R. M. Slevinsky and H. Safouhi. A comparative study of numerical steepest descent, extrapolation, and sequence transformation methods in computing semi-infinite integrals. *Numer. Algor.*, 60:315–337, 2012.
- [Ste73] F. Stenger. Integration formulas based on the trapezoidal formula. *J. Inst. Math. Appl.*, 12:103–114, 1973.
- [Ste81] F. Stenger. Numerical methods based on the Whittaker cardinal, or sinc functions. *SIAM Rev.*, 23:165–224, 1981.
- [Ste93] F. Stenger. *Numerical Methods Based on Sinc and Analytic Functions*. Springer Series in Computational Mathematics 20. Springer-Verlag, New York, 1993.
- [Ste00] F. Stenger. Summary of Sinc numerical methods. *J. Comp. Appl. Math.*, 121:379–420, 2000.
- [STMS10] R. M. Slevinsky, T. Temga, M. Mouattamid, and H. Safouhi. One- and two-center ETF-integrals of first order in relativistic calculation of NMR parameters. *J. Phys. A: Math. Theor.*, 43:225202, 2010.
- [Sug97] M. Sugihara. Optimality of the double exponential formula - functional analysis approach -. *Numer. Math.*, 75:379–395, 1997.
- [Sug02] M. Sugihara. Double exponential transformation in the Sinc-collocation method for two-point boundary value problems. *J. Comp. Appl. Math.*, 149:239–250, 2002.

- [Sug03] M. Sugihara. Near optimality of the sinc approximation. *Math. Comp.*, 72:767–786, 2003.
- [SW77] E. O. Steinborn and E. J. Weniger. Advantages of reduced Bessel functions as atomic orbitals: An application to  $H_2^+$ . *Int. J. Quantum Chem. Symp.*, 11:509–516, 1977.
- [SW78] E. O. Steinborn and E. J. Weniger. Reduced Bessel functions as atomic orbitals: Some mathematical aspects and an LCAO-MO treatment of  $HeH^{++}$ . *Int. J. Quantum Chem. Symp.*, 12:103–108, 1978.
- [TD98] L. N. Trefethen and T. A. Driscoll. Schwarz-Christoffel mapping in the computer era. *Proc. Intl. Cong. Math.*, 3:533–542, 1998.
- [TM71] H. Takahasi and M. Mori. Error estimation in the numerical quadrature of analytic functions. *Appl. Anal.*, 1:201–229, 1971.
- [TM73] H. Takahasi and M. Mori. Quadrature formulas obtained by variable transformation. *Numer. Math.*, 21:206–219, 1973.
- [TM74] H. Takahasi and M. Mori. Double exponential formulas for numerical integration. *Publ. RIMS, Kyoto Univ.*, 9:721–741, 1974.
- [TOMS13] K. Tanaka, T. Okayama, T. Matsuo, and M. Sugihara. DE-Sinc methods have almost the same convergence property as SE-Sinc methods even for a family of functions fitting the SE-Sinc methods: Part II: indefinite integration. *Numer. Math.*, 125:545–568, 2013.
- [Tre80] L. N. Trefethen. Numerical computation of the Schwarz-Christoffel transformation. *SIAM J. Sci. Sta. Comput.*, 1:82–102, 1980.
- [TS83] H. P. Trivedi and E. O. Steinborn. Fourier transform of a two-center product of exponential-type orbitals. Application to one- and two-electron multicenter integrals. *Phys. Rev. A.*, 27:670–679, 1983.
- [TSM04] K. Tanaka, M. Sugihara, and K. Murota. Numerical indefinite integration by double exponential sinc method. *Math. Comp.*, 74:655–679, 2004.
- [TSM09] K. Tanaka, M. Sugihara, and K. Murota. Function classes for successful DE-Sinc approximations. *Math. Comp.*, 78:1553–1571, 2009.

- [TSMM09] K. Tanaka, M. Sugihara, K. Murota, and M. Mori. Function classes for double exponential integration formulas. *Numer. Math.*, 111:631–655, 2009.
- [TT06] T. W. Tee and L. N. Trefethen. A rational spectral collocation method with adaptively transformed Chebyshev grid points. *SIAM J. Sci. Comput.*, 28:1798–1811, 2006.
- [Wat66] G. N. Watson. *A Treatise on the Theory of Bessel Functions*. Cambridge University Press, Second Edition, Cambridge, England, 1966.
- [WB06] A. Wächter and L. T. Biegler. On the implementation of a primal-dual interior point filter line search algorithm for large-scale nonlinear programming. *Math. Prog.*, 106:25–57, 2006.
- [Wei78] M. Weissbluth. *Atoms and molecules*. Academic, New York, 1978.
- [Wen82] E. J. Weniger. *Reduzierte Bessel-Funktionen als LCAO-Basisatz: Analytische und numerische Untersuchungen*. PhD thesis, Universität Regensburg, 1982.
- [Wen89] E. J. Weniger. Nonlinear sequence transformations for the acceleration of convergence and the summation of divergent series. *Comput. Phys. Rep.*, 10:189–371, 1989.
- [Wen01] E. J. Weniger. Irregular input data in convergence acceleration and summation processes: General considerations and some special Gaussian hypergeometric series as model problems. *Comput. Phys. Comm.*, 133:202–228, 2001.
- [Wen04] E. J. Weniger. Mathematical properties of a new Levin-type sequence transformation introduced by čížek, Zamastil, and Skála. I. Algebraic theory. *J. Math. Phys.*, 45:1209–1246, 2004.
- [WGS86] E. J. Weniger, J. Grotendorst, and E. O. Steinborn. Unified analytical treatment of overlap, two-center nuclear attraction and Coulomb integrals of  $B$  functions via the Fourier-transform method. *Phys. Rev. A.*, 33:3688–3705, 1986.
- [WS82] E. J. Weniger and E. O. Steinborn. Programs for the coupling of spherical harmonics. *Comput. Phys. Commun.*, 25:149–157, 1982.
- [WS83] E. J. Weniger and E. O. Steinborn. The Fourier transforms of some exponential-type functions and their relevance to multicenter problems. *J. Chem. Phys.*, 78:6121–6132, 1983.

- [WS88] E. J. Weniger and E. O. Steinborn. Overlap integrals of  $B$  functions. A numerical study of infinite series representations and integrals representation. *Theor. Chim. Acta.*, 73:323–336, 1988.
- [Wyn56] P. Wynn. On a device for computing the  $e_m(S_n)$  transformation. *Math. Tables Aids Comput.*, 10:91–96, 1956.
- [Xu96] Y.-L. Xu. Fast evaluation of Gaunt coefficients. *Math. Comput.*, 65:1601–1612, 1996.
- [Zwi92] D. Zwillinger. *The Handbook of Integration*. Jones and Bartlett Publishers, London, England, 1992.